SEPTEMBER **18– 22, 2017**

PRAGUE, CZECH REPUBLIC

MODELLING AND OBSERVING

DENSE STELLAR SYSTEMS

MODEST **UNDER** **PRAGUE'S** STARRY **SKIES**

Kepler

Doppler

Brahe

Einstein

Mach

MODEST 17

BOOK OF ABSTRACTS

This book contains the abstracts of oral and poster presentations of the MODEST 17 conference held in Prague from September 18tth to September 22nd 2017. The abstracts in the first part of the book are orderd according to the programme. The second part of the book publishes the presented posters.

Scientific organising committee:

Melvyn Davies
Francesco Ferraro
Jaroslav Haas (co-chair)
Douglas Heggie
Pavel Kroupa (co-chair)
Steffen Mieske
Mark Morris
Simon Portegies Zwart
Rainer Spurzem
Ladislav Šubr (chair)

Local organising committee:

Jörg Dabringhausen
Nela Dvořáková
Jaroslav Haas
Jan Kára
Petr Kepčija
Pavel Kroupa
Jozef Krutel
Lýdia Štofanová
Ladislav Šubr
Nicol Tomková

Contents

List of participants

Aarseth, Sverre
University of Cambridge
sverre@ast.cam.ac.uk

Alfaro Cuello, Mayte
Max-Planck-Institut für Astronomie
alfaro@mpia.de
p. 37

Arca Sedda, Manuel
Astronomisches Rechen-Institut - Zentrum fur Astronomie der Universitat Heidelberg
m.arcasedda@ari.uni-heidelberg.de
p. 70

Arifyanto, Mochamad Ikbal
Dept. of Astronomy, Institut Teknologi Bandung
ikbal@as.itb.ac.id
p. 112

Askar, Abbas
Nicolaus Copernicus Astronomical Center, Polish Academy of Sciences
askar@camk.edu.pl
p. 79

Bae, Yeong-Bok
Korea Astronomy and Space Science Institute
baeyb@kasi.re.kr
p. 75

Ballone, Alessandro
INAF-OAPd
alessandro.ballone@oapd.inaf.it
p. 46, 96

Banerjee, Sambaran
University of Bonn
sambaran@astro.uni-bonn.de
p. 80

Beccari, Giacomo
ESO
gbeccari@eso.org
p. 24

Belczynski, Krzysztof
Copernicus Center, Poland
chrisbelczynski@gmail.com
p. 74

Belloni, Diogo
Nicolaus Copernicus Astronomical Center
belloni@camk.edu.pl
p. 28

Benacquista, Matthew
University of Texas Rio Grande Valley
benacquista@icloud.com
p. 30

Bertelli Motta, Clio
ARI - ZAH - University of Heidelberg
cbertelli@ari.uni-heidelberg.de
p. 130

Bianchini, Paolo
McMaster University
bianchip@mcmaster.ca
p. 68

Bobrick, Alexey
Lund Observatory
alexey@astro.lu.se
p. 102

Boekholt, Tjarda
Universidade de Aveiro
tjardaboekholt@gmail.com
p. 104

Boily, Christian
Observatoire astronomique de Strasbourg
christian.boily@astro.unistra.fr
p. 22

Bojnordi Arbab, Behzad
Sharif University of Technology
behzadbojnordi@gmail.com
p. 90

Bortolas, Elisa
University of Padova / INAF-OAPd
elisa.bortolas@phd.unipd.it
p. 78, 110

Boubert, Douglas
University of Cambridge
d.boubert@ast.cam.ac.uk
p. 118

Breen, Phil
University of Edinburgh
Phil.Breen@ed.ac.uk
p. 9

Buckner, Anne
University of Leeds
a.s.m.buckner@leeds.ac.uk
p. 124

Cai, Maxwell Xu
Leiden Observatory
cai@strw.leidenuniv.nl
p. 15

Capuzzo Dolcetta, Roberto
Dep. of Physics, Sapienza, Univ. of Roma, Italy
roberto.capuzzodolcetta@uniroma1.it
p. 48

Casetti, Lapo
Università di Firenze, INFN and INAF-Arcetri, Italy
lapo.casetti@unifi.it
p. 19

Cattolico, Raffaele Stefano
University Sapienza
stefano.cattolico@uniroma1.it

Charbonnel, Corinne
Dept of Astronomy, University of Geneva (CH) and CNRS (F)
corinne.charbonnel@unige.ch
p. 34

Chaves Velasquez, Luis Leonardo
INAOE, México
leonardochaves83@gmail.com
p. 120

Claydon, Ian
University of Surrey
i.claydon@surrey.ac.uk
p. 7

Concha-Ramírez, Francisca
Leiden Observatory
fconcha@strw.leidenuniv.nl
p. 131

Cuevas Otahola, Bolivia Teresa
INAOE
bolivia@inaoep.mx
p. 134

Dabringhausen, Joerg
Astronomical Institute, Charles University
joerg@sirrah.troja.mff.cuni.cz
p. 41

Davari, Nazanin
University of Rome La Sapienza
nazanin.davari@uniroma1.it

Davies, Melvyn
Lund University
mbd@astro.lu.se
p. 58

Di Cintio, Pierfrancesco
CNR-IFAC & INFN Firenze
p.dicintio@ifac.cnr.it
p. 108

Dinnbier, František
Universitaet zu Koeln
dinnbier@ph1.uni-koeln.de

Do, Tuan
UCLA
tdo@astro.ucla.edu
p. 44

Dvorakova, Nela
Astronomical Institute of Charles University
dvorakova.nela@seznam.cz

Fellhauer, Michael
Departamento de Astronomia, Universidad de Concepcion, Chile
mfellhauer@astro-udec.cl
p. 59

Ferraro, Francesco R.
University of Bologna
francesco.ferraro3@unibo.it

Fragione, Giacomo
Hebrew University of Jerusalem Israel
giacomo.fragione90@gmail.com
p. 69, 94

Giersz, Mirek
Nicolaus Copernicus Astronomical Centre, Polish Academy of Sciences
mig@camk.edu.pl
p. 64

Gilmore, Gerry
Institute of Astronomy, Cambridge
gil@ast.cam.ac.uk
p. 31

Grudić, Michael
Caltech
mgrudich@caltech.edu
p. 27

Haas, Jaroslav
Astronomical Institute of Charles University, Prague
haas@sirrah.troja.mff.cuni.cz

Hacar, Alvaro
Leiden Observatory
hacar@strw.leidenuniv.nl
p. 20

Haghi, Hossein
Institute for Advanced Studies in Basic Sciences (IASBS)
haghi@iasbs.ac.ir
p. 40

Hong, Jongsuk
KIAA-PKU
jongsuk.hong@pku.edu.cn
p. 35

Jaehnig, Karl
Vanderbilt University
karl.o.jaehnig@vanderbilt.edu

Jerabkova, Tereza
HISKP, University of Bonn
tereza@sirrah.troja.mff.cuni.cz
p. 38

Jørgensen, Timmi
Lund Observatory
timmi@astro.lu.se
p. 86

Kacharov, Nikolay
Max Planck Institute for Astronomy - Heidelberg
kacharov@mpia.de
p. 36

Kára, Jan
Charles University
Honza.chris@gmail.com

Karas, Vladimir
Astronomical Institute, Czech Academy of Sciences
vladimir.karas@cuni.cz
p. 92

Kaur, Karamveer
Raman Research Institute, Bangalore
karamveer@rri.res.in
p. 50

Kepcija, Petr
Charles University
pkepcija@gmail.com

Khalaj, Pouria
Institute of Planetology and Astrophysics of Grenoble
pouria.khalaj@univ-grenoble-alpes.fr

Kocsis, Bence
Eotvos University
bkocsis@gmail.com
p. 81

Kremer, Kyle
Northwestern University-CIERA
kylekremer23@gmail.com
p. 100

Kroupa, Pavel
University of Bonn; Charles University, Praha
pavel@astro.uni-bonn.de

Krutel, Jozef
Charles University
jkrutel@icloud.com

Lee, Joowon
Kyung Hee University
joowon.lee@khu.ac.kr
p. 133

Lilley, Edward
Institute of Astronomy, University of Cambridge
ejl44@cam.ac.uk
p. 114

Luetzgendorf, Nora
ESA/STScI
nluetzge@cosmos.esa.int
p. 55

Martinez, Luis
Astronomy Institute, UNAM
lamartinez@astro.unam.mx
p. 11

Mastrobuono Battisti, Alessandra
Max Planck Institute for Astronomy
mastrobuono@mpia.de
p. 47

McMillan, Steve
Drexel University
steve@physics.drexel.edu
p. 2

Megeath, Tom
University of Toledo
tommegeath@gmail.com
p. 18

Meiron, Yohai
Eötvös Loránd University
sahmes@gmail.com
p. 10

Mieske, Steffen
ESO
smieske@eso.org
p. 71

Morris, Mark
University of California, Los Angeles
morris@astro.ucla.edu
p. 45

Moyano Loyola, Guido Rodrigo Ismael
Lund Observatory
gmoyano@astro.lu.se
p. 8

Ordenes Briceño, Yasna
Heidelberg University and Catholica University of Chile
yordenes@astro.puc.cl
p. 51

Panamarev, Taras
ARI/ZAH Heidelberg
taras@ari.uni-heidelberg.de
p. 54

Park, So-Myoung
Kyung Hee University
smpark12@khu.ac.kr
p. 116

Pavlík, Václav
Astronomical Institute of Charles University, Prague
pavlik@sirrah.troja.mff.cuni.cz
p. 4, 98

Picotti, Arianna
MPIA
picotti@mpia.de
p. 49

Pinto, Luis Diego
Sapienza, University of Rome
luisdiego.pinto@uniroma1.it
p. 16

Pooley, David
Trinity University
dpooley@trinity.edu
p. 32

Portegies Zwart, Simon
Leiden Observatory
spz@strw.leidenuniv.nl
p. 14

Raso, Silvia
University of Bologna
silvia.raso2@unibo.it
p. 60

Rasskazov, Alexander
Eötvös Loránd University
alexander.rasskazov@gmail.com
p. 76

Rastello, Sara
Università di Roma, La Sapienza
sara.rastello@uniroma1.it
p. 106, 128

Reina-Campos, Marta
Heidelberg University
reina.campos@uni-heidelberg.de
p. 6

Rieder, Steven
RIKEN AICS
steven@rieder.nl
p. 23

Rodriguez, Carl
MIT
carlrodr@mit.edu
p. 65

Ryabova, Marina
Southern Federal University, Russia
rgyaf@yandex.ru
p. 129

Ryabov, Denis
Southern Federal University, Russia
dryabov@yandex.ru

Sahu, Snehalata
Indian Institute of Astrophysics, Bengaluru
snehalata@iiap.res.in
p. 61

Seleznev, Anton
Ural Federal University, UrFU
anton.seleznev@urfu.ru
p. 21

Shin, Jihye
Korea Institute for Advanced Study
jhshin.jhshin@gmail.com
p. 132

Simunovic, Mirko
Gemini Observatory
msimunovic@gemini.edu
p. 88

Sippel, Anna
MPIA
sippel@mpia.de
p. 66

Sitek, Monika
Astronomical Observatory of Warsaw University
monika@sitek.com.pl
p. 126

Sollima, Antonio
INAF Osservatorio Astronomico di Bologna
antonio.sollima@oabo.inaf.it
p. 39

Spurzem, Rainer
National Astronomical Observatories, CAS, Beijing, China
spurzem@nao.cas.cn
p. 77

Stofanova, Lydia
Astronomical Institute of the Charles University, Prague
lydiastofan@gmail.com

Stutz, Amelia
Universidad de Concepcion
amelia.stutz@gmail.com
p. 25

Subr, Ladislav
Astronomical Institute, Charles University
subr@sirrah.troja.mff.cuni.cz

Tiongco, Maria
Indiana University
mtiongco@indiana.edu
p. 12

Tomková, Nicol
Charles University
nicol.tomkova@gmail.com

Trani, Alessandro Alberto
SISSA
aatrani@gmail.com
p. 52

Valencia-Enríquez, Diego
INAOE
diegovalencia5@gmail.com
p. 122

Varri, Anna Lisa
University of Edinburgh, UK
annalisa.varri@gmail.com
p. 5

Vasiliev, Eugene
Oxford University
eugvas@lpi.ru
p. 53

Wang, Long
RIKEN AICS
longwang.astro@live.com
p. 3

Zeidler, Peter
Space Telescope Science Institute (STScI)
zeidler@stsci.edu
p. 26

Zocchi, Alice
University of Bologna
alice.zocchi2@unibo.it
p. 67

Programme

Sunday, September 17

18:00 – 21:00	**Welcome reception in the historical building of Charles University / registration**

Monday, September 18

07:30 – 08:30	**Registration**
08:30 – 10:25	**Stellar dynamics and numerical methods (chair: Ladislav Subr)**
08:30 – 09:10	Steve McMillan: *Modeling Massive Cluster Formation with Stellar Feedback using FLASH and AMUSE*
09:10 – 09:35	Long Wang: *A new high-performance particle^3 tree code designed for realistic massive star cluster simulations*
09:35 – 10:00	Václav Pavlík: *Fitting self-similar core collapse in N-body models*
10:00 – 10:25	Anna Lisa Varri: *Leveraging the phase space richness of star clusters: primordial and evolutionary features*
10:25 – 10:55	**coffee break**
10:55 – 12:35	**Stellar dynamics and numerical methods (chair: Anna Lisa Varri)**
10:55 – 11:20	Marta Reina-Campos: *The E-MOSAICS project: simulating the formation and evolution of galaxies and their globular cluster systems*
11:20 – 11:45	Ian Claydon: *Modelling globular clusters with potential escapers*
11:45 – 12:10	Guido Rodrigo Ismael Moyano Loyola: *The effect of unresolved binary systems on the determination of dynamical masses*
12:10 – 12:35	Phil Breen: *The physical origin of stellar envelopes around globular clusters*
12:35 – 14:55	**Lunch**
14:55 – 16:10	**Stellar dynamics and numerical methods (chair: Simon Portegies Zwart)**
14:55 – 15:20	Yohai Meiron: *Relaxation and mixing of constants of motion in globular clusters*
15:20 – 15:45	Luis Martinez: *On the origin and evolution of the old, yet metal-rich, open cluster NGC 6791*
15:45 – 16:10	Maria Tiongco: *Dynamical evolution of tidally limited rotating star clusters*
16:10 – 16:40	**coffee break**
16:40 – 18:10	**Dynamics of (exo)planetary systems in star clusters (chair: Maria Tiongco)**
16:40 – 17:20	Simon Portegies Zwart: *The evolution of planetary systems in dense star clusters*
17:20 – 17:45	Maxwell Xu Cai: *Stability of Multiplanetary Systems in Star Clusters*
17:45 – 18:10	Luis Diego Pinto: *A Smoothed Particle Hydrodynamics approach to young protoplanetary disks around single and binary stars*
18:10 – 18:40	**Poster presentations (chair: Jaroslav Haas)**

Tuesday, September 19

08:30 – 10:25	**Young star clusters and star forming regions (chair: Corinne Charbonnel)**
08:30 – 09:10	Tom Megeath: *The spatial distribution of young stars and gas in giant molecular clouds and the implications for cluster formation.*
09:10 – 09:35	Lapo Casetti: *Non-thermal states of galactic filaments from the dynamics of two-dimensional self-gravitating systems*
09:35 – 10:00	Alvaro Hacar: *Fibers in the NGC1333 proto-cluster*
10:00 – 10:25	Anton Seleznev: *Stellar clusters in the star formation complexes G173 and G192*
10:25 – 10:55	**coffee break**
10:55 – 12:35	**Young star clusters and star forming regions (chair: Alessandra Mastrobuono Battisti)**
10:55 – 11:20	Christian Boily: *The Evolution of Tight Binaries in Star Forming Regions*
11:20 – 11:45	Steven Rieder: *Simulations of young star clusters: the MYSTIX case*
11:45 – 12:10	Giacomo Beccari: *Discrete episodes of star formation in the ONC?*
12:10 – 12:35	Amelia Stutz: *Cluster formation in Orion: the Slingshot mechanism*
12:25 – 14:30	**Lunch**
14:30 – 15:45	**Young star clusters and star forming regions (chair: Tereza Jerabkova)**
14:30 – 14:55	Peter Zeidler: *Young massive star clusters in the era of integral field spectroscopy*
14:55 – 15:20	Michael Grudić: *The Structure of Young Massive Clusters via Hierarchical Star Formation*
15:20 – 15:45	Diogo Belloni: *On Cataclysmic Variables in Globular Clusters*
15:45 – 16:15	**coffee break**
16:15 – 18:00	**New observational frontiers (chair: Steffen Mieske)**
16:15 – 16:55	Matthew Benacquista: *Gravitational Wave Detection of Compact Binaries*
16:55 – 17:35	Gerry Gilmore: *New observational frontiers - Gaia, and others*
17:35 – 18:00	David Pooley: *The Lynx X-ray Mission*
19:00 – 22:00	**Conference dinner**

Wednesday, September 20

08:30 – 10:25	**Stellar populations in star clusters (chair: Amelia Stutz)**
08:30 – 09:10	Corinne Charbonnel: *Multiple stellar populations in globular clusters - Observational constraints and theoretical challenges*
09:10 – 09:35	Jongsuk Hong: *Dynamical origin of multiple populations in star clusters in the Magellanic Cloulds*
09:35 – 10:00	Nikolay Kacharov: *Stellar populations and star formation histories in the nuclei of nearby galaxies*
10:00 – 10:25	Mayte Alfaro Cuello: *Connecting globular and nuclear star clusters through the enigmatic M54*
10:25 – 10:55	**coffee break**
10:55 – 12:35	**Stellar populations in star clusters (chair: Nora Luetzgendorf)**
10:55 – 11:20	Tereza Jerabkova: *Stellar populations in extreme star burst clusters and UCDs*
11:20 – 11:45	Antonio Sollima: *The initial and present-day mass function of Galactic globular clusters*
11:45 – 12:10	Hossein Haghi: *The mass-to-light ratio-metallicity relation of globular clusters in M31*
12:10 – 12:35	Joerg Dabringhausen: *Are globular clusters in the Fornax Cluster different from those in the Virgo Cluster?*
12:35 – 14:30	**Lunch**
14:30 – 16:00	**Discussion on perspectives of NBODY6/7 with Sverre Aarseth (chair: Rainer Spurzem)**
16:00 – 18:00	**Guided tour through Prague / free programme**
18:30 – 20:00	**Concert in the representative hall of the Faculty of Mathematics and Physics**

Thursday, September 21

08:30 – 10:25	**Galactic centre / nuclear star clusters (chair: Jaroslav Haas)**
08:30 – 09:10	Tuan Do: *Observations of the Milky Nuclear Star Cluster*
09:10 – 09:35	Mark Morris: *The Dust-Enshrouded "G" Sources Orbiting the Galactic Black Hole: Fluffy Stellar Merger Products*
09:35 – 10:00	Alessandro Ballone: *A compact source scenario for the Galactic Center cloud G2*
10:00 – 10:25	Alessandra Mastrobuono Battisti: *The build up of nuclear star clusters: simulations and observations*
10:25 – 10:55	**coffee break**
10:55 – 12:35	**Galactic centre / nuclear star clusters (chair: Giacomo Beccari)**
10:55 – 11:20	Roberto Capuzzo Dolcetta: *Nuclear Star Clusters and Super Massive Black Holes as Compact Massive Objects*
11:20 – 11:45	Arianna Picotti: *XSHOOTER Survey of the Nearest Nuclear Star Clusters*
11:45 – 12:10	Karamveer Kaur: *Response of a Nuclear Star Cluster to the Slow Accumulation of Gas*
12:10 – 12:35	Yasna Ordenes Briceño: *Nucleated dwarf galaxies in the central region of the Fornax Galaxy Cluster: Nuclear cluster analysis*
12:35 – 14:30	**Lunch**
14:30 – 16:10	**Galactic centre / nuclear star clusters (chair: Elisa Bortolas)**
14:30 – 14:55	Alessandro Alberto Trani: *Circumnuclear disks and rings of gas as probes of supermassive black hole presence*
14:55 – 15:20	Eugene Vasiliev: *The adventures of a stellar cusp in the Galactic Center*
15:20 – 15:45	Taras Panamarev: *Direct N-body simulation of the Galactic Centre*
15:45 – 16:10	Nora Luetzgendorf: *An upper limit on the mass of a central black hole in the large magellanic cloud*
16:10 – 16:40	**coffee break**
16:40 – 18:35	**Blue stragglers / stellar collisions and their products (chair: Yasna Ordenes Briceño)**
16:40 – 17:20	Melvyn Davies: *Stellar collisions and their products*
17:20 – 17:45	Michael Fellhauer: *Pop III star clusters: The crucial interplay between accretion and collisions*
17:45 – 18:10	Silvia Raso: *The "UV-route" to Search for Blue Straggler Stars in Globular Clusters: First Results from the HST UV Legacy Survey*
18:10 – 18:35	Snehalata Sahu: *UV bright population in Globular Cluster NGC 288 - insights from UVIT*
19:30 – 21:00	**Mark Morris: Extreme Stars at the Center of the Galaxy (public lecture)**

Friday, September 22

08:30 – 10:25	**Compact objects in star clusters (chair: Sambaran Banerjee)**
08:30 – 09:10	Mirek Giersz: *Compact objects in star clusters*
09:10 – 09:35	Carl Rodriguez: *Binary Black Hole Mergers from Dense Star Clusters*
09:35 – 10:00	Anna Sippel: *A black hole love story*
10:00 – 10:25	Alice Zocchi: *Kinematical signatures of intermediate-mass black holes in globular clusters*
10:25 – 10:55	**coffee break**
10:55 – 12:35	**Compact objects in star clusters (chair: Mirek Giersz)**
10:55 – 11:20	Paolo Bianchini: *The dynamical M/L of globular clusters*
11:20 – 11:45	Giacomo Fragione: *Millisecond pulsars and the gamma-ray excess in the Galactic Center*
11:45 – 12:10	Manuel Arca Sedda: *Evolution of intermediate-mass and stellar binary black holes in galactic nuclei*
12:10 – 12:35	Steffen Mieske: *Super-massive black holes in ultra-compact dwarf galaxies*
12:35 – 14:30	**Lunch**
14:30 – 16:25	**Astrophysical sources of gravitational waves (chair: Joerg Dabringhausen)**
14:30 – 15:10	Krzysztof Belczynski: *GW170104 and the origin of heavy, low-spin binary black holes via classical isolated binary evolution*
15:10 – 15:35	Yeong-Bok Bae: *Dynamically Formed Black Hole Binaries as Gravitational Wave Sources*
15:35 – 16:00	Alexander Rasskazov: *Evolution of massive black hole binaries in rotating stellar nuclei and its implications for gravitational wave detections*
16:00 – 16:25	Rainer Spurzem: *Extragalactic Globular Star Clusters as Sources of Gravitational Wave Events*
16:25 – 16:55	**coffee break**
16:55 – 18:35	**Astrophysical sources of gravitational waves (chair: Melvyn Davies)**
16:55 – 17:20	Elisa Bortolas: *Star Cluster Disruption by a Supermassive Black Hole Binary*
17:20 – 17:45	Abbas Askar: *Gravitational Waves and High Energy Sources Originating From Globular Clusters*
17:45 – 18:10	Sambaran Banerjee: *Stellar-mass black holes in young massive and open stellar clusters and their role in gravitational-wave generation*
18:10 – 18:35	Bence Kocsis: *Gravitational wave sources in galactic nuclei*

Monday, September 18

Stellar dynamics and numerical methods

Modeling Massive Cluster Formation with Stellar Feedback using FLASH and AMUSE

Steve McMillan
Drexel University

I describe some applications a hybrid simulation code designed to explore the formation and assembly of massive star clusters. It combines the magnetohydrodynamics code FLASH, handling gas dynamics and star formation, with the AMUSE software environment, which manages the dynamics and evolution of stars and binary systems. The gravitational interaction between the gas and the stars is treated via a symplectic gravity bridge. Radiative, wind, and supernova feedback are followed in FLASH based on information provided by the AMUSE system. The context for our simulations is provided by kiloparsec-scale simulations of a turbulent, supernova-driven, stratified ISM, which set both the initial conditions and the boundary conditions for our (100-pc scale) simulations. I will present results focusing on stellar feedback during the early phases $(1-2)$ Myr of the cluster's lifetime.

A new high-performance particle^3 tree code designed for realistic massive star cluster simulations

Long Wang
RIKEN AICS

As Wang (2016) provided the first million-body simulations of globular clusters (GCs) using Nbody6++GPU, the realistic GC modelling become possible. However, to perform such a simulation requires years of computing time on GPU supercomputers due to the very time-consuming force calculation and complex few-body dynamic algorithms. This limits its application for general GC studies that require many simulations for parameter sampling. To overcome this bottleneck, we are developing a new N-body code based on a high-performance particle-particle particle tree method combined with sophisticated few-body algorithms used in Nbody6(++). With this new code, high-computing-speed $N > 10^6$ simulations including all important dynamical processes involved in collisional dynamical systems can be possible. Thus, it will become a powerful tool for efficient realistic modelling of massive star clusters or more massive systems like Ultra Compact Dwarfs and Nuclear star clusters.

Fitting self-similar core collapse in N-body models

Václav Pavlík
Astronomical Institute of Charles University, Prague

Core collapse is a typical evolutionary stage of star clusters. It is known that in an idealised case, clusters evolve in a self-similar, or homologous, way prior the core collapse, e.g. the density outside the core scales as $\rho \propto r^{(-\alpha)}$. As in N-body models the complete collapse is prevented by the transfer of binding energy of the cluster to binary stars, its time is difficult to identify. Assuming that N-body clusters evolve self-similarly, we developed a method to estimate the time of core collapse. We analysed hundreds of realisations of two models: one single-component and one with Salpeter's IMF. Both have patterns of homologous evolution, although, with different power-law index: the former has $\alpha \approx 2.3$, the latter has $\alpha \approx 1.5$. Further, we realised that the multi-component model went through several homologous collapses with similar properties. Finally, we found a significant correlation between the time of core collapse and the time of formation of the first hard binary.

Leveraging the phase space richness of star clusters: primordial and evolutionary features

Anna Lisa Varri
University of Edinburgh, UK

The study of the structure and dynamics of collisional stellar systems is often pursued under a relatively stringent set of simplifying assumptions, such as isotropy in the velocity space and the absence of ordered motions (e.g. rotation), which limit significantly the opportunity to explore the kinematic richness of star clusters. None the less, recent and forthcoming observational programmes are unveiling an unexpected degree of phase space complexity, which offers a refreshingly new and fertile degree of freedom to enrich our fundamental understanding of the formation and evolution of this class of stellar systems. We will present some new theoretical insight emerging from a more realistic treatment of the three-dimensional velocity space of star clusters, with emphasis on the distinction between signatures resulting from the early formation stage ("primordial features") or from long-term dynamical processes ("evolutionary features").

The E-MOSAICS project: simulating the formation and evolution of galaxies and their globular cluster systems

Marta Reina-Campos
Heidelberg University

We present the E-MOSAICS project (MOdelling Star cluster system Assembly In Cosmological Simulations in the context of EAGLE): a suite of cosmological, hydrodynamical simulations run with the EAGLE model that includes the semi-analytic model MOSAICS for star cluster formation and disruption. This is the first work to self-consistently model the formation and evolution of the entire star cluster population through cosmic history in fully cosmological, hydrodynamical simulations of galaxy formation. The project includes zoom simulations of Milky Way-like analogues, galaxy groups and massive galaxy clusters. We will show how globular cluster and young massive cluster populations form through the same mechanisms and how globular cluster population properties have finally become quantitative tracers of the formation histories of their host galaxy.

Modelling globular clusters with potential escapers

Ian Claydon
University of Surrey

An increasing number of observations of globular clusters have shown a flattening of the velocity dispersion profile and elevated surface density profile in the outer regions. Explanations include the effects of a dark matter halo and modified gravity theories. Alternatively, a population of energetically unbound stars trapped within the Jacobi surface can explain these observables. From exploring the effects of these stars in N-body simulations we can make predictions for effects on the rotation and velocity dispersion anisotropy and by including the contribution of these energetically unbound stars in self-consistent models of GC's we show that their properties are sensitive to the details of the Galactic tides, opening the window to use the potential escapers, as a complementary tool to other methods, to infer the Galactic mass profile. Understanding this behaviour is paramount to correctly understanding the wealth of data that will be available from upcoming Gaia data releases.

The effect of unresolved binary systems on the determination of dynamical masses

Guido Rodrigo Ismael Moyano Loyola
Lund Observatory

The determination of dynamical masses of star clusters relies on having kinematic information of its members and, at the very least, line-of-sight velocity dispersion information for both single stars and binary systems. The presence of unresolved close binary systems contaminate the determination of velocity dispersion leading to an overestimation of the dynamical mass of a given star cluster. In order to quantify this overestimation we have modelled a range of star clusters with different masses and primordial binary systems, for which we calculate the dynamical mass of each of them using observational constrains.

The physical origin of stellar envelopes around globular clusters

Phil Breen
University of Edinburgh

Recent observational evidence suggests that a number of globular clusters in the Local Group may be surrounded by diffuse spherical envelopes of stars, extending out to several hundred parsecs (e.g., see M2, NGC 5694, NGC 1851 in the Milky Way and MGC1 in M31). In isolation, star clusters can naturally develop diffuse envelopes which may be characterised by different structural and kinematic properties depending on whether they are populated by slow diffusion or rapid ejection of cluster stars. In the presence of an external galactic potential, this picture becomes more complicated as the envelopes respond significantly to the effects of the tidal field. We investigate several possible formation and disruption mechanisms of these tenuous envelopes, with emphasis on the role played by the orbital history of the star cluster, the possible presence of a dark matter mini-halo, or modified theories of gravity.

Relaxation and mixing of constants of motion in globular clusters

Yohai Meiron
Eötvös Loránd University

We explore the relaxation and mixing of energies and angular momenta in globular clusters using N-body simulations and the diffusion equation. We show that relaxation time is only a useful concept when considering the cluster as a whole, but when considering particles of particular orbital families, the mixing time gives a better picture on how quickly those particles' constants of motion diffuse. We also show that there is an interesting difference between how energy and angular momentum mix.

On the origin and evolution of the old, yet metal-rich, open cluster NGC 6791

Luis Martinez
Astronomy Institute, UNAM

Due to a unique set of properties, the studies about NGC 6791 are diverse; from orbital analyses, going through a detailed study of its density distribution, and more recently, to a deep analysis of its chemical composition. In this talk I will present a new approach and tools employed to understand how this peculiar cluster was formed and evolved. Since its metallicity suggests it was born in the inner thin disk, we test a possible radial migration scenario for the orbit of NGC 6791. Then, we explore how the different possible Galactic environments the cluster went through determined its evolution. Finally, by using nbody6tt to simulate NGC 6791, we find the properties of the cluster at its formation time, which let us understand how it managed to live so long, being metal-rich, and still very massive.

Dynamical evolution of tidally limited rotating star clusters

Maria Tiongco
Indiana University

Many observational studies are providing a rich and growing amount of information on the internal kinematics of globular clusters. Driven by the opportunity to address a number of open questions on the dynamical evolution of globular clusters with this new information, I have investigated by means of N-body simulations, the evolution of the internal kinematical properties of rotating star clusters evolving in the external tidal field of their host galaxies. I will focus my presentation on the results concerning the evolution of the rotation curve and the velocity anisotropy and show how the evolution of anisotropy and rotation are affected by the cluster internal evolution and the interaction with the external tidal field. I will present a number of results illustrating how the interplay between a cluster's internal evolution and the interaction with the host galaxy can produce a significant complexity in the cluster's morphological and kinematical properties.

Monday, September 18

Dynamics of (exo)planetary systems in star clusters

The evolution of planetary systems in dense star clusters

Simon Portegies Zwart
Leiden Observatory

The evolution of planetary systems in dense star clusters Planetary systems in star clusters are affected by internal dynamical processes and interactions with other stars. Using large scale numerical simulations I will quantize these effects and discuss the consequences.

Stability of Multiplanetary Systems in Star Clusters

Maxwell Xu Cai
Leiden Observatory

More than 3500 exoplanets are discovered, but only $\sim 1\%$ of them are found in star clusters. To understand the roles of star cluster environments in shaping the dynamical evolution of planetary systems, we carry out direct N-body simulations of four planetary systems models in three different star cluster environments. I will report the results of these simulations. For details, see: `https://arxiv.org/abs/1706.03789`

A Smoothed Particle Hydrodynamics approach to young protoplanetary disks around single and binary stars

Luis Diego Pinto
Sapienza, University of Rome

Exoplanetary systems likely rise by condensation of the primordial protoplanetary disks around young stars. During the last 30 years, such processes have been widely investigated by studying the gas evolution around both single and binary stars. Of course, circumstellar disks may be present not only in an isolated environment but also in more or less crowded environment. Open Clusters are good examples of regions rich of young stars likely surrounded by a gaseous disk. Recent numerical investigations have put in evidence the complex mechanism in which a protoplanetary disk in an open cluster can be perturbed (impulsively or secularly) by the other stars. We present here an hydrodynamical code we developed to investigate the evolution of self-gravitating gaseous disks which interact with stars. We present some applications to the evolution of protoplanetary disks around single stars (embedded in open clusters) and some investigations on the gas gravitational feedback to isolated binary star.

Tuesday, September 19

Young star clusters and star forming regions

The spatial distribution of young stars and gas in giant molecular clouds and the implications for cluster formation.

Tom Megeath
University of Toledo

Understanding the emergence of stellar clusters and associations from the complex spatial distributions of young stars found in molecular clouds is a key problem in astrophysics. I will overview our understanding of the formation and early evolution of stellar groups, clusters, and associations, with a focus on the low mass stars that make up the bulk of the stellar mass. Taking a primarily observational perspective, I will initially concentrate on surveys of molecular clouds in the nearest 1 kpc, where young low mass stars and protostars can be detected and studied in detail. Of particular interest is the interplay of turbulence, gravitational collapse, magnetic fields, fragmentation, accretion and feedback from the 10000 AU scales of individual protostars to the parsec scales of clusters. I will also discuss potential differences with more distant and extreme regions and the prospects for extending observational studies to these more distant regions with JWST and ALMA.

Non-thermal states of galactic filaments from the dynamics of two-dimensional self-gravitating systems

Lapo Casetti
Università di Firenze, INFN and INAF-Arcetri, Italy

Observations suggest that filaments in galactic molecular clouds are in a non-thermal state. As a simple model of a filament we study a two-dimensional system of self-gravitating particles by means of numerical simulations of the dynamics. In cold collapses, after the damping of virial oscillations the system settles in a non-thermal steady state whose radial density profile is very similar to the observed ones. Moreover, for sufficiently small initial virial ratio the density and kinetic temperature profiles are anticorrelated, i.e., exhibit temperature inversion, again a feature that has been found in observations. The same happens in the state reached after a strong perturbation of an initially isothermal cylinder. Finally, we discuss our results in the light of recent findings in other contexts (including non-astrophysical ones) and argue that the same kind of non-thermal states may be observed in any physical system with long-range interactions, including condensed matter ones.

Fibers in the NGC1333 proto-cluster

Alvaro Hacar
Leiden Observatory

Whether these gas properties for clustered star formation are similar to those found in isolation remains a matter of strong debate. In a recent paper (Hacar et al. 2017), we carried out a comprehensive and high-sensitivity study of the internal structure, density, temperature, and kinematics of the dense gas content of the NGC 1333 region in Perseus, one of the nearest and best studied embedded proto-clusters. The detailed characterization of the gas kinematics reveals an intricate underlying gas organization both in space and velocity. We identified a total of 14 velocity-coherent, (tran-)sonic structures within NGC 1333, with similar physical and kinematic properties than those quiescent, star-forming (aka fertile) fibers previously reported in low-mass star-forming clouds (see Hacar et al. 2013). These fibers are arranged in a complex spatial network, build-up the observed total column density, and contain the dense cores and protostars in this cloud. Our results suggest that the observational dichotomy between clustered and non-clustered star-forming regions might be naturally explained by the distinct spatial density of fertile fibers in these environments. During my talk I will discuss how these fibers can potentially unify our current description of the star formation process in clusters of increasing complexity and mass.

Stellar clusters in the star formation complexes G173 and G192

Anton Seleznev
Ural Federal University, UrFU

It is well known that stars are forming generally inside star clusters and associations, in a single process with the formation of planetary systems. Then the study of star clusters with different ages gives us the possibility to trace the history of star formation in the Galactic disk during several giga years. An extremely young star clusters are of a special interest, they are observed directly in the process of formation inside gas-dust clouds, many stars, being cluster members, have observable protostellar/protoplanetary disks. An investigation of extremely young clusters provides an opportunity to find out an initial stellar mass function, to understand an order of formation of stars with different masses and the duration of star formation process, to make conclusions about an early dynamical evolution of star clusters and star formation region as a whole. This talk presents results of an investigation of star clusters in star formation regions G173 and G192.

The Evolution of Tight Binaries in Star Forming Regions

Christian Boily
Observatoire astronomique de Strasbourg

Stars form over large $\sim$ pc scale regions of arbitrary geometry along filaments and clumps. I will review recent models and observations that motivate a simplified approach to the dynamics of these regions and in particular the internal dynamics of their sub-structures. I will argue that many of the observed characteristics of the stellar populations observed must be set in the very late stages of the formation epoch. I will offer some prospects for multiple-stars based on results from an on-going project combining dynamics and photometry.

Simulations of young star clusters: the MYSTIX case

Steven Rieder
RIKEN AICS

Initial conditions for star cluster simulations are often based on simplified models, which resemble clusters in an evolved state. We investigate how clusters are affected by their initial conditions, by modelling them after observed clusters from the MYStIX observations. Using an AMUSE star cluster simulation model that include stellar dynamics, stellar evolution and gas dynamics, we investigate for three different cluster configurations how they evolve over a period of 10 Myr. Each cluster configuration is run with a number of different realisations, varying unknown parameters like the relative position and velocity of sub-clusters to study how these affect the evolution of these young star clusters.

Discrete episodes of star formation in the ONC?

Giacomo Beccari
ESO

As part of the Accretion Discs in Halpha with OmegaCAM (ADHOC) survey, we imaged in r, i and H-alpha a region of 12×8 square degrees around the Orion Nebula Cluster. Thanks to the high-quality photometry obtained, we discovered three well-separated pre-main sequences in the colour-magnitude diagram towards the cluster's center. Although several reasons could be invoked to explain these sequences including unresolved binaries, independent high-resolution spectroscopy supports the interpretation that these correspond to discrete episodes of star formation, each separated by about a million years. Our observations reveal that these star-forming events occurred in the densest central regions of the cloud. The stars from the two youngest populations rotate faster than the older ones, in agreement with the evolution of stellar rotations observed in pre-main sequence stars younger than 4 Myr in several star forming regions. If confirmed these results prompt for a revised look at the formation mode and early evolution of stars in clusters.

Cluster formation in Orion: the Slingshot mechanism

Amelia Stutz
Universidad de Concepcion

The Integral Shaped Filament (ISF) is home to the nearest significant protocluster, the Orion Nebula Cluster. Recently we proposed the "Slingshot" mechanism, requiring that the ISF oscillate. In this work we investigate the "Slingshot" effect on the ONC structure. We show that the stellar density follows a Plummer profile with inner softening scale $a =$ 0.36 pc, while the gas follows a cylindrical power law. The stellar contribution to the gravitational field is nearly equal to that of the gas at $r = a$. At all other radii the field is gas-dominated. The cluster crossing time is ≈ 0.5 Myr, nearly identical to the filament oscillation timescale. These results reveal an intimate connection between the stars and the gas, such that tidal effects due to filament oscillations may set the protocluster structure. We suggest that clusters that form in oscillating filaments are ultimately ejected, thereby ending their formation phase.

Young massive star clusters in the era of integral field spectroscopy

Peter Zeidler
Space Telescope Science Institute (STScI)

With an age of 1 – 2 Myr at a distance of 4 kpc and a total stellar mass of 37000 solar masses, Westerlund 2 (Wd2) is the second most massive young massive star cluster (YMC) in the Milky Way. The numerous OB stars and the surrounding HII region make Wd2 a perfect testbed to study the interactions of YMCs with their parental molecular gas cloud. We are mapping Wd2 with the integral field spectrograph MUSE for a complete spectrophotometric survey of the cluster region. In combination with our deep multiband Hubble Space Telescope (HST) photometric catalog we are able to extract stellar spectra down to 1 solar mass using the software package "Pampelmuse". A precise wavelength calibration using OH skylines to accurately measure stellar radial velocities, in combination with multi-epoch HST data to measure proper motions, provides us with the necessary information on the internal stellar velocity dispersion to study, for the first time, the 3D kinematics and evolution of a YMC.

The Structure of Young Massive Clusters via Hierarchical Star Formation

Michael Grudić
Caltech

Young massive clusters (YMCs) of widely varying mass, size, and environment have been observed to have a similar outer surface brightness profile: a power law with a ”shallow” slope between -2 and -3. We show that the surface brightness profiles of star clusters formed in multi-physics MHD star formation simulations including stellar feedback are in agreement with observations. This validates a novel approach to simulating star cluster formation without resolving individual stars. We show that these shallow outer power-law profiles are the natural consequence of phase-space mixing in the hierarchical merging of sub-clusters that eventually form a bound star cluster. This gives physical motivation to the observational fitting function, and has implications for the initial structure of young globular clusters at high redshift.

On Cataclysmic Variables in Globular Clusters

Diogo Belloni
Nicolaus Copernicus Astronomical Center

Cataclysmic variables (CVs) are interacting binaries composed of a white dwarf undergoing stable mass transfer from (usually) a low-mass main sequence star and they are expected to exist in non-negligible numbers in globular clusters (GCs) that are natural laboratories for testing theories of stellar dynamics and evolution. I will present the main aspects related to our understanding regarding GC CV populations based on the analysis of MOCCA (Hypki & Giersz 2013) numerical simulations performed by Belloni et al. (2016, 2017a, 2017b) and Hong et al. (2017). Emphasis will be given to the main differences in present-day CV properties with respect to CV evolution models; common envelope phase parameters; influence of nova eruptions on CV evolution and of dynamics on CV formation; initial cluster conditions; and initial binary populations; and how all these factors influence CV ages, duty cycles and detectability.

Tuesday, September 19

New observational frontiers

Gravitational Wave Detection of Compact Binaries

Matthew Benacquista
University of Texas Rio Grande Valley

In light of the recent detections of binary black hole coalescences with LIGO, I will review the detection process for these binaries and the methods of determining their properties. I will also discuss the prospects for future detections at lower frequencies with LISA.

New observational frontiers - Gaia, and others

Gerry Gilmore
Institute of Astronomy, Cambridge

Gaia is here! This changes the observational everything by orders of magnitude. I will give an update. But for precision studies of specific systems, such as clusters, one needs precise complementary data, especially radial velocities and abundances to isolate relevant samples in phase space. These data are being obtained from many projects. I will show examples from one, the Gaia-ESO Survey.

The Lynx X-ray Mission

David Pooley
Trinity University

Lynx is a strategic X-ray mission concept with large collecting area, sub-arcsecond angular resolution over a large field of view, and high spectral resolution. It is one of four mission concept studies initiated by NASA for the 2020 Decadal Survey. In addition to enabling frontier science from the first accretion light in the Universe to finding the missing baryons to galaxy formation and evolution, it will also be the only large mission after Chandra that will have the spatial resolution necessary to study X-ray sources in globular clusters. I will discuss the proposed mission capabilities and the next steps going forward into the Decadal Survey, which will require broad community support and input.

Wednesday, September 20

Stellar populations in star clusters

Multiple stellar populations in globular clusters - Observational constraints and theoretical challenges

Corinne Charbonnel
Dept of Astronomy, University of Geneva (CH) and CNRS (F)

In this talk I will review the characteristics of the multiple stellar populations observed in globular clusters, and discuss the various scenarios that have been developed to explain their origin. I will focus on the (many) current theoretical issues and open questions.

Dynamical origin of multiple populations in star clusters in the Magellanic Cloulds

Jongsuk Hong
KIAA-PKU

Numerical simulations were carried out to study the origin of multiple stellar populations in the intermediate-age clusters NGC 411 and NGC 1806 in the Magellanic Clouds. We performed NBODY6++ simulations based on two different formation scenarios, an ad hoc formation model where second-generation (SG) stars are formed inside a cluster of first-generation (FG) stars using the gas accumulated from the external intergalactic medium and a minor merger model of unequal mass ($M_{\rm SG}/M_{\rm FG} = 0.05$–$0.10$) clusters with an age difference of a few hundred million years. In this talk, I will present the comparison between our simulation results and the observations and will provide some observable properties for the future observations for a better illustration of the origin of the multiple populations in the Magellanic Cloud clusters.

Stellar populations and star formation histories in the nuclei of nearby galaxies

Nikolay Kacharov
Max Planck Institute for Astronomy - Heidelberg

The majority of galaxies harbour massive star clusters at their centres. These nuclear clusters are the densest stellar aggregates in the Universe but their origin and evolution are not well established to date. Being morphologically similar to the most massive globular clusters, they have multiple, distinct stellar populations covering a large range of age and metallicity. This is indicative of a merger history or prolonged star formation, sometimes continuing to the present day. In this talk I will present recent results on the star formation histories of the nuclei of 6 nearby galaxies (< 7 Mpc) based on X-Shooter unresolved spectroscopy and comprehensive composite population models.

Connecting globular and nuclear star clusters through the enigmatic M54

Mayte Alfaro Cuello
Max-Planck-Institut für Astronomie

M54 is the second most massive globular cluster (GC) in the Milky Way, sitting at the photocenter of the Sagittarius dwarf galaxy, it is one of the nearest nuclear star clusters (NSCs). M54 shows a large spread in metallicity and age, as an evidence of its complex star formation history. These facts and its proximity ($D = 27.4$ kpc) make M54 an ideal laboratory for studying the still unknown connection between massive GCs and NSCs. We present a large MUSE data set ($\approx 3.25' \times 3.25'$) covering ≈ 2.5 Reff of M54. We have extracted kinematic information and metallicity estimates for ≈ 7000 individual member stars, being able to disentangle the existence of at least two stellar populations, one old and metal poor and other young and more metal rich, with clear kinematic differences. Through these dynamical properties and chemical enrichment information we will be able to constrain the star formation history of M54. This may pave the way to uncover the origin of the most massive GCs in the Milky Way.

Stellar populations in extreme star burst clusters and UCDs

Tereza Jerabkova
HISKP, University of Bonn

The stellar initial mas function (IMF) has been described as being invariant, bottom heavy or top-heavy in extremely dense star burst conditions. To provide usable observable diagnostic we calculate redshift dependent spectral energy distributions of stellar populations in extreme star burst clusters which are likely to have been the precursors of present day massive globular clusters (GCs) and of ultra compact dwarf galaxies (UCDs). Their redshift dependent photometric properties are calculated as predictions for the James Webb Space Telescope (JWST) observations. While the present day GCs and UCDs are largely degenerate concerning bottom-heavy or top-heavy IMFs, a metallicity- and density-dependent top-heavy IMF implies the most massive UCDs to appear as objects with quasar-like luminosities with a variability on a monthly time scale. Implications of the physical environment in these extreme star burst objects for the emergence of multiple stellar populations will also be discussed.

The initial and present-day mass function of Galactic globular clusters

Antonio Sollima
INAF Osservatorio Astronomico di Bologna

I present the results of a survey aimed at deriving the global mass functions of a sample of 35 Galactic globular clusters. By comparing deep Hubble Space Telescope photometry with suitable multi-mass dynamical models we were also able to determine dynamical parameters, mass-to-light ratios and the mass fraction of dark remnants. The shape of the derived global mass functions as well as their correlations with dynamical and general parameters is analysed and interpreted in terms of the dynamical evolution of these stellar systems. I will also discuss the implications of the obtained correlations on the shape and universality of the Initial Mass Function.

The mass-to-light ratio-metallicity relation of globular clusters in M31

Hossein Haghi
Institute for Advanced Studies in Basic Sciences (IASBS)

The structural properties, kinematical properties and the M/L ratios of 163 GCs in the M31 galaxy in the near infrared (K-band) and optical (V-band) are derived by Strader et al. ($2009 - 2011$). Their sample of GCs exhibits M/L ratios which are considerably lower than what is predicted from SSP models of GCs with a canonical IMF. In addition, one expects that the M/L ratios of SSP models show a positive correlation with metallicity. In this talk, I will address this discrepancy and will propose solutions which are mainly based on the depletion of low-mass stars either due to dynamical evolution, a metallicity- and density-dependent top-heavy IMF, and the relation between the age and the metallicity of the GCs.

Are globular clusters in the Fornax Cluster different from those in the Virgo Cluster?

Joerg Dabringhausen
Astronomical Institute, Charles University

The Fornax Cluster and the Virgo Cluster are two nearby galaxy clusters in which thousands of globular clusters (GCs) have been observed with the Hubble Space Telescope. Using the Chandra Point Source Catalog, I have matched this optical data on GCs with X-ray point sources. X-ray point sources that can be matched with a GC are interpreted as binary stars in which one component is a neutron star that accretes matter from its companion. This makes the frequency of X-ray point sources a valuable indicator for the properties of the stellar populations of the host GCs. First results do indeed show a noticable difference between the GCs in the Fornax Cluster and the Virgo Cluster: Luminous GCs in the Fornax Cluster appear to be rather poor in X-ray sources in comparison to similar GCs in the Virgo Cluster. One possible interpretation of that finding is that the stellar initial mass function in luminous GCs in the Fornax Cluster is different from that of comparable GCs in the Virgo Cluster, but further research is needed to clarify this question.

Thursday, September 21

Galactic centre / nuclear star clusters

Observations of the Milky Nuclear Star Cluster

Tuan Do
UCLA

Due to its proximity, the Milky Way nuclear star cluster provides us with a wealth of data not available in other galactic nuclei. In particular, we can observe the properties of individual stars. These properties include the position in two dimension and the velocity in three dimensions. With the rapid advances integral field and multi-object spectroscopy, we can also derive the physical properties of individual stars, such as the effective temperature, abundances, and surface gravity. I will discuss how the pass decade of adaptive optics measurements from HST, Keck, and Gemini have been used to derive physical properties of the cluster and constraints on its origins. While these analyses have been very successful at helping us understand its structure and star formation, there is still enormous untapped potential in these data sets. I will discuss new work on the physical properties of the stars, such as their metallicity, and how they will help us understand the origin and evolution.

The Dust-Enshrouded "G" Sources Orbiting the Galactic Black Hole: Fluffy Stellar Merger Products

Mark Morris
University of California, Los Angeles

The recently recognized objects G1 and G2 are self-luminous objects with cold dust photospheres. They follow eccentric orbits around the supermassive black hole at the Galactic centre, and come close enough at periapse to suffer tidal removal of some of their extended material. Given that both G1 and G2 have survived their periapse passages, it is now evident that they are stellar objects rather than compact dust clouds. We argue that these objects are the result of relatively recent stellar mergers of binary pairs whose internal orbits underwent rapid evolution toward extremely high eccentricities in response to the gravitational influence of a third body, the Galactic black hole. The evolution was mediated by the eccentric Kozai-Lidov effect, which is manifested in the octupole approximation. The mergers should equilibrate to normal single stars on a Kelvin-Helmholtz time scale, but such induced mergers should be sufficiently commonplace that other G-type sources are likely present.

A compact source scenario for the Galactic Center cloud G2

Alessandro Ballone
INAF-OAPd

Since its discovery in 2012, the gas and dust cloud G2, orbiting Sgr A* on a very eccentric orbit, has caught the attention of the astronomical community. G2 has passed pericenter in early 2014, but there is still a large debate on the nature and origin of this object. I will focus on a "compact source" model, where G2 is the outflow from a mass-losing star. 3D adaptive mesh refinement hydrosimulations with the grid code PLUTO allowed me to perform a more detailed and realistic comparison to the observed position velocity diagrams: a slow (50 km/s) outflow can reproduce G2, while a faster one might be able to simultaneously reproduce G2 and its following tail G2t. I will finally show that the outflow parameter needed to match the observations are roughly those of a T Tauri star and that in few years the central source should decouple from the previously ejected material, this being the smoking gun evidence for such a scenario.

The build up of nuclear star clusters: simulations and observations

Alessandra Mastrobuono Battisti
Max Planck Institute for Astronomy

Nuclear star clusters (NSCs) are dense stellar systems known to exist in galactic nuclei. Although their evolution is connected to that of the host galaxy, their origin is still unknown. Here we explore one of the possible formation channels in which globular clusters inspiral to the center of the galaxy, disrupt and build up the NSC. We use several N-body simulations and models constrained by observations from the Milky Way (MW) to follow the formation and evolution of NSCs. We find that the simulated system can show properties that make it comparable with the MW NSC, including significant rotation, a fact that has been so far attributed to gas infall and in situ star formation. We explore the kinematic evolution of the simulated NSC to illustrate how the merger history can imprint fossil records on its dynamical structure. We conclude that the cluster inspiral is a viable mechanism for the formation of NSCs and we provide fundamental tools to understand their assembly history.

Nuclear Star Clusters and Super Massive Black Holes as Compact Massive Objects

Roberto Capuzzo Dolcetta
Dep. of Physics, Sapienza, Univ. of Roma, Italy

Basing also on an enlarged data collection of NSC and SMBH data related to host galaxies properties, I present some discussion useful to enlighten about the origin of such Compact Massive Objects in galactic centers.

XSHOOTER Survey of the Nearest Nuclear Star Clusters

Arianna Picotti
MPIA

To unveil the formation and evolutionary pathways of nuclear star clusters it is essential to understand the dynamical properties of both stars and gas at the centre of different galactic environments. I will present stellar kinematics and the gas content of our XSHOOTER Survey of the Nearest Nuclear Star Clusters. The survey sample consists of 19 nearby (< 10 Mpc) nuclear star clusters embedded in a diverse range of galaxy hosts masses and morphological types along the Hubble sequence. Our dataset allows us to retrieve near-infrared based stellar kinematic profiles, as well as to estimate the molecular and ionized hydrogen content and to reveal possible signatures of AGN activity in the nucleus of each galaxy. Additionally, the survey is ideal for measuring dynamical masses of nuclear star clusters and identifying candidates for gas-dynamical black hole mass determinations.

Response of a Nuclear Star Cluster to the Slow Accumulation of Gas

Karamveer Kaur
Raman Research Institute, Bangalore

The young stars at the Galactic Centre form a compact cluster, and were probably born in situ in a massive accretion disc around the supermassive black hole. So there must have been substantial accumulation of gas in the central parsecs before their birth. We are interested in the secular response of the cusp of old stars to a slowly growing gaseous disc. We present a simple model in which a spherical cluster of old stars, with anisotropic velocity dispersions, deforms adiabatically to an axisymmetric configuration. A simple formula for the perturbed phase space distribution function is derived using linear theory, using which we compute the spheroidal distortion of the density profile. Linear theory accounts only for stellar orbits whose apses circulate. The non-linear theory of adiabatic capture into resonance is used to understand orbits whose apses librate. The process is likely generic in galactic nuclei, and the dynamical stability of the deformed cluster is of interest.

Nucleated dwarf galaxies in the central region of the Fornax Galaxy Cluster: Nuclear cluster analysis

Yasna Ordenes Briceño
Heidelberg University and Catholica University of Chile

We present the analysis of 66 dwarf nucleated galaxies (dEN) in the central region ($R <$ 350 kpc) of the Fornax Galaxy Cluster. The sample dEN were identified as part of the Next Generation Fornax Survey (NGFS) using deep u, g and i-band images obtained with the 4-meter Blanco telescope at CTIO. The dEN sample covers a previously unexplored luminosity range which reaches more than five magnitudes deeper than the ACS Fornax Cluster Survey (ACSFCS). We have analyzed the dEN inner regions, after subtracting the surface brightness profile of the spheroids, using various light-profile types fitting to study the nuclei to obtain their total magnitudes and structural parameters. We have found complex nuclei in our sample ($\approx 20\%$) with cuspy centres, double nuclei, and nearby satellite globular clusters. The rest of nuclei seems to be relatively isolated nuclei with simple surface brightness profile. This is a benchmark dataset for testing theoretical predictions of nucleus formation scenarios.

Circumnuclear disks and rings of gas as probes of supermassive black hole presence

Alessandro Alberto Trani
SISSA

An increasing number of observations are finding circumnuclear gas in nearby galactic nuclei (GNs), where the dynamics can be dominated by a supermassive black hole (SMBH). I explore the link between the properties of circumnuclear gas and the properties of GNs, specifically the mass of the SMBH and the nuclear star cluster. I present the first systematic study of the formation of circumnuclear rings/disks in GNs by means of smoothed particle hydrodynamics simulations. Not only the kinematics, but also the morphology of circumnuclear gas shows distinct features of the presence of SMBHs, displaying a disk structure in SMBH dominated GNs and ring-like structures in nuclear-star-cluster dominated GNs. I discuss the implication of this result for the measurement of SMBH mass in nearby GNs. I also show that stars formed from circumnuclear gas can decouple from the gas and have a different dynamical evolution. This has strong implications for the formation of stellar disks around SMBHs.

The adventures of a stellar cusp in the Galactic Center

Eugene Vasiliev
Oxford University

I present evolutionary models of the Milky Way nuclear star cluster based on a novel Fokker–Planck method in action space. I demonstrate that a Bahcall-Wolf cusp forms in much less than a Hubble time under realistic assumptions about the mass spectrum, and the subsequent evolution proceeds nearly self-similarly. These models, especially including a moderate amount of continuous star formation, agree well with the recently detected weak cusp in the surface brightness profile.

Direct N-body simulation of the Galactic Centre

Taras Panamarev
ARI/ZAH Heidelberg

We study the dynamics and evolution of nuclear star cluster of the Milky Way galaxy performing direct million-Body simulations. We focus on interaction of the stellar system with the supermassive black hole. We obtain stellar density profiles for different stellar species, rate of tidal disruption events and detection of gravitational waves emitted by accretion of compact objects onto the central black hole. We discuss possible presence of millisecond pulsars in the galactic centre.

An upper limit on the mass of a central black hole in the large magellanic cloud

Nora Luetzgendorf
ESA/STScI

We constrain the possible presence of a central black hole (BH) in the center of the Large Magellanic Cloud (LMC). This requires spectroscopic measurements over an area of order a square degree, due to the poorly known position of the kinematic center. Such measurements are now possible with the impressive field of view of the Multi Unit Spectroscopic Explorer (MUSE) on the ESO Very Large Telescope. We used the Calcium Triplet (850 nm) spectral lines in many short-exposure MUSE pointings to create a two-dimensional integrated-light line-of-sight velocity map from the 10^8 individual spectra, taking care to identify and remove Galactic foreground populations. The data reveal a clear velocity gradient at an unprecedented spatial resolution of 1 arcmin^2. We fit kinematic models to arrive at a 3sigma upper-mass-limit of $\approx 10^7 M_\odot$ for any central BH - consistent with the known scaling relations for supermassive black holes and their host systems.

Thursday, September 21

Blue stragglers / stellar collisions and their products

Stellar collisions and their products

Melvyn Davies
Lund University

In this invited talk I review the possible outcomes of stellar collisions within the crowded cores of stellar clusters. Collisions have a number of consequences: they can alter the distribution of stellar masses, for example producing more massive main-sequence stars through the merger of two lower-mass stars. Collisions involving compact objects and red giants will produce a zoo of exotic objects including those which will spiral in to contact via the emission of gravitational waves.

Pop III star clusters: The crucial interplay between accretion and collisions

Michael Fellhauer
Departamento de Astronomia, Universidad de Concepcion, Chile

The formation of the very first stars still holds a lot of mysteries. Modern metal-free hydrodynamical simulations show that we do not expect monolithic collapses of thousands of solar masses into single objects but that we rather have fragmentation into smaller stars. Our new models show that with the interplay of accretion and collisions in those star clusters, we still are able to form massive objects.

The "UV-route" to Search for Blue Straggler Stars in Globular Clusters: First Results from the HST UV Legacy Survey

Silvia Raso
University of Bologna

In this talk I present a detailed study of the Blue Straggler Star (BSS) population in four intermediate/high density systems (NGC 2808, M15, NGC 6541 and NGC 6388) based on data acquired within the HST UV Legacy Survey of Galactic Globular Clusters. The data were analysed by using a "UV-guided" approach, where the master list of detected stars is obtained from the UV exposures, and the PSF-fitting of each star is then forced to the images acquired in the other filters. This approach optimizes the detection of hot stars, allowing to obtain complete samples of BSSs even in the central regions of high density clusters. I show the advantages of this method by comparing our selections with those obtained in previous works based on an "optical-guided" approach. Finally, I discuss the dynamical evolution stage reached by the four target clusters, as determined from the observed BSS radial distributions and the A+ parameter defined in Alessandrini et al. (2016) and Lanzoni et al. (2016).

UV bright population in Globular Cluster NGC 288 - insights from UVIT

Snehalata Sahu
Indian Institute of Astrophysics, Bengaluru

We present the early results of moderately deep Ultraviolet Imaging Telescope (UVIT) observations of NGC 288 in 3 UV filters. We have performed crowded-field photometry on the UVIT images and created the Color-Magnitude Diagrams (CMDs). We have fitted the CMDs with the isochrones generated for UVIT filters using the Flexible Stellar Population Synthesis (FSPS) model and identified different evolutionary sequences. Taking the advantage of large FOV of UVIT as compared to HST, we detect the full Horizontal Branch (HB) and Blue Straggler stars (BSS) in near-UV covering the entire cluster. We also detect 3 probable Extreme-HB candidates in the cluster. We have compared our UVIT CMDs with HST-ACS and ground observations. We found that in the NUV CMD, all the sequences may not be fitted with one isochrone. We plan to model the UV CMD and estimate parameters using synthetic CMDs. The UVIT image of NGC 288, put together from our observations, can be seen in the website http://uvit.iiap.res.in.

Friday, September 22

Compact objects in star clusters

Compact objects in star clusters

Mirek Giersz
Nicolaus Copernicus Astronomical Centre, Polish Academy of Sciences

In the first part of my talk, I will give a very brief and biased, by my scientific interests, summary about the observations of compact objects present in globular clusters. Namely, white dwarfs, neutron stars, black holes, intermediate mass black holes and all kinds of binaries harbouring those objects. From the theoretical point of view I will shortly discuss the possible influence of such objects on overall globular cluster evolution and observational imprints which they may leave. In the second part of my talk, I will discuss what kind of constraints on the presence of compact objects in globular clusters can be imposed from the analysis of the MOCCA Survey Database of globular clusters models. I will very briefly refer to the works done with my collaborators on cataclysmic variables, formation of intermediate mass black holes, formation of black hole subsystems, rates of black hole - black hole mergers, properties of black hole - main sequence binaries which escaped from globular clusters and rates of tidal disruption events with intermediate mass black holes.

Binary Black Hole Mergers from Dense Star Clusters

Carl Rodriguez
MIT

The recent detections of gravitational waves from merging binary black holes have the potential to revolutionize our understanding of compact object astrophysics. But to fully utilize this new window into the universe, we must compare these observations to detailed models of binary black hole formation throughout cosmic time. In this talk, I will review our current understanding of cluster dynamics, describing how binary black holes can be formed through gravitational interactions in dense stellar environments such as globular clusters. I will review the properties and merger rates of binary black holes from the dynamical formation channel. Finally, I will describe how the initial configuration of a binary black hole is determined by its formation history, and how we can use this to discriminate between dynamically-formed binaries and those formed from isolated evolution in galactic fields.

A black hole love story

Anna Sippel
MPIA

By use of a direct N-body model of a globular cluster, I will illustrate the path two single stellar mass black holes take to end up in a binary system that can ultimately merge generating gravitational waves. Many few-body encounters are necessary and not only facilitate to form our black hole binary, but also create havoc in the cluster core.

Kinematical signatures of intermediate-mass black holes in globular clusters

Alice Zocchi
University of Bologna

Finding an intermediate-mass black hole (IMBH) in a globular cluster, or proving its absence, is a crucial ingredient in our understanding of galaxy formation and evolution. The challenge is to find a unique signature of an IMBH that cannot be accounted for by other processes. Observational claims of IMBH detection are often based on analyses of the kinematics of stars, such as a rise in the velocity dispersion profile towards the cluster centre, but this signature is degenerate with other scenarios. Here we analyse the case of ω Cen by comparing the observed profiles to those calculated from models that account for the presence of radial anisotropy and of multiple mass components segregated in the system. We can partially explain the shape of the projected velocity dispersion profile, even if models that do not include an IMBH do not exhibit a cusp in the centre. Our analysis cannot rule out the presence of an IMBH, but puts some caution on the amount of mass that it could have.

The dynamical M/L of globular clusters

Paolo Bianchini
McMaster University

The mass-to-light ratio (M/L) of globular clusters is a fundamental tool to link their luminosity to their dynamical mass, unveil their total gravitational potential and their current stellar population. Using a set of Monte Carlo cluster simulations we investigate the role of 2-body relaxation in shaping the M/L. Our study shows that M/L profiles are not constant and dynamically younger clusters display a central peak up to $\approx 20\ M/L_{\odot}$ due to the retention of dark remnants, suggesting a novel strategy to understand the degeneracy with the presence of intermediate-mass black holes. Moreover, we show that the dependence of the M/L on the dynamical state of a cluster is primarily driven by the dynamical ejection of dark remnants, offering the possibility to constrain the number of dark remnants based on accurate measurements of the M/L. Finally, we illustrate the relevance of our work for dynamical studies of other dense stellar systems, like Nuclear Star Clusters and Ultra Compact Dwarfs.

Millisecond pulsars and the gamma-ray excess in the Galactic Center

Giacomo Fragione
Hebrew University of Jerusalem Israel

The Fermi Large Area Telescope has provided the most detailed view of the emission toward the Galactic Center (GC) in high-energy gamma-rays. Besides interstellar emission and point-source contributions, data suggest the presence of a residual gamma-ray excess. The striking similarity of its spatial distribution with standard dark matter profiles have made people claim this may be evidence for dark matter particle annihilations. However, the signal is also compatible with emission from millisecond pulsars (MSPs) formed in dense globular clusters and left in the GC as a consequence of cluster tidal disruption and evaporation. By taking into account the fate of star clusters across the Milky Way's history and the spin-down rate due to magnetic-dipole breaking, the population of residual MSPs can be modeled. The final gamma-ray amplitude and spatial distribution are in agreement with Fermi observations and provide an astrophysical proof of the GC excess.

Evolution of intermediate-mass and stellar binary black holes in galactic nuclei

Manuel Arca Sedda
Astronomisches Rechen-Institut - Zentrum fur Astronomie der Universitat Heidelberg

A large fraction of the observed galaxies host in their centre a supermassive black hole (SMBH), often surrounded by a dense nuclear cluster (NC). The processes that drive NC formation likely involve strong interactions between massive star clusters (GCs) and the super-massive black hole. Using N-body simulations, we modelled the evolution of stellar BH binaries (BHBs) and intermediate-mass black holes (IMBHs) hosted in the infalling GCs. We show that: i) the SMBH tidal field can induce a significant increase of the BHB eccentricity, favouring the BHB coalescence; ii) if a triple system composed of 2 IMBH and an SMBH form, there is a 30% probability that one of the IMBH undergoes a merging with the SMBH within 1 Gyr. We discuss the outcomes of our models in the framework of our current knowledge of the MW centre and the implications for current and future gravitational waves detections.

Super-massive black holes in ultra-compact dwarf galaxies

Steffen Mieske
ESO

I propose to give an update on the ongoing search for super-massive black holes in ultra-compact dwarf galaxies (UCDs). Recently it was shown that the globally elevated dynamical mass-to-light ratios of UCDs could plausibly be explained by SMBHs having $5-15\%$ of the UCD stellar mass (Mieske et al. 2013). Finding SMBHs in UCDs would thus provide a very direct support for the hypothesis that those UCDs are the tidally stripped remnants of originally much more massive galaxies, and that UCDs as a class may harbour a previously unaccounted for population of SMBHs. In my presentation I will highlight the observational challenges in detecting the kinematical signal of a central black hole in a UCD and discuss alternative explanations for such a signal (e.g. stellar-mass remnants) and how the dynamical modelling constraints those alternatives. Finally, I will discuss the cosmological relevance of the frequency of UCDs as signposts of tidal disruption of low-mass dark matter halos.

Friday, September 22

Astrophysical sources of gravitational waves

GW170104 and the origin of heavy, low-spin binary black holes via classical isolated binary evolution

Krzysztof Belczynski
Copernicus Center, Poland

The Advanced LIGO has observed four BH-BH mergers thus far. The effective spin of GW170104 has an 82 percent probability of being negative, which would indicate spin-orbit misalignment. It has been suggested that LIGO's detections favour a population of binaries with frequent and significant spin-orbit misalignment, hence supporting dynamical formation over classical isolated binary evolution. However, it is also well known that massive stars can have efficient transport of angular momentum within the star and have strong winds that carry away substantial angular momentum. The progenitors of the heaviest stellar-mass BHs ($M > 30M_\odot$) are expected to efficiently reduce their angular momentum, producing BHs with low spin (consistent with existing LIGO constraints). A stellar evolution model that incorporates rotation is used to determine the natal spins of the BHs produced by core collapse. These natal spins are incorporated into our population synthesis code which follows the evolution of Population I/II stars across cosmic time and predicts the BH-BH population in the universe. Our classical isolated binary evolution model produces a BH-BH population that is consistent with the observed LIGO population. In particular, it produces systems that are consistent with the measured properties of GW170104; total mass, mass ratio, effective spin and the overall BH-BH merger rate. Neither strong natal BH kicks nor dynamical interactions are required to recover GW170104. LIGO's observations do not provide evidence for dynamical formation over classical isolated binary formation and it is not yet possible to establish the evolutionary channel through which GW170104 was formed.

Dynamically Formed Black Hole Binaries as Gravitational Wave Sources

Yeong-Bok Bae
Korea Astronomy and Space Science Institute

Gravitational waves (GWs) from binary black holes (BBHs) had been detected by advanced LIGO. The estimated BH masses of GW150914 are about 30 $M_{\odot}$, rather than 10 $M_{\odot}$ which has been considered as a typical mass of BHs. In this talk, we will pay our attention to effects of a BH mass function on dynamically formed BBHs in globular cluster. We have performed direct N-body simulations assuming BH populations with (a) two mass components and (b) continuous BH mass function generated from a low metallicity environment. The hardness distribution of ejected BBH depends on the central velocity dispersion of the cluster, and the mass ratios between two BHs are close to 1. The formation efficiency of BBH is larger for higher-mass BHs, which means that an observed BH mass function inferred from GW detections can be biased toward heavier BH population. If time allows, we will also show our latest results on dynamical capture of BHs driven by gravitational radiation with relativistic simulations.

Evolution of massive black hole binaries in rotating stellar nuclei and its implications for gravitational wave detections

Alexander Rasskazov
Eötvös Loránd University

The subject of our study is a binary supermassive black hole (BSBH) in the center of a galactic nucleus. We model the evolution of its orbit due to interactions with the stars of the galaxy by means of 3-body scattering experiments. Our model includes a new degree of freedom - the orientation of the BSBH's orbital plane - which is allowed to change due to interaction with the stars in a rotating nucleus. The binary's eccentricity also evolves in an orientation-dependent manner. We find that the dynamics are qualitatively different compared with non-rotating nuclei: 1) The BSBH's orbital plane evolves toward alignment with the plane of rotation of the nucleus; 2) The BSBH's eccentricity decreases for aligned BSBHs and increases for counter-aligned ones. We then apply our model to calculate the effects of stellar environment on the gravitational wave background spectrum produced by BSBHs. Using the results of recent N-body/Monte-Carlo simulations we account for different rates of stellar interaction in spherical, axisymmetric and triaxial galaxies. We also consider the possibility that SBH masses are systematically lower than usually assumed. The net result of the new physical mechanisms included here is a spectrum for the stochastic gravitational wave background that has a significantly lower amplitude than in previous treatments, which could explain the discrepancy that currently exists between the models and the upper limits set by pulsar timing array observations.

Extragalactic Globular Star Clusters as Sources of Gravitational Wave Events

Rainer Spurzem
National Astronomical Observatories, CAS, Beijing, China

The first realistic full direct N-body simulation of a globular cluster simulation with a million stars and including all required astrophysical effects (the DRAGON simulation, obtained by a Chinese-European collaboration on massively parallel GPU accelerated supercomputers) will be shown. The results on distributions of luminous and non-luminous objects (e.g. black holes and neutron stars, and binaries with them) over up to 12 Gyr evolutionary time will be shown. I will focus then on the single and binary black holes of stellar origin, which are naturally present in our simulations. We record some events of binary black hole mergers (by using high-order Post-Newtonian dynamics when necessary), which are very similar to those who generated recently the gravitational wave source GW150914 in LIGO. We plot the LIGO detections and our fictitious detections in the supercomputer together in one plot, compare them, and deduce some information about the sources (distances, ages). Also we show synthetic gravitational wave signals (waveforms) from our objects in different wavebands, not only LIGO; so we can e.g. predict how our computed sources would show up in new Chinese or European space based GW instruments.

Star Cluster Disruption by a Supermassive Black Hole Binary

Elisa Bortolas
University of Padova / INAF-OAPd

Massive black hole binaries (BHBs) are expected to be one of the most powerful sources of low-frequency gravitational waves (GWs). BHBs are believed to form in the late stages of galaxy mergers, then harden by close encounters with interacting stars until GWs lead the BHBs to coalescence. It has been argued that BHBs may stall at $\approx$ 1pc scale and never enter the GW stage if stars are not continually fed to the binary loss cone. In this talk, I will discuss the possibility that the loss cone is refilled by the infall of a star cluster (SC) onto a pc-scale binary. I will present the results of N-body simulations exploring different orbits for the SC infall. I will show that SCs reaching the BHB on non-zero angular momentum orbits (with eccentricity ≈ 0.7) fail to enhance the binary hardening, while SCs approaching the BHB on radial orbits considerably contribute to its shrinking and may shorten the BHB path towards GWs.

Gravitational Waves and High Energy Sources Originating From Globular Clusters

Abbas Askar
Nicolaus Copernicus Astronomical Center, Polish Academy of Sciences

Dynamical interactions in extremely dense stellar systems like globular clusters can lead to the formation of exotic binary systems that can be potential sources of gravitational waves or high energy electromagnetic radiation. The detection of gravitational waves from at least three coalescing binary black holes by the LIGO detectors has sparked the debate about whether such binary systems may have formed in dense stellar clusters. X-ray observations of globular clusters also show that they harbour many accreting binary systems. In this talk, I will present results from a survey of thousands of star cluster models that were simulated using the MOCCA (MOnte Carlo Cluster simulAtor) code that follows the long term evolution of star clusters. The results will focus on the formation channel and properties of gravitational wave sources like binary black holes and X-ray sources like accreting compact objects that originate from globular clusters.

Stellar-mass black holes in young massive and open stellar clusters and their role in gravitational-wave generation

Sambaran Banerjee
University of Bonn

The study of stellar-mass black holes (BH) in dense stellar clusters is under the spotlight, in the era of the LIGO's detections. This study presents a set of evolutionary models of compact open- or young massive-type stellar clusters of varying metallicity. Including the state-of-the-art schemes for stellar wind and remnant formation, such model clusters are evolved, for the first time, using the state-of-the-art direct N-body evolution program NBODY7, for at least 10 Gyr or until dissolution. In contrast to earlier studies, the BBH mergers obtained in these models show a prominence in in-cluster, triple-mediated mergers compared to those occurring among the dynamically-ejected BBHs. This remains to be true in the presence of a realistic primordial-binary population which, in fact, boosts such in-situ mergers. These BBH mergers are well consistent with the LIGO-detected events and suggest a full-sensitivity LIGO detection rate of 10s-100s BBH mergers from stellar clusters, per year.

Gravitational wave sources in galactic nuclei

Bence Kocsis
Eotvos University

With the detections of the gravitational waves emitted during black hole mergers, LIGO has recently opened the field of gravitational wave astrophysics. In this talk I will discuss some of the astrophysical processes that may be responsible for the observed events. Although less than 0.5% of the stellar mass is in dense stellar systems, I will argue that a large fraction of the black hole mergers may originate in these environments. In particular, I will review black hole mergers in galactic nuclei, including gravitational wave capture events, LIGO mergers driven by the central supermassive black holes, and those which are accelerated by gaseous disks. The event rate distribution may be used to understand the astrophysical origin of the observed gravitational wave events.

Posters

MODEST 17 official poster

Michal Anelt
sans&serif

SEPTEMBER **18—22, 2017**

PRAGUE, CZECH REPUBLIC

MODELLING AND OBSERVING

DENSE STELLAR SYSTEMS

MODEST **UNDER** **PRAGUE'S** STARRY **SKIES**

Kepler

Doppler

Brahe

Einstein

Mach

MODEST17

SOC /

Melvyn Davies
Francesco Ferraro
Jaroslav Haas (CO-CHAIR)
Douglas Heggie
Pavel Kroupa (CO-CHAIR)
Steffen Mieske
Mark Morris
Simon Portegies Zwart
Ladislav Subr (CHAIR)

SCIENTIFIC TOPICS /

Galactic centre / Nuclear star clusters •
Young star clusters and star forming regions •
Stellar dynamics and numerical methods •
Stellar populations in star clusters •
Blue stragglers (stellar collisions and their products) •
Compact objects in star clusters •
Astrophysical sources of gravitational waves •
Dynamics of (exo)planetary systems in star clusters •
New observational frontiers (LIGO, GAIA, JWST, FAST...) •

M67 and the origin of the Sun

Timmi Jørgensen
Lund Observatory

We investigate the stellar cluster M67, in which we believe the Sun might have been born. The indication for this is that both the Sun and M67 have a common age and metallicity, and the solar twins in M67 have more Sun-like abundances than field solar twins. We use Nbody simulations to study the dynamics of stars in M67 as it orbits a Milky Way potential, which include a galactic bar, spiral arms and giant molecular clouds (GMCs). These components of the Milky Way heat the orbit of M67. Encounters with GMCs in particular can push M67 up to the high-altitude orbit on which it is currently observed. In the process M67 loses some of its stars. We then investigate the orbits of stars that are ejected from M67 and in particular whether they are consistent with the Galactic orbit of the Sun.

The Dynamical Evolution of M67 and the Origin of the Sun

Timmi Jørgensen, Ross Church and Bengt Gustafsson

Lund Observatory, Department of Astronomy and Theoretical Physics, Lund University

email: timmi@astro.lu.se

1 Project

We investigate the stellar cluster M67, in which we believe the Sun might have been born. The indication for this is that both the Sun and M67 have a common age and metallicity, and the solar twins in M67 have more Sun-like abundances than field solar twins.

We use Nbody simulations to study the dynamics of stars in M67 as it orbits a Milky Way potential, which include a galactic bar, spiral arms and giant molecular clouds (GMCs). These components of the Milky Way heat the orbit of M67 (Gustafsson et al. 2016). Encounters with GMCs in particular can push M67 up to the high-altitude orbit on which it is currently observed.

In the process M67 loses some of its stars. We then want to investigate the orbits of stars that are ejected from M67 and in particular whether they are consistent with the Galactic orbit of the Sun.

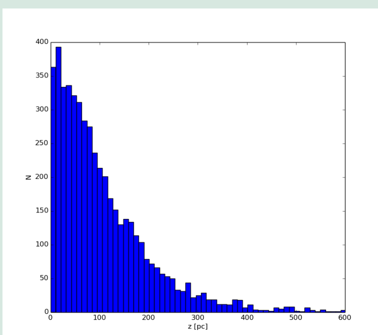

Fig. 1

The |z| distribution of 5000 test particles after 4.6 Gyr. At this point in time, 2.3 % of the test particles have |z| > 400 pc.

Milky Way Model

For the Galactic model we made a replica of the one used in Gustafsson et al. (2016). The Galactic model consists of an axially symmetric potential according to Potential I of Binney (2012). Additional to this potential we added a galactic bar represented by a prolate spheroid and two spiral arms which are represented by 100 oblate spheroids for each arm. Our Milky Way model is scaled such that it is consistent with a circular speed of 220 km/s at a galactocentric distance of 8 kpc. Also included in the model are 2500 GMCs which are born along the spiral arms. Each GMC will live for 40 Myr before a new one is born.

We run a simulation of 5000 test particles in our Milky Way model for a period of 4.6 Gyr. The end result of heating by the spiral arms and GMCs can be seen in Fig. 1. This is consistent with the results found in Gustafsson et al. (2016).

2

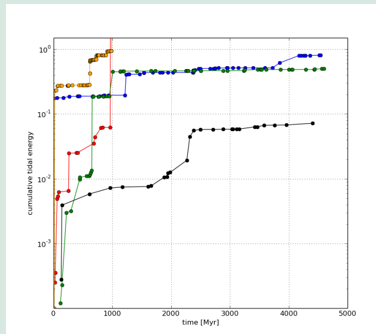

Fig. 2

The GMC encounter history for 5 different particles represented by different colors. Each of these particles reaches a height of |z| > 400 pc. The circles indicates GMC encounters. If the cumulative tidal energy injected into the cluster exceeds unity the cluster is destroyed.

Cluster Survival

The survival of a stellar cluster through GMC interactions is determined by how much tidal energy it recieves during the encounter. If the encounter is too strong the stellar cluster will be destroyed. This tidal energy for each encounter can be described by the change in the inner kinetic energy. If the tidal energy becomes equal or higher than the initial kinetic energy in the cluster, the cluster will be destroyed.

For each test particle there is a GMC encounter history. The cumulative tidal energy injected into the cluster at each encounter can be seen in Figure 2 for 5 different particles. Each of these particles reaches a height of |z| > 400 pc. Each color represents a different particle and the circles indicates GMC encounters. If the cummulative tidal energy reaches unity or above, the cluster is destroyed. The survival rate for the clusters that get scattered to |z| > 400 is 27.8 %.

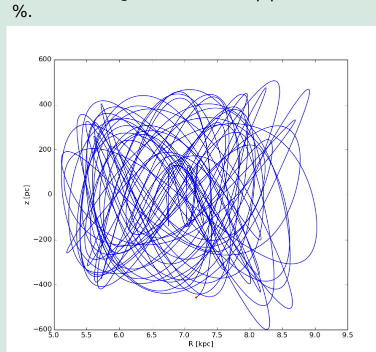

Fig. 3

The orbit of a test particle in our Milky Way model followed for 4.6 Gyr in the R-z plane. The red point specifies where the test particle is after 4.6 Gyr. This particle survives up to high |z|.

3 Nbody Simulations

For the Nbody simulations we are going to be using nbody6tt, a version of nbody6 (Aarseth 2003) where tidal tensors can be implemented, by Renaud et al. (2011). We generate the tidal tensors from our Milky Way model and stop the simluation for each big GMC encounter.

Each of these GMC encounters are then done in nbody6. For M67 we assume a total number of stars of 36 000 with a binary fraction of 50 %. In Fig. 4 a simulation of M67 has been done where a total tidal energy input of 0.8 has been injected into the cluster during one GMC encounter. The red dots show the initial cluster, whereas the black dots shows the stars after 20 Myr. The blue line shows the path of the GMC in the simulation where an impact parameter of 10 pc was used.

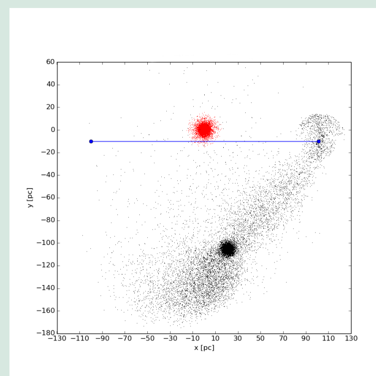

Fig. 4

Nbody simulation of an encounter between M67 and a GMC. The initial cluster has 36 000 stars with a binary fraction of 50 %. The red points represents the initial stars in the clusters, whereas the black points are the stars at the end of the simulation. The blue line represents the path of the GMC.

Conclusion and Future Work

As of now, we have the GMC encounter histories of the test particles that get to high |z| which corresponds to the similar heating that is produced in Gustafsson et al. (2016). We are also able to reproduced the velocity dispersion in U, V and W that is observed for solar-type stars in the solar neighborhood by Holmberg et al. (2009). The next step is to run the Nbody simulations.

Our Milky Way model has a constant spiral and bar pattern which we want to eliminate in future work, since it is improbable that these structures would be constant during a time scale of 4.6 Gyr. Thus, instead of using our current Milky Way model, we want to extract a new model from a galaxy/cosmology simulation.

Searching for Triple Populations in Galactic Globular Clusters

Mirko Simunovic
Gemini Observatory

We combine multi-epoch HST photometric catalogs and select proper-motion members for multiple galactic globular clusters. We refine the photometry by applying differential reddening corrections to our catalogues and are able to accentuate the features in the colour-magnitude diagram such as the main-sequence and the binary sequence. From here, we perform a series of data quality assessment steps to find statistically significant detections brighter and redder than the equal-mass binary line. We compare our selected samples to the expected triple populations from MOCCA dynamical evolution simulations of globular clusters, as well as contaminants expected from the field population using galactic models.

Searching for Triple Populations in Galactic Globular Clusters

Mirko Simunovic[1], Nathan Leigh
[1]Gemini Observatory, Hilo, Hawaii / msimunovic@gemini.edu

Introduction

Direct dynamical interactions involving binary star systems are thought to be catalysts for the formation of exotic stellar populations in globular clusters. The gravitational binding energy of a few very close binaries rivals that of the rest of the million stars in a GC [1]. These few stars will have a big effect on the dynamical evolution of GCs, and the formation and destruction of rich populations of stellar exotica in their cores. Detailed knowledge of the properties of multiple star systems in dense GCs is sorely lacking, particularly at low mass-ratios and intermediate- and long-periods. Binary-binary interactions are predicted by theory and numerical experiments to produce stable triple star systems [2], but their existence has not been observationally confirmed.

Data Description

- Multi-epoch HST photometric data from the HST/ACS globular cluster survey [3] and the HST/WFC3-UVIS globular cluster survey [4].
- The photometry is further refined with a measure of the differential reddening across the filed of view.
- The catalogs are cleaned from bad photometry sources and objects near bright saturated stars.

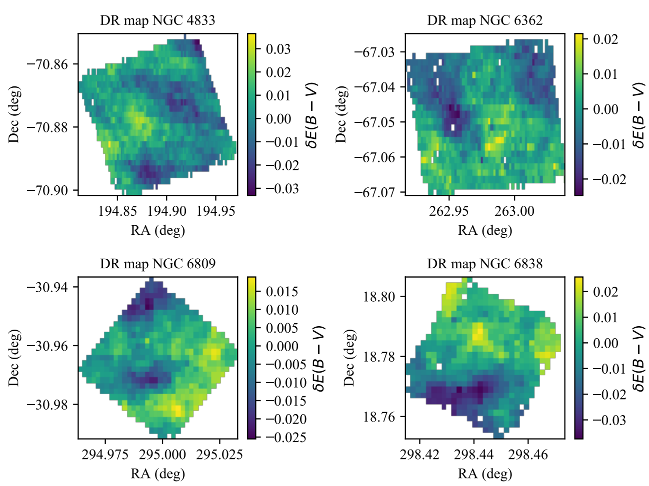

Figure 1. Differential reddening maps for a sample of four Galactic GCs, derived using the procedure described in [5]. The color scale used to illustrate the reddening corrections across the field of view are shown to the right of each inset. The maps are able to recover complex structures in the distribution of dust across the field of view.

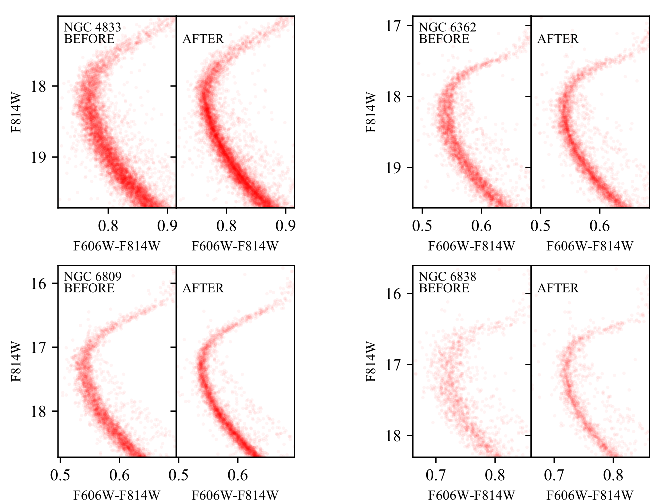

Figure 2. Color-magnitude diagrams for the four Galactic GCs shown in Fig. 1. The left and right panels of each inset show, respectively, the CMDs before and after applying our differential reddening correction procedure. The CMDs illustrate the power of the method to effectively accentuate the features of the CMD. In particular, the binary sequence and the main-sequence become better defined after the correction.

Candidate Selection

- We select cluster members through proper motion measurements from [6].
- We are able to eliminate virtually all foreground and background contaminants whose proper motions do not match that of the ensemble of cluster stars.
- Objects falling above the equal-mass binary sequence in the cluster CMD (see the dashed red lines in Figure 3) are therefore appropriate candidates of being triple systems.
- We use the photometric error distribution to calculate the probability of false positives having colors redder than the equal-mass binary sequence, for an arbitrary magnitude.
- Statistically significant candidates are inspected for flux contamination from nearby sources.

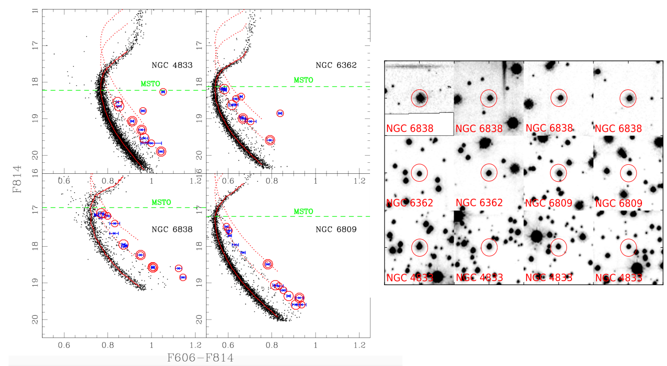

Figure 3. Left: Proper-motion cleaned and differential reddening corrected color-magnitude diagrams for a sample of GCs in the (F606W-F814W)-F814W-plane. Only objects classified as cluster members from the proper motions in [6] are shown. All preliminary triple star candidates are highlighted with blue crosses. Triples identified as having no nearby bright objects in the images are highlighted by red circles. The solid red lines show our fiducial fits to the MS, and the dashed lines show the equal-mass binary and triple sequences. Right: HST/ACS F814W filter images for a sample of triple star candidates. The host GC is shown in red at the bottom left of each inset. The images are each 5 x 5 arcsec in size.

Figure 4. The time evolution (in Myr) of the number of stable triple star systems for two different simulations. The simulations were performed with the MOCCA code for GC evolution [7] by Mirek Giersz and Arkadiusz Hypki. The 200k and 50k models have initial binary fractions of, respectively, 0.2 and 0.1. All stellar-mass BHs are ejected from their host cluster within the first < 30 Myr, after which point the numbers of triples increases. The number of predicted triples are comparable to the sample sizes found for photometric triple candidates. This suggests that the observed triple star candidates can be used to constrain the presence of stellar-mass BHs in their host clusters, since they tend to destroy triples directly during dynamical interactions.

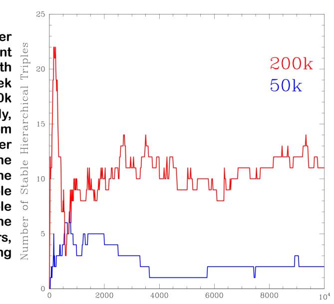

Gemini GMOS-S follow-up

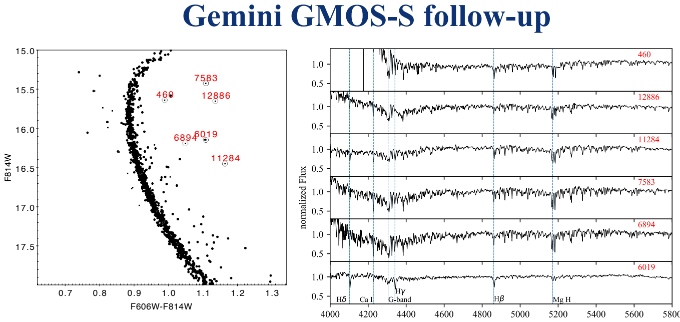

Figure 5. Left: CMD of NGC 6121. The highlighted symbols are triple star candidates recently observed with the GMOS-S spectrograph. Right: Normalized spectra of the triple candidates shown in the left panel. Several strong absorption features in the spectra are labeled. The spectra will allow a determination of spectral types and the search for multi-component SEDs.

References

[1]. Hut P., ApJL 272, 29L (1983)
[2]. Leigh N. W. C. et al., MNRAS 463, 3311 (2016)
[3]. Sarajedini A. et al., AJ 133, 1658 (2007)
[4]. Piotto G. et al., AJ 149, 91 (2015)
[5]. Milone A. P. et al., A&A 540, 16 (2012)
[6]. Simunovic M. & Puzia T. H., MNRAS 462, 3401 (2016)
[7]. Giersz M. et al., MNRAS 454, 3150 (2015)

AURA

GEMINI OBSERVATORY
Exploring the Universe, Sharing its Wonders

The impact of near stellar flybys on the habitability of planets

Behzad Bojnordi Arbab
Sharif University of Technology

With discovery of each exoplanet in habitable zone around a star, where we have the right properties of the star and the planet for supporting life at the present time, we expect to find life. But life is not born in a day; if our search is for advanced or intelligent type of life, there must be enough time for it to evolve and it takes billions of years. If the planet is ripped off of its life-supporting properties in midst of its evolution by a hazard, advanced species will not be born. My work is on the near stellar flyby hazard. I examine earth-like planets in different environments (spiral arms, galactic center, star clusters, elliptical galaxies and collisional galaxies) to calculate the chances for the planet to stay in the habitable zone in different periods of time needed for life to evolve to advanced stages of life. In this talk I will discuss the different outcomes of stellar flybys and how much is their chance in long periods of time in different environments. I will also show how it affects the chances of finding life in different regions of our galaxy and other galaxies.

The Impact of Near Stellar Flybys on the Habitability of Planets

Behzad Bojnordi Arbab
Sharif University of Technology, Department of Physics

Introduction

Earth is the only place we have found life, but one of the greatest efforts are on finding life in other places in the universe. The search for life is mostly the search for habitable planet but complicated life can not be born in a short time. The life we see today has evolved for billions of years and if we want to see this type of life in another planet, life must have time to evolve. In this work we investigate the hazard of stellar encounters that can change the orbit of the planet to non-habitable orbit.

Simulation and parameters

we use REBOUND N-body integrating software package, using non-symplectic IAS15 integrator.

we have simulated a system consisting of a sun-like star (we call it the primary star), an earth-like planet and a secondary star (with mass = 1M(sun)). The planet is on a 1AU circular orbit. The aim is to simulate all possible flybys with in this system and for each simulation, we have 4 parameters:

- Impact parameter of the secondary
- Inclination of the star's path to the orbital plane of the planet
- Longitude of the ascending node of the planet orbit
- True anomaly of the planet in the beginning of the simulation

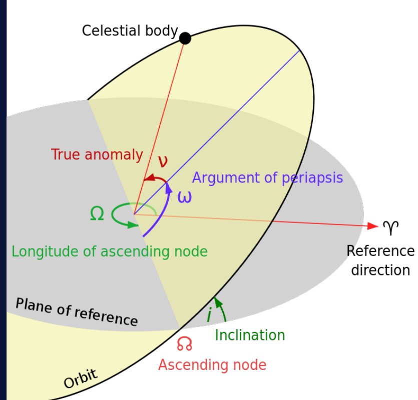

Figure 1: True anomaly, Longitude of ascending node, argument of periapsis and inclination are shown in this figure

Chance of remaining in HZ

If the after the star passes by, the planet's orbit exceeds the habitable zone, then we call it out. We do this simulation for many phases in the 4D parameter space. The ratio of total number of simulations remaining in the habitable zone by the total number of simulations can be seen as a probability

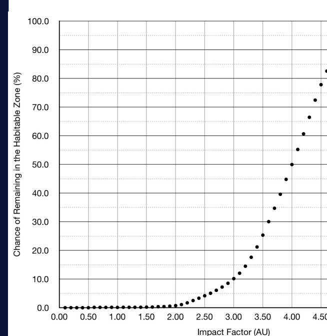

Figure 2: portion (or chance) of orbits with different parameters that remained fully in habitable zone

Results are dependant of all four parameters

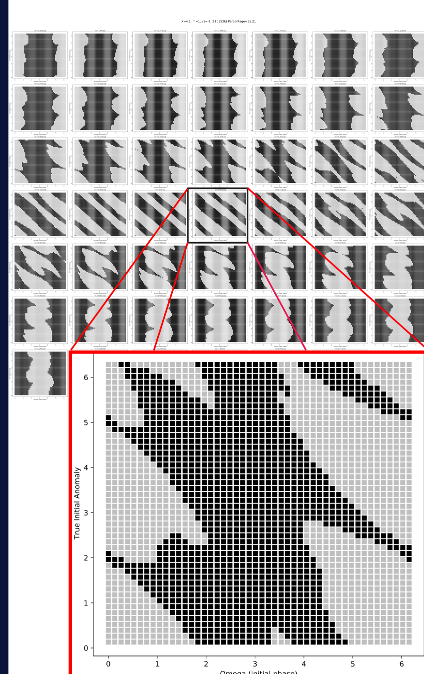

Figure 3: The data blocks and sets as the simulations are done for each set of parameters. dark squares are the simulations that the planet remains in the habitable zone

Having this data, if we know the velocity dispersion and the number density of the stars around the planetary system, we can estimate the rate of encounters with specific velocities and therefor the chance of the planet to have a dangerous stellar encounter. By our calculations, the chance of an earth-like planet in the current position of the system in milky way, the chance are very low (about 0.001%) to have a dangerous encounter in 4 billion years

Sensitivity of HCIP to Habitable Zone width and velocity

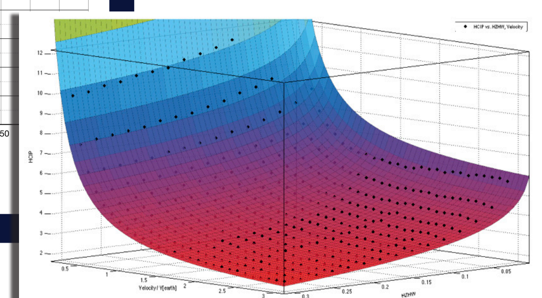

Figure 4: Half Chance Impact Parameter plotted for different Habitable Zone Half Width (HZHW) and velocities

Another interesting result is how this calculations are sensitive to the boundaries and stellar velocity. So for different Habitable Zone Half Width we have the figure 4.

And from this simulations, we fitted a surface to better understand the how the Half Chance Impact Parameter (the impact parameter with half chance for remaining in the habitable zone) changes with the different definitions of habitable zone boundary with each stellar velocity.
(HZHW= Habitable Zone Half Width)
(HCIP= Half Chance Impact Parameter)

$$D_{HCIP} = -\ln(W_{HZHW}) + av^{-1} + b$$

As the chances are very low, the changes in definitions of boundaries will not change the result significantly. For a planet like earth in the galaxy, if life starts to grow in the planet, there is very low chance for the planet to get out of the habitable zone and therefor, life will not be threatened by this hazard

- Simulations in this paper made use of the REBOUND code which can be downloaded freely at http://github.com/hannorein/rebound
- used the IAS15 integrator, Rein and Spiegel (2015)
- Martínez-Barbosa, C. A., Jílková, L., Zwart, S. P., & Brown, A. G. A. (2016, September 28). The rate of stellar encounters along a migrating orbit of the Sun. arXiv.org.
- Bailer-Jones, C. A. L. (2015). Close encounters of the stellar kind. Astronomy & Astrophysics, 575, A35. http://doi.org/10.1051/0004-6361/201425221

contact information:
Email: behzadbojnordi@gmail.com

Plunging neutron stars as origin of temporary organised magnetic field component near SMBH

Vladimir Karas
Astronomical Institute, Czech Academy of Sciences

A hidden population of neutron stars is expected to be present in the central Nuclear Star Cluster in the centre of the Milky Way. These are endowed with dipole-type magnetic field and the process of orbital decay should bring them gradually towards the central Supermassive Black Hole. Despite the fact that black holes do not support their own internal magnetic field, the event horizon can be threaded by organised field lines along which plasma streams may flow. Various magnetohydrodynamical mechanisms have been suggested to generate turbulent magnetic fields on small scales, however, the origin of the large-scale component is unclear. We propose that magnetic fields can be brought onto SMBH by magnetic stars, in particular, strongly magnetised neutron stars (this contribution based on https://arxiv.org/abs/1705.09820).

Plunging neutron stars

as origin of temporary organised magnetic field near SMBH

Astronomical Institute
of the Czech Academy of Sciences

STRONGGRAVITY
EU FP7-SPACE research project 312789 2013 - 2017

Vladimír Karas[1], Michal Zajaček[2,3], Devaky Kunneriath[4], & Andreas Eckart[2,3]

[1]*Astronomical Institute, Czech Academy of Sciences, Prague, Czech Republic*
[2]*I. Physikalisches Institut der Universität zu Köln, D-50937 Cologne, Germany*
[3]*Max-Planck-Institut für Radioastronomie, Auf dem Hügel 69, D-53121 Bonn, Germany*
[4]*National Radio Astronomy Observatory, Charlottesville, VA, United States*

A hidden population of neutron stars is expected to be present in the central Nuclear Star Cluster in the centre of the Milky Way. These are endowed with dipole-type magnetic field and the process of orbital decay should bring them gradually towards the central Supermassive Black Hole. Despite the fact that black holes do not support their own internal magnetic field, the SMBH's event horizon can be threaded by organised field lines along which plasma streams may flow. Various magnetohydrodynamical mechanisms have been suggested to generate turbulent magnetic fields on small scales, however, the origin of the large-scale component is unclear. We propose that magnetic fields can be brought onto SMBH by magnetic stars, in particular, strongly magnetised neutron stars (this contribution based on Karas et al. 2017, https://arxiv.org/abs/1705.09820).

1. Introduction

Black holes cannot support their own internal magnetic field like, for example, compact stars can. Despite this fact observations indicate that event horizons of supermassive black holes (SMBH) are threaded by field lines along which plasma streams flow. Various magnetohydrodynamical mechanisms have been suggested to generate turbulent magnetic fields on small scales, however, the origin of the large-scale component is unclear. In this write-up we describe our progress in an on-going work and discuss the possibility of dipole-type magnetic fields being brought onto SMBH by magnetized neutron stars, which are expected to drift inward from a hidden population in the Nuclear Star Cluster. This can contribute to an organised component of the magnetic field on the characteristic length-scale of the stellar size, which thread the horizon during the final stages of the magnetized star plunge into or its close flyby around SMBH. Because of mass–size scaling relations for black holes, the effect is more important for lower-mass SMBH.

2. Magnetic tubes near a black hole in motion

Effects of mutual interaction between strong gravitational and electromagnetic fields play an important role in shaping structures and driving processes in the inner regions of galactic nuclei. These are governed by the system of Einstein-Maxwell equations, which represent a highly non-linear set of coupled partial differential equations [2]. Special solutions can be derived by imposing various idealized assumptions and symmetries, however, astrophysically realistic solutions can only be found by numerical approaches or approximative methods, such as linearization.

In galactic nuclei, gravity is determined by the central black hole which dominates within its sphere of influence, $r \lesssim r_{\rm s}$,

$$r_{\rm s} \simeq 1.7 \frac{M_\bullet}{4\times10^6 M_\odot}\left(\frac{\sigma}{100\,{\rm km/s}}\right)^{-2}\,{\rm pc}, \qquad (1)$$

where $M_\bullet$ is the mass of the black hole expressed in units of the inferred mass of the Galactic centre black hole and σ denotes the line-of-sight stellar velocity dispersion in the central region.

Further out, contributions to the gravitational field arise from stars in the Nuclear Star Cluster (NSC), as well as gas and dust in an accretion disc and a circum-nuclear torus. Nonetheless, the latter terms can be neglected close to the black hole horizon, where the solution of Einstein's field equations (in geometric units, $c=G=1$), is given by Kerr metric to high degree of accuracy,

$$R_{\alpha\beta} - \tfrac{1}{2}Rg_{\alpha\beta} = 8\pi T_{\alpha\beta}. \qquad (2)$$

Vacuum space-times have the right-hand side of eq. (2) vanishing, whereas for a more general electro-vacuum case the energy-momentum tensor $T_{\alpha\beta}$ is determined by electromagnetic terms:

$$T^{\alpha\beta} \equiv T^{\alpha\beta}_{\rm EMG} = \frac{1}{4\pi}\left(F^{\alpha\mu}F^{\beta}_{\mu} - \tfrac{1}{4}F^{\mu\nu}F_{\mu\nu}g^{\alpha\beta}\right) \simeq \mathcal{O}(\mathcal{E}^2+\mathcal{B}^2). \qquad (3)$$

The electromagnetic field tensor $F^{\alpha\beta}$ contributes to the source, however, astrophysically realistic fields are not strong enough and their gravitational influence to the space-time metric terms vanishes when linearized in electric ($\mathcal{E}$) and magnetic ($\mathcal{B}$) intensities.

Gravitational radius, $r = r_{\rm g} = 1.475\times10^5 M/M_\odot\,{\rm cm}$, characterizes the typical length-scale in a system which involves action of strong gravity near a black hole. In the units of gravitational radius, the horizon of a rotating black holes has radius equal to $r_+(a) = 1+\sqrt{1-a^2}$, which gradually decreases with black hole dimensionless spin a: $r_+ = 2$ for a non-rotating (Schwarzschild) black hole, and $r_+ = 1$ for a maximally spinning (Kerr) black hole. These represent asymptotically flat vacuum solutions endowed with a regular event horizon, which is present in the Kerr metric for $a^2 \leq 1$.

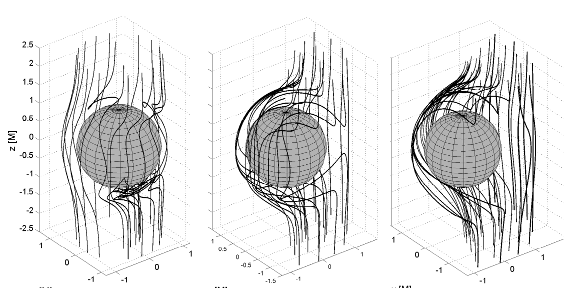

Fig. 2. Structure of asymptotically homogeneous (vertically aligned) magnetic field lines influenced by translatory boost of the black hole (horizon $r = r_+$ is indicated by the shaded sphere). The case of extreme rotation ($a = 1$) of Kerr black hole is shown and the field lines are defined with respect to ZAMO observers. The field becomes expelled out of the horizon (Meissner-type effect) for the vanishing drift velocity, but it can thread the horizon with an increasing flux when the black hole moves. The direction of boost velocity has been set to coincide with the horizontal axis of the stereometric projection: $v_x > 0$, $v_y = -v_x$ and $v_z = 0$. In the above-shown panels, from left to right, velocity with respect to speed of light ($c = 1$) grows according to the following sequence: $v_x = 0.1$, 0.3, and 0.7, respectively. Larger velocity causes the accumulation of field lines and, hence, stronger intensity of the magnetic field on the front side.

Magnetic fields near accreting black holes operate on vastly different length-scales, ℓ, which range from small-scale turbulent fields ($\ell \ll r_+$, likely due to magneto-rotational instability), to organized fields operating on larger scales exceeding the radius of horizon, $\ell \gtrsim r_+$. In the present contribution, we are interested in the latter possibility. While it has been suggested that organized field lines could support the process of launching and pre-collimating jets, the origin of filamentary structures remains unclear. Here we propose that the horizon of a supermassive black hole may be threaded by a dipole-type magnetic component that originates in a strongly magnetized neutron star in its vicinity. A significant number of remnant (isolated) neutron stars is expected to exist in the Nuclear Star Cluster, where they can gradually sink towards the black hole.

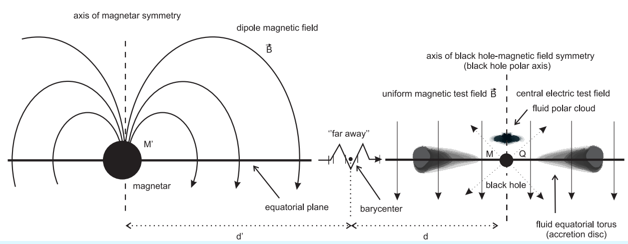

Fig. 1. An artistic sketch of a binary system of a magnetized neutron star interacting with a supermassive black hole. Magnetic field has dipolar topology near the surface of the neutron star (on the left side of the diagram), which we assumed to be non-rotating for simplicity. At larger distances, within a limited volume surrounding the companion black hole, the imposed magnetic field resembles a homogeneous filament of (almost) parallel lines (on the right side).

Figure 1 illustrates the basic idea about magnetic stars as the origin of external magnetic field [3]. A similar set-up was proposed as a model for the origin of accretion disc coronae levitating because of the presence of an organized magnetic field above the equatorial plane and in polar regions near an accreting black hole. Let us note that the presence of a magnetar has been reported in the neighbourhood of the Galactic centre, however, the distance $\simeq 0.5\,$pc is too large to provide a convincing example of the system envisaged in our present discussion.

3. A hidden population of isolated neutron stars in NSC

We have adopted a rotating black-hole solution to Einstein field equations (2) together with the solution of Maxwell equations for a weak, asymptotically uniform magnetic field, eq. (3), i.e. linearized with respect to $\mathcal{E}$ and $\mathcal{B}$. We performed a translatory boost to take linear motion into account. This can be achieved by a straightforward (albeit tedious) calculation of the Lorentz transformation of the field components, which rotates the asymptotical direction of the field lines. Unlike the case of a non-drifting black hole, an electric component is induced.

The resulting magnetic field is plotted in Figure 2 for three cases of boost velocity. Let us note that the shape of lines of force depends on the choice of reference frame; we employ zero-angular-momentum observers (ZAMO) as preferred fiducial observers for which the lines of force have been constructed in a stereometric projection. We notice that the translational motion of the black hole enriches the resulting structure very significantly. We can observe formation of a boundary zone, where narrow layers surround the event horizon. Such layers are typical sites of magnetic reconnection and the subsequent acceleration of electrically charged particles.

So far there have been just very few reports of neutron star candidates near Galactic centre, which has led to a persisting "missing pulsar problem". However, among confirmed pulsar detections and other evidence for magnetized neutron stars we can mention two highly dispersed pulsars at an angular offset of $\lesssim 0.3$ deg from Sgr A*. Also, reported the detection of three pulsars with a large dispersion measure, indicating the location at a similar distance from us as the Galactic centre itself.

The above-given arguments motivate a scenario where a SMBH is embedded in an organized, uniform-like filament of an externally generated magnetic field. However, because of fast linear speed of the source (given by the orbital motion of the neutron star according to our picture), we need to take the effect of the translatory boost into account. To this end we adopted a suitable formalism to treat weak magnetic fields near the black hole in arbitrary motion. Let us note that a complementary approach can be applied to explore the magnetic field of a moving dipole near a black hole within Rindler's approximation. Both methods reveal the interaction between electromagnetic and gravitational effects that are inherent to the coupled system of Einstein-Maxwell equations.

To summarize, we have illustrated the structure of an initially organized (uniform-like) magnetic lines close to the horizon, where they can be distorted by the translatory motion of the supermassive black hole. Despite a complicated structure of the field lines, a clear degree of self-organization persists, which distinguishes the field structures discussed here from highly turbulent small-scale magnetic fields that are thought to develop within accretion flows.

4. Conclusions

We discussed the possibility that strongly magnetized neutron stars can impose an ordered (organized) component of their dipole-type field onto a nearby supermasive black hole. To this end we discussed a likely scenario with numerous neutron stars produced as end-points of stellar evolution within the central Nuclear Star Cluster, such as the one surrounding Sgr A* in the Galactic centre. The intensity of the dipole-type field decreases with the distance from the neutron-star surface with cube of radius in the near zone. Hence, the resulting component of the organized field comes out rather weak, although the realistic situation gets complicated beyond the light cylinder where the field lines open up and the magnetic intensity decays with radius in slower pace. Some members of the neutron star population are expected to sink very close to the black hole or even plunge into the horizon as a result of the orbital decay caused by hydrodynamical friction with the ambient gaseous environment and the emission of gravitational waves. Because of their compactness, neutron stars are not disrupted by SMBH tidal forces and they can support the magnetic intensity at and above 1 G on the SMBH horizon during the final stage of the infall.

References

[1] Karas V., Kopáček O., Kunneriath D., Zajaček M., Araudo A., Eckart A., & Kovář J. (2017), Contrib. Astron. Obs. Skalnate Pleso 47, 124-132 (https://arxiv.org/abs/1705.09820)

[2] Karas V., Kopáček O., & Kunneriath D. (2012), Classical and Quantum Gravity, Volume 29, Issue 3, id. 035010

[3] Kovář J., Kopáček O., Karas V., & Stuchlík Z. (2010), Classical and Quantum Gravity, 27, id. 135006

E-mail: vladimir.karas@cuni.cz

A steeper stellar cusp in the Galactic Center from binary disruptions and its implications for EMRIs

Giacomo Fragione
Hebrew University of Jerusalem Israel

The relaxed distribution of stars around a massive black hole is known to follow a cusp profile $n(r) \propto r^{-\alpha}$ with characteristic slope $\alpha = 7/4$. This follows from energy conservation and a scattering rate as given by two body encounters. However, we show that injection of stars close to the black hole modifies this profile. In the steady-state configuration, the cusp develops a central region with typical slope $\alpha = 9/4$ in which stars diffuse outward. Binary disruption by the intense tidal field of the massive black hole is among the phenomena that take place in the Galactic Center. In such disruption, one of the binary members remains bound to the black hole, thus providing a source term of stars close to the black hole. We show that for the parameters of the Galactic Center, this source is strong enough to modify the cusp profile. If the binary fraction at the influence radius is of order unity and the orbits of all the captured stars are efficiently circularized, the steeper cusp extends almost as far as the radius of influence of the black hole.

Steeper stellar cusps in galactic centers from binary disruptions and its implications for EMRIs

Giacomo Fragione & Re'em Sari
The Hebrew University of Jerusalem, Israel

האוניברסיטה העברית בירושלים
THE HEBREW UNIVERSITY OF JERUSALEM

Introduction

The relaxed distribution of stars around a massive black hole (BH) is known to follow a cusp profile $\rho(r) \propto r^{-\alpha}$ with characteristic slope $\alpha = 7/4$. This follows from energy conservation and a scattering rate as given by two body encounters [2]. In this picture, the injection of stars close to the BH modifies this profile. Binary disruption by the intense tidal field of the massive BH is among the phenomena that take place in the Galactic Center (GC). In such disruption, one of the binary members remains bound to the BH, thus providing a source term of stars [3].

Binary Disruption

A binary of total mass M_* undergoes tidal breakup when passes inside the tidal radius [1]

$$r_{bt} = a\left(\frac{M_{BH}}{M_*}\right)^{1/3} , \qquad (1)$$

where a is the binary semi-major axis. One of the stars is expelled the with velocities of hundreds km s^{-1}, while the other one remains bound to the massive BH with semimajor axis [3]

$$r_{BH} \approx a_b\left(\frac{M_{BH}}{m}\right)^{2/3} \qquad (2)$$

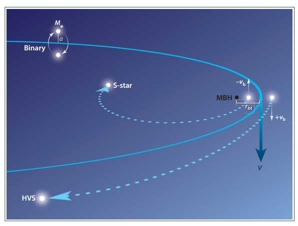

If we assume that the binary semi-major axis are distributed according to $f(a_b) \propto 1/a_b$, the typical r_{BH} of captured stars will follow the same distribution scaled by a factor $Q^{2/3} = (M_{BH}/m)^{2/3}$.

Cusp with binaries

Let r_{min} be the distance at which we inject these stars with rate η/P_h, where $\eta = \eta_b\,\omega$ is a numerical factor that depends on the binary fraction (η_b) and on the effective number of injected stars that circularize (ω), and P_h is the period at the influence radius r_h [1,3]. The stars will scatter each other via 2-body process, transporting themselves away from the injection point. If the rate of injection is significant enough, the flux would be in both inward and outward directions. The inward flux is identical to the standard case, and a constant energy flow dictates $\rho \propto r^{-7/4}$ for $r < r_{min}$. For the outward flow of stars from the injection point $r > r_{min}$, energy conservation is less restrictive than stellar number conservation. The energy flux would be very small, with a constant stellar flux given by $\dot{N}_{inj} = N(r)/T_{2b}(r) \propto r^{-2\alpha+9/2} = const$. Therefore, $\alpha = 9/4$, in the outer cusp. The extent of such a region depends on η [4]

$$N(r) = \frac{M}{m} \times \begin{cases} \left(\frac{\eta r_h}{r_{min}}\right)^{1/2}\left(\frac{r}{r_h}\right)^{5/4} & \text{for } r < r_{min} \\ \eta^{1/2}\left(\frac{r}{r_h}\right)^{3/4} & \text{for } r_{min} < r < R_{max} = \eta r_h \\ \left(\frac{r}{r_h}\right)^{5/4} & \text{for } R_{max} = \eta r_h < r \end{cases} \qquad (3)$$

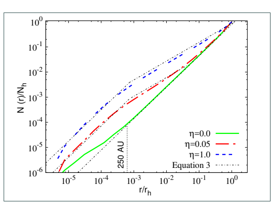

Comparison between the analytical predictions for the distribution of stars obtained from Eq. 3 along with the results from simulations in the cases $\eta = 0.05$ and $\eta = 1$, when $r_{min} = 250$ AU. In the case $\eta = 1$, $R_{max} = r_h$ and the region with the steeper slope $\alpha = 9/4$ extends up to the influence radius. In the case $\eta = 0.5$, the cusp is steeper up to $R_{max} = 0.05\,r_h$, while returns to the [2] beyond it.

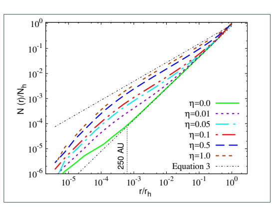

Modified cusps for different values of η. For the Milky Way's GC, if we assume that the binary fraction at r_h is 0.1 [5] and $\omega = 0.35$ [4], we would get $\eta \approx 0.035$. Such η is enough to modify the cusp within ≈ 0.07 pc [4]. The binary-modified profile would be ≈ 8 times denser than the standard cusp at $r < r_{min} = 250$ AU. Such effect may not be observable because of the source crowding and bright stars contamination within ≈ 0.07 pc.

Recent observational data have shown that the old population of 1-2 $M_\odot$ stars follow 3D star distribution with slope ≈ 1.2 up to ≈ 3 pc [7]. Several factors of uncertainty

- challenging observations $\lesssim 0.07$ pc [7]
- uncertain number of binaries at the influence radius [5]
- our model has no initial mass function for binaries [4]
- possible top-heavy initial mass function for disrupted binaries [3]

Implication for EMRIs

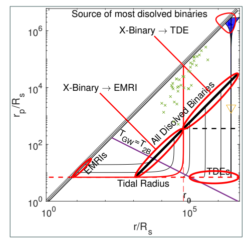

Particles of mass m on eccentric orbits change significantly their angular momentum on a timescale

$$T_{rel}(r, r_p) = \frac{P(r)}{N(r)}\left(\frac{M_{BH}}{m}\right)^2\left(\frac{r_p}{r}\right) , \qquad (4)$$

where $P(r)$ is the period, $N(r)$ is the number of particles, r_p and r the particle pericenter and semi-major axis. Gravitational waves circularize highly eccentric orbits, while keeping the pericenter roughly fixed, on a timescale

$$T_{GW}(r, r_p) = \frac{R_S}{c}\frac{M_{BH}}{m}\left(\frac{r_p}{R_S}\right)^4\left(\frac{r}{r_p}\right)^{1/2} , \qquad (5)$$

where R_S is the Schwarzschild radius and c the velocity of the light.

For small enough galaxies, tidal disruption mass transfer occurs before the star hits the Schwarzschild radius. If this encounter happens on an extremely eccentric orbit, this result in a violent tidal disruption event (TDE) of the star over its dynamical time at $r_t = R_*(M_{BH}/m)^{1/3}$. If the star approaches on a slowly shrinking circular orbit, the star transfers mass to the BH on the gravitational wave timescale as an EMRI (extreme-mass ratio inspiral). The rate of TDEs is dominated by the supply from roughly circular orbits at the radius of influence [6]

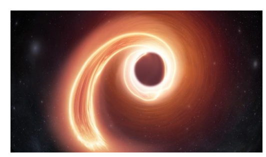

$$R_{TDE} = \frac{N(r_h)}{T_{rel}(r_h)} = \frac{1}{P(r_h)} \qquad (6)$$

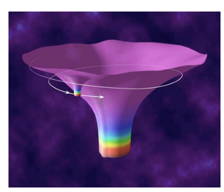

The rate of EMRIs is given by the supply of from roughly circular orbits of the largest radius that does result in a TDE ($r_0 = r_h(R_S/r_t)^2$) [6]

$$R_{EMRI} = \frac{N(r_0)}{T_{rel}(r_0)} = \frac{(R_S/r_t)^2}{P(r_h)} \qquad (7)$$

Binary injection changes the typical distribution of stars $N(r)$ inside r_h as in Eq. 3. These stars are on highly eccentric orbits and are more prone to evolution by gravitational waves when [6]

$$\frac{r_{BH,p}}{R_S} < \left(\frac{r_h}{r_{BH}}\right)^{1/2} \qquad (8)$$

Conclusions

- binary tidal disruptions can changes the slope of the cusp external to the source position leading to a steeper slope $\alpha = 9/4$ when the rate is high enough
- if we assume that the binary fraction in the GC is 0.1, binary injection is strong enough to modify the cusp within ≈ 0.07 pc
- larger number of stars useful to measure relativistic precession with GRAVITY
- implications for BH-BH mergers due to Kozai-Lidov oscillations
- implications for EMRIs

References

[1] Alexander, T. 2017, Ann. Rev. Astron. Astrophys., 55
[2] Bahcall, J. N., & Wolf, R. A. 1976, ApJ, 209, 214
[3] Brown W. R. 2015, Annu. Rev. Astron. Astrophys., 53, 15
[4] Fragione G., & Sari R. 2017, submitted to ApJ
[5] Hopman, C. 2009, ApJ, 700, 1933
[6] Sari R., Fragione G., & Weissbein A. in prep.
[7] Schödel, R. et al. 2017, preprint, arXiv:1701.03817

giacomo.fragione90@gmail.com

3D adaptive mesh refinement simulations of star formation in the inner parsecs of the Milky Way

Alessandro Ballone
INAF-OAPd

The Galactic Center is a dense environment, hosting a supermassive black hole and a variegated stellar population, with hundreds of young stars within the central parsec. Analytic work and smoothed-particle hydrodynamics simulations show that the young stars can be born out of molecular clouds, infalling from larger distances. Recent studies also highlighted the presence of gas streamers, possibly connected to the +20 km/s and +50 km/s molecular clouds. Whether the young stars formed already in the central parsec or in these gas streamers, few parsecs away from Sgr A*, is still an open question. I present a set of 3D adaptive mesh refinement hydrodynamic simulations of star formation in the Galactic Center, performed with the code RAMSES. I explore a wide range of initial gas cloud properties. I discuss for which cases star formation occurs only in the central parsec (when the cloud has disrupted and formed a dense disk), or already in gas streamers, still on their way toward Sgr A*.

3D AMR simulations of star formation in the inner parsecs of the Milky Way

State of the art

The inner few parsecs of the Galactic Center are an extremely dense environment, with several components:

- **SgrA***, a **supermassive black hole** with mass of 4×10^6 M$_\odot$;
- a **late-type star cluster** (cusp);
- a **disk of young** (O/WR type) **stars**;
- few tens of B-type stars (the so-called **S-stars**) with isotropically oriented, highly eccentric orbits in the inner 0.05 pc from the SMBH;
- a circumnuclear disk (**CND**) of molecular/neutral gas and dust, at 2-7 pc from SgrA*;
- 2 near **molecular clouds**, often named +20 km/s and +50 km/s, possibly interacting with the CND from outside through streamers;
- The "**minispiral**", a inward spiral pattern of ionized gas inside (and possibly fed by) the CND.

Objectives

Many studies have showed that in-situ fragmentation by the infall and tidal disruption of a molecular cloud could lead to star formation in the inner parsecs of the Milky Way (e.g., Mapelli & Trani, 2016, and references therein). A key problem still remains unsolved: **were the observed stars already born in gas streamers reaching SgrA* from tens of parsecs distance or, later, in a gravitationally unstable disk formed by the material directly impinging on the SMBH?**
Answering this question is linked to the past star formation history, as well as to the current and future interplay between all the different components of SgrA*'s near environment.

Methods

AMR simulations of molecular clouds plunging into SgrA* were never attempted. For this purpose, we used the **code RAMSES** (Teyssier, 2002) and its sink particle formation algorithm to study the formation and dynamics of the putative stars (star clusters).
In order to understand how star formation occurs, depending on the initial properties of the plunging cloud, we ran a set of **12 (2x2x2x2) simulated turbulent clouds** with
2 masses, **10^4 and 10^5 M$_\odot$**;
2 radii, **5 and 10 pc**;
2 distances from SgrA*, **30 and 60 pc**;
2 initial velocities, **10 and 100 km/s**.
We currently assumed an isothermal equation of state and a temperature of 100 K for the molecular gas. The gravitational potential of the SMBH, the old stellar cusp and the galactic bulge have been included in the simulation.

First Results

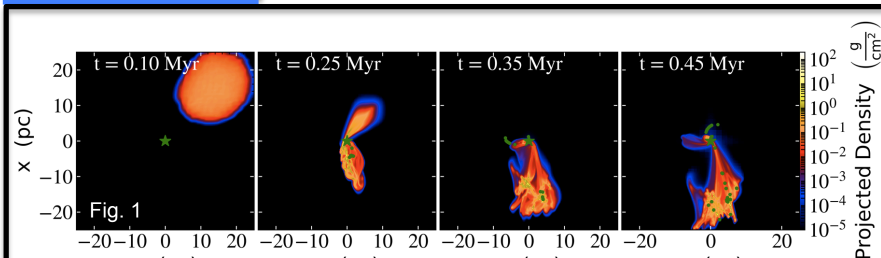

Fig. 1 shows the time evolution of our model with mass equal to 10^5 M$_\odot$, initial radius of 10 pc, distance from SgrA* of 30 pc and velocity of 10 km/s. The latter is a small fraction of the escape velocity from the SMBH+cusp potential, at that distance. For this reason, the molecular cloud reaches SgrA* on a very eccentric orbit.

Part of the cloud has formed a disk at few pc distance from SgrA*. The remaining gas is forming stars and it is partially keeping on receeding from the SMBH and partially feeding the disk in a long streamer. This model might remind the current configuration of the +20 km/s molecular cloud, which also shows indication of recent star formation (Lu+, 2015) and seems to be interacting with the CND (e.g., Liu+, 2012; Takekawa+, 2017).

A first burst of coheval stars forms around 2×10^5 yr of the simulation, at the cloud's pericenter passage, where the tidal squeezing of the cloud is maximum; A second population forms more gradually later on, in the density peaks arising from turbulence (Fig. 2 shows a cumulative timeline of sink formation). Fig.3 (the cloud is seen edge-on, here) also shows that the orbital plane of the first group of stars is basically equal to the one of the cloud (the white line shows the orientation of its angular momentum), while the second population has various heights with respect to this plane.

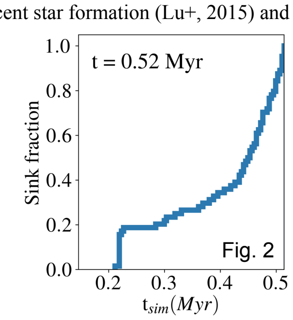

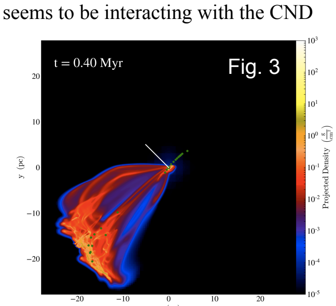

References

- Liu et al., 2012, ApJ, 756, 195
- Lu et al., 2015, ApJ, 814, 18L
- Mapelli & Trani, 2016, A&A, 585, 161
- Takekawa et al., 2017, ApJ, 834, 121
- Teyssier, 2002, A&A, 385, 337

Contacts

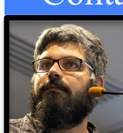

Alessandro Ballone
alessandro.ballone@oapd.inaf.it

Michela Mapelli
michela.mapelli@oapd.inaf.it

… but also ask anybody in the ForDyS group!
http://web.pd.astro.it/mapelli/group.html

The black hole retention fraction in star clusters

Václav Pavlík
Astronomical Institute of Charles University, Prague

Recent works, e.g. Peuten (2016) and Baumgradt & Sollima (2017), have been constraining the retention fraction of black holes (BHs) in globular clusters by comparing the degree of mass segregation with N-body simulations. They are consistent with an upper limit of the retention fraction being 50 % or less (e.g. 10 %). In this work we focus on direct simulations of the dynamics of BHs in star clusters, aiming to constrain the distribution of natal kicks which BHs receive during supernovae explosions. To do so, we modified the Aarseth's `nbody6` code so that we can measure the retention fraction of BHs for a given set of parameters which are: the initial mass of a star cluster, the initial half-mass radius and σ, the value of the Maxwellian BH velocity kick distribution. We compare these direct N-body models with our analytic estimates and observational constraints derived by Peuten (2016) and Baumgardt & Sollima (2017). Our results as well as this poster are available online at `http://sirrah.troja.mff.cuni.cz/~pavlik/bh/`.

The black hole retention fraction in star clusters

Václav Pavlík[1,†] and **Tereza Jeřábková**[1,2,3,⋆]

1 Astronomical Institute of the Charles University, Prague, Czech Republic
2 Helmholtz-Institut für Strahlen- und Kernphysik, Universität Bonn, Bonn, Germany
3 European Southern Observatory, Garching bei München, Germany
† pavlik@sirrah.troja.mff.cuni.cz ⋆ tjerabko@eso.org

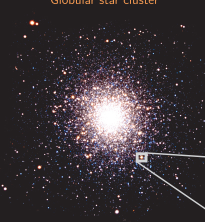

Asymmetric SN explosion leads to a BH kick

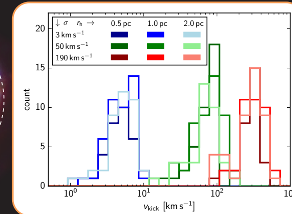

Distribution of kick velocities is Maxwellian (e.g. the data from our model with 25k stars)

Abstract

Recent works, e.g. Peuten (2016) and Baumgradt & Sollima (2017), have been constraining the retention fraction of black holes (BHs) in globular clusters by comparing the degree of mass segregation with *N*-body simulations. They are consistent with an upper limit of the retention fraction being 50 % or less (e.g. 10 %). In this work we focus on direct simulations of the dynamics of BHs in star clusters, aiming to constrain the distribution of natal kicks which BHs receive during supernovae explosions. To do so, we modified the Aarseth's `nbody6` code so that we can measure the retention fraction of BHs for a given set of parameters which are: the initial mass of a star cluster, the initial half-mass radius and σ, the value of the Maxwellian BH velocity kick distribution. We compare these direct *N*-body models with our analytic estimates and observational constraints derived by Peuten (2016) and Baumgardt & Sollima (2017).

Numerical models

We performeded over 1 100 *N*-body simulations of isolated star clusters. Our models have 1k, 10k, 25k, 50k, and 100k stars with the Kroupa (2001) IMF in the range from 0.08 to 150 $M_\odot$. Smaller clusters were evolved in the single CPU `nbody6` integrator and larger models in the parallel `nbody6.sse` version (Aarseth 2003; Nitadori & Aarseth 2012). All models started from the Plummer (1911) distribution with an initial half-mass radius of either 0.5, 1.0 or 2.0 pc. The stellar evolution was based on an algorithm from Hurley, Pols & Tout (2000). We assumed the average metallicity of globular clusters in the Galaxy (Baumgardt & Sollima 2017), i.e. [Fe/H] $= -1.30$. Finally, we considered three values of the velocity dispersion for the supernova (SN) kicks, namely $\sigma = 3$, 50 and 190 km s^{-1}.

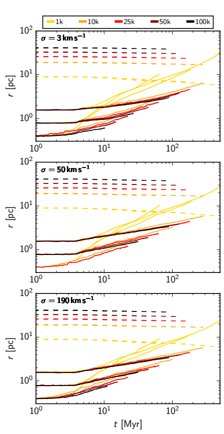

We show the evolution of our models on the left by the means of their **half-mass (solid lines)** and **tidal radii (dashed lines)**. The latter comes from

$$r_t = R_g \left(\frac{M_c}{2M_g} \right)^{\frac{1}{3}},$$

where M_c is the cluster's mass within the tidal radius, R_g is its distance from the centre of the Galaxy ($\stackrel{\text{def}}{=} 5$ kpc), and M_g is the mass of the Galaxy up to R_g ($\approx 5 \cdot 10^{10}\,M_\odot$, from Faber & Gallagher 1979).

Retention fraction

In each realisation of our models, we tracked the positions of all newly formed and existing BHs. The retention fraction, denoted as η_{BH}, corresponds to the fraction of BHs that are inside a certain radius, e.g. the half-mass radius or the tidal radius. The plots on the right show the evolution of the mean η_{BH} in our models with the initial half-mass radius of 1.0 pc and $\sigma = 3$ km s^{-1}. After a certain amount of time, the retention fraction reaches a stacionary value which depends on the number of stars in the model, i.e. its initial mass. The oscillations or a slight decrease of this value that we see after all BHs **(black line)** formed are due to ejections through close encounters of BHs and other stars.

The plots of η_{BH} in other models and the animations of our star clusters are available online.

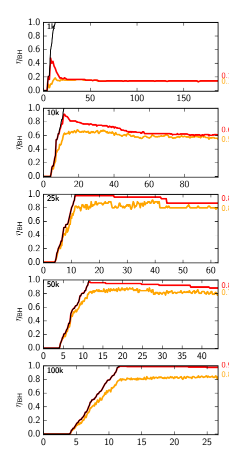

Analytic estimate in comparison to *N*-body models

We generated star clusters with the Kroupa (2001) IMF in the same mass range as our *N*-body models. First, we assume that at the time of the kick the systems are Plummer (1911) models with the parameter a and that the kick velocities follow the Maxwell–Boltzmann distribution with a velocity dispersion σ. Then, we consider every star above 8 $M_\odot$ to be a black hole. The estimated BH retention fraction, η_{BH}, is the fraction of BHs that did not ecsape from the cluster, assuming that the stellar remnants are lost if their velocity after a SN kick is larger than the escape velocity at their current radius. The limit velocity is defined as

$$v_{esc}(r) = \left(\frac{2Gm}{\sqrt{r^2 + a^2}} \right)^{\frac{1}{2}},$$

where m is the mass of the black hole and r is its current distance from the centre of the star cluster.

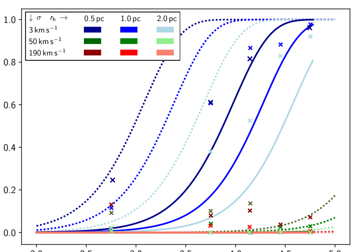

The results are plotted in the figure above. The **upper limit of η_{BH} (dotted lines)** is calculated as if all the BHs were ejected directly from the centre. For the **lower limit (solid lines)**, we assumed the ejections from $r = 10$ pc, which corresponds to the radius of an expanded cluster. The data from our ***N*-body results** are marked by **'x'**. There is a general agreement within the analytic estimates and the *N*-body simulations. The main effect causing the differences between these two is the dynamical evolution of star clusters which was not accounted for in the analytic predictions.

Conclusions

The preliminary results shown here indicate that:

i) The black hole retention fraction grows with an increasing initial star cluster mass. This is shown by direct *N*-body simulations which corroborate the analytical estimates. Thus, it is possible to estimate the BH retention fraction using a simple analytical formula, taking into account the tidal radius of a given cluster. The estimate agrees well with the *N*-body results, especially for star clusters with the initial mass greater than $10^4\,M_\odot$.

ii) Given the predicted velocity dispersion of SN kicks ($\gtrsim 190$ km s^{-1}), no BH would remain in even a very massive globular cluster. The only possible BHs retained are the most massive ones due to two reasons: **a)** The BH kick velocity might be scaled with its mass (conservation of momentum), or **b)** the most massive stars might implode leaving BH remnants without a kick.

iii) If the retention fraction of BHs is about 50 % in globular clusters (Peuten 2016; Baumgardt & Sollima 2017), then the velocity distribution of kicks cannot be a simple Maxwellian with a velocity dispersion of 190 km s^{-1} or larger. This suggests implosions or a bimodal kick velocity distribution (as it has been found for neutron stars by Verbunt et al. 2017) are valid.

References & Acknowledgements

Aarseth, S. J. 2003, Gravitational N-Body Simulations, Cambridge University Press, Cambridge, UK
Baumgardt, H. & Sollima, A. 2017, ArXiv e-prints [arXiv:1708.09530]
Faber, S. M. & Gallagher, J. S. 1979, ARA&A, 17, 135
Hurley, J. R., Pols, O. R., & Tout, C. A. 2000, MNRAS, 315, 543
Kroupa, P. 2001, MNRAS, 322, 231
Nitadori, K. & Aarseth, S. J. 2012, MNRAS, 424, 545
Peuten, M., Zocchi, A., Gieles, M., Gualandris, A., & Hénault-Brunet, V. 2016, MNRAS, 462, 2333
Plummer, H. C. 1911, MNRAS, 71, 460
Verbunt, F., Igoshev, A., & Cator, E. 2017, ArXiv e-prints [arXiv:1708.08281]

Go to http://sirrah.troja.mff.cuni.cz/~pavlik/bh/ or use the QR code to download this poster and to see more online content, e.g. the animations from our simulations.

This study was supported by the Charles University grants SVV-260441 and GAUK-186216. We also greatly appreciate access to the computing and storage facilities owned by parties and projects contributing to the National Grid Infrastructure MetaCentrum, provided under the programme *Projects of Large Research, Development, and Innovations Infrastructures* (CESNET LM2015042).

Mass-transferring black hole binaries in globular clusters

Kyle Kremer
Northwestern University-CIERA

We explore the formation of mass-transferring binary systems containing black holes (BHs) within globular clusters (GCs). We show that it is possible to form mass-transferring BH binaries with main sequence, giant, and white dwarf companions with a variety of orbital parameters in GCs which span large ranges in various initial cluster properties. We demonstrate that the formation of these systems is dominated by binary-mediated strong dynamical scattering encounters within the cluster. Furthermore, we show that at any given time, the number of mass-transferring BH systems within a GC has little correlation with the total number of BHs retained by the GC at that time. Our results strongly suggest that the presence of observed BH X-ray binaries in GCs cannot put any constraints on the total number of (unobservable) BHs the host clusters may retain today.

Dynamical Formation of Mass-transferring Black Hole Binaries in Globular Clusters

Northwestern University

Kyle Kremer, Sourav Chatterjee, Carl Rodriguez, & Fred Rasio
Northwestern University
Center for Interdisciplinary Exploration and Research in Astrophysics (CIERA)

CIERA
CENTER FOR INTERDISCIPLINARY EXPLORATION AND RESEARCH IN ASTROPHYSICS

Motivation

Modeling dense star clusters such as **globular clusters** is one of the most challenging problems in computational astrophysics. We have developed a highly parallelized and advanced Monte Carlo approach to stellar dynamics that allows us to model clusters with up to N~10^6 particles in at most ~1 week of computing time. Our parallelized Monte Carlo approach allows us to model clusters significantly more rapidly than a traditional N-body integrator, enabling us to fully explore the population of dense star clusters found in the Milky Way and other galaxies.

Globular Cluster 47 Tuc
ESO/M.-R. Cioni/VISTA Magellanic Clour survey

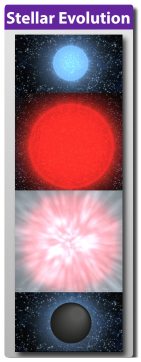

Our **Cluster Monte Carlo code (CMC)** contains all the relevant dynamics for modeling dense star clusters, including two-body scatterings, 3- and 4- body strong encounters, and three-body binary formation. CMC also contains detailed prescriptions for single and binary stellar evolution, equivalent to the most recent population synthesis studies of isolated binary evolution in galactic fields.

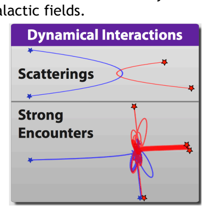

CMC can be used to model in detail the dynamical formation of binary systems containing black holes. If these systems are mass-transferring at late times, they could potentially be observed as **Black Hole X-ray binaries (BH XRBs).**

In recent years, several stellar mass BHs have been observed as X-ray and Radio sources within Milky Way and extragalactic globular clusters.

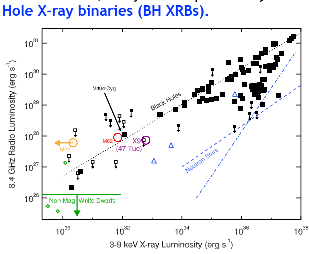

Observed BH XRBs in globular clusters. From Strader et al. (2012).

Dynamical Formation of BH XRBs

Using a collection of 70 fully-evolved globular cluster models, we identified all BHs found in a mass-transferring binary (MTB) at t > 8 Gyr. All identified MTBs are dynamically created; the median number of strong encounters involving the BHs in these systems is 30. These binaries are formed through two distinct dynamical channels:

(1) **Binary-mediated formation**, in which binary star evolution and a series of scattering and/or exchange interactions drive a BH-non-BH binary to mass-transfer.

(2) **Triple-mediated formation**, in which a hierarchical triple with a BH-non-BH inner binary is formed through a binary-binary interaction. The inner binary is driven to Roche-lobe overflow through Lidov-Kozai oscillations.

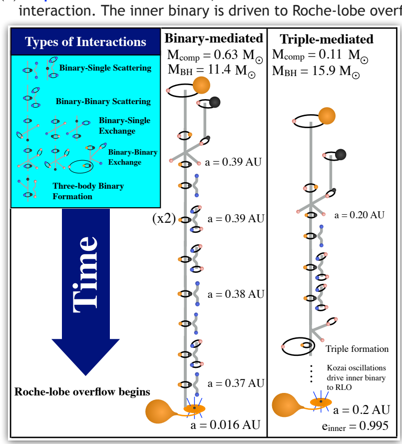

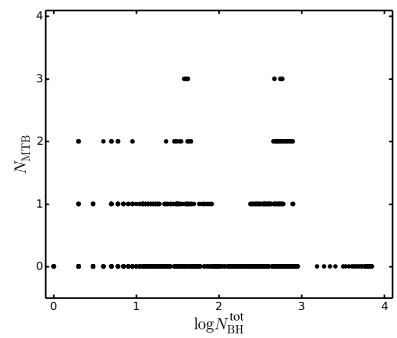

Number of MTBs (N_{MTB}) versus total number of BHs (N_{BH}^{tot}) in each cluster for all snapshots with t > 8 Gyr. **We conclude no correlation exists between the number of BH XRBs and total number of BHs in a globular cluster.**

Understanding the Lack of Correlation

BH-non-BH binaries that may eventually become BH XRBs form in regions of the cluster where BHs and non-BHs mix. The formation rate of BH-non-BH binaries within this mixing zone (MZ), given by the equation below, is found to be nearly independent of the total number of BHs within a cluster. We assume that the interactions are dominated by the widest non-BH binaries at the hard-soft boundary in the MZ.

When a large population of BHs is present, the density in the mixing zone is low, keeping the dynamical formation rate of BH-non-BH binaries low. As more BHs are ejected from the cluster, the density in the mixing zone increases, but the rate of formation is then regulated by the low number of remaining BHs. This dynamical self-regulation of the formation rate of BH XRBs is directly responsible for the lack of correlation between the number of BH XRBs and the number of BHs in a globular cluster.

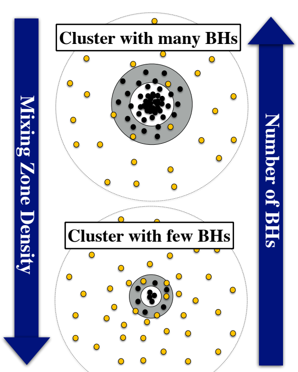

Formation rate of BH-non-BH binaries:

$$\Gamma \propto n_b \Sigma \sigma_v N_{\rm BH} \propto n \sigma_v^{-3} N_{\rm BH}$$

n_b : number density of non-BH binaries in the MZ
Σ : interaction cross section in the MZ
σ_v : velocity dispersion of BHs in the MZ
N_{BH} : number of BHs in the MZ
n : number density of non-BHs in the MZ

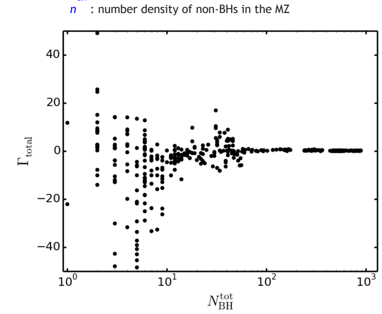

References

1) CMC Code Paper: Pattabiraman et al., 2013, ApJS, 204, 15
2) Black holes in Globular Clusters: Morscher et al., 2015, ApJ, 800, 9
3) Observed Stellar Mass BHs in Globular Clusters: Strader et al., 2012, Nature, 490, 71
4) Chomiuk, L., Strader, J., Maccarone, T. J., Miller-Jones, J. C. A., Heinke, C., Noyola, E., Seth, A. C., & Ransom, S. 2013, ApJ, 777, 69

This work was supported by NASA's ATP Grant NNX14AP92G, Chandra Theory Grant TM5-16004X/NAS8-03060, HST award HST-AR-14555.001-A, and NSF Grant AST-1716762. KK was supported by an NSF GRFP.

Mass transfer in white dwarf-neutron star binaries

Alexey Bobrick
Lund Observatory

White dwarf-neutron star binaries are an important source of ultra-compact X-ray binaries in globular clusters. These binaries inspiral and come into contact due to emission of gravitational waves. The ensuing onset of mass transfer either leads to stably transferring ultra-compact X-ray binaries or to a tidal disruption of the donor star. I will describe how the loss of mass and angular momentum in these binaries determines the outcome of mass transfer. In our recent study we showed that only helium white dwarfs with masses below about 0.2 $M_{\odot}$ evolve into stably transferring systems. We used a combination of hydrodynamic simulations and long term modelling. I will summarise the key ideas behind our approach and provide the main observational implications of the result. In particular, chemical compositions of the observed ultra-compact X-ray binaries put constraints on whether they formed from white dwarfs or non-degenerate helium-burning stars.

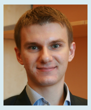

Mass Transfer in White Dwarf-Neutron Star Binaries

Alexey Bobrick, Melvyn B. Davies, Ross Church
Lund Observatory, Department of Astronomy and Theoretical Physics, Lund University

LUND UNIVERSITY

1 Abstract

The present work introduces a new method for modelling the long-term evolution of white dwarf neutron star binaries by using hydrodynamical simulations. We find that the critical mass dividing stable and unstable outcomes is about $0.2 M_\odot$, much smaller than previously thought. The eccentricity is observed to have no effect on the angular momentum loss, and may be important only if it changes on timescales shorter than those of mass transfer.

2 Observations

- About 150 detached WD-NS binaries in the Galaxy, observed as binary radio pulsars
- 10 of them will inspiral into contact in less than a Hubble time due to GW emission
- 14 systems are stably transferring material, observed as ultra-compact X-ray binaries
- Twelve Calcium-rich gap transients observed, possibly outcomes of mergers of these systems

3 Globular Clusters

- Contain about one third of known detached and transferring WD-NS binaries
- Direct collisions of neutron stars and background post-MS stars are thought to be an important formation channel
- May contain a population of radio-quiet detached WD-NS binaries which formed through exchange encounters

4 Hydrodynamical Simulations

We use a modified Smoothed Particle Hydrodynamics scheme called Oil-on-Water. It treats the stellar body (Water) separately from the atmosphere (Oil). This allows us to model arbitrarily small mass transfer rates. The present project improves on the original research by Church et al. (2009).

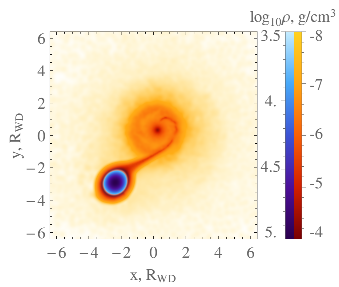

Figure: Density section in the orbital plane for a $0.15 M_\odot$ He white dwarf in a binary with a $1.4 M_\odot$ neutron star with eccentricity of 0.04. The snapshot is taken after 13 orbital periods since the beginning of the simulation.

5 Angular Momentum Loss

We use the results of our simulations to measure the amount of angular momentum lost by white dwarf neutron star binaries through mechanical disc winds. This is used to construct a model of their long-term evolution. We additionally investigate the role of eccentricity on mass transfer.

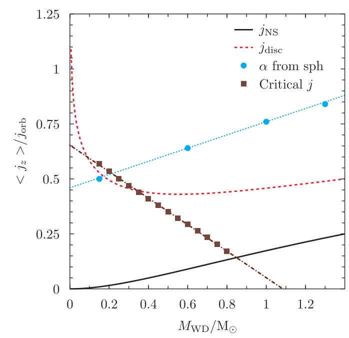

Figure: Stable systems are below the brown curve. Standard mass loss model through a jet predicts relatively low angular momentum loss (black curve). We measure that the disc winds, occurring at rates above a few $\dot{M}_{Edd}$, carry away more angular momentum, thus making more systems unstable (blue curve). This is in agreement with a semi-empirical estimate assuming that the material is removed at circularisation radius of the disc (red curve).

Below: A $0.15 M_\odot$ white dwarf in a binary with $1.4 M_\odot$ neutron star. Initially, the mass transfer rate grows exponentially over time, but then turns over, leading to formation of an ultracompact X-ray binary.

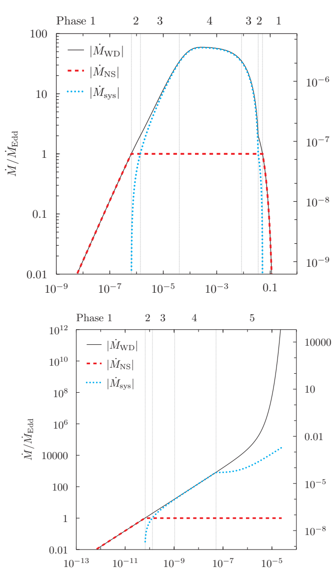

Above: A $0.75 M_\odot$ white dwarf initially undergoes a similar evolution, but the mass transfer rate does not stabilize over time, leading to a tidal disruption of the white dwarf. During phases 2-3 the jet is still visible, whereas during phases 4-5 the system is surrounded by a thick opaque envelope.

6 Long-term Evolution

- The binary spirals in due to GW emission
- The mass transfer rates reach the Eddington limit, leading to mass loss
- The coupled loss of angular momentum is critical to stability of the binaries
- Binaries containing a low-mass donor turn into stably transferring X-ray binaries
- Binaries containing a high-mass donor lead to a tidal disruption of the donor

7 Evolutionary Channels

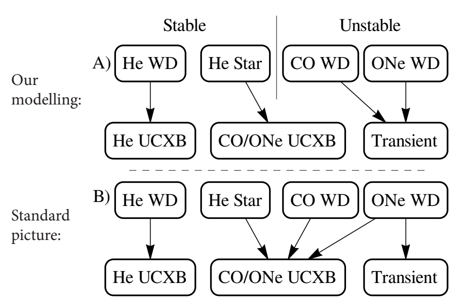

Figure: Evolutionary channels for WD-NS binaries as implied by our modelling (Panel A). The diagram differs from the one which follows from the standard jet-only model of mass loss (Panel B). Most importantly, we predict more systems to be unstable than previously thought.

WD: white dwarf, NS: neutron star, He Star: helium burning star without a hydrogen envelope, UCXB: ultra-compact X-ray binary, Transient: Ca-rich gap transient.

8 Rates and Implications

- All C-O and O-Ne white dwarfs lead to unstable mass transfer
- Ultra-compact X-ray binaries transferring C/O/Ne must have formed from non-degenerate donors, e.g. through collisions of neutron stars and horizontal branch stars
- Empirical galactic merger rates of UCXBs, binary pulsars and the observed rates of Ca-rich gap transients are consistent with our modelling

Key references:
Bobrick, Davies and Church, (2017), MNRAS, 467, 3556; Church et al, (2009), MNRAS, 395, 1127; Verbunt, (1987), ApJ, 312, L23; Ivanova et al, (2008), MNRAS, 386, 553.

E-mail: alexey@astro.lu.se, mbd@astro.lu.se, ross@astro.lu.se.

Testing the Slingshot: stellar dynamics in an oscillating filament

Tjarda Boekholt
Universidade de Aveiro

We describe a new gravitational potential based on observations of the integral shaped filament (ISF) in Orion A. The potential has two main characteristics: (1) it is cylindrical, and (2) it is time dependent as the filament shows signs of oscillatory motion. We use AMUSE to couple this potential to N-body dynamics of test particles ("stars"). We investigate the early dynamical evolution of the "stars" in the potential. We reproduce the observed spread of actual young stars in the ISF, but only when the potential is oscillating. This confirms the previously proposed Slingshot mechanism. Furthermore, stellar ejection from the filament cuts protostars off from the dense gas where they accrete their mass. We find that a constant "stellar" accretion rate, combined with the oscillating potential, can produce a Salpeter slope in the mass function.

Testing the Slingshot:
stellar dynamics in an oscillating filament

Theory & Star Formation Group

T. Boekholt, A. Stutz, M. Fellhauer, D. Schleicher and D. Matus Carrillo
Theory and Star formation Group
University of Concepcion

1. The Integral Shaped Filament in Orion A

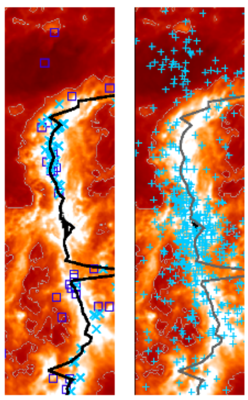

On the left we show a column density map (red shade) of the Integral Shaped Filament ((ISF) in Orion A.

Superposed are the positions of protostars (left panel) and stars with disks (right panel) (in blue). The latter are much more spread out.

What is the mechanism for this early dynamical heating of young stars?

2. The Slingshot Mechanism

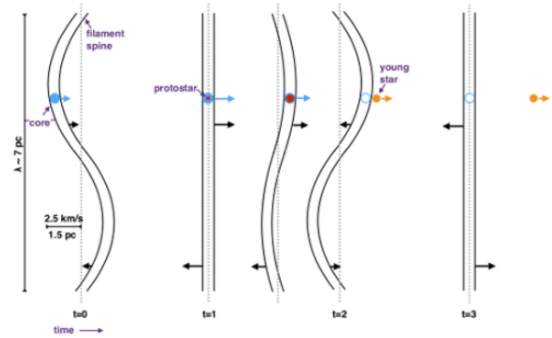

The Slingshot Mechanism provides an explanation (see cartoon above). It starts with a protostar born in the center of a gas filament, which is represented by an oscillating cylinder. The protostar becomes more massive by accreting gas. At the same time it experiences an acceleration due to the moving filament. The protostar is ejected if its inertia has grown beyond some threshold.

3. Numerical Simulations of the Slingshot

AMUSE

To test the Slingshot Mechanism we perform numerical simulations. We derive a gravitational potential based on observations of the ISF profile and let it oscillate sinusoidally. We populate the cylinder with point-particles (stars) and couple the dynamics of the potential with the stars using the AMUSE framework.

On the right we present three simulations with increasing oscillation speeds..

In the top row the filament is oscillating slowly and we hardly observe any ejections.

In the middle row, some stars are ejected towards the right, and some towards the left, leading to a spread of stars, similar to what is observed.

In the borrom row, the filament moves to fast, and all the stars are ejected.

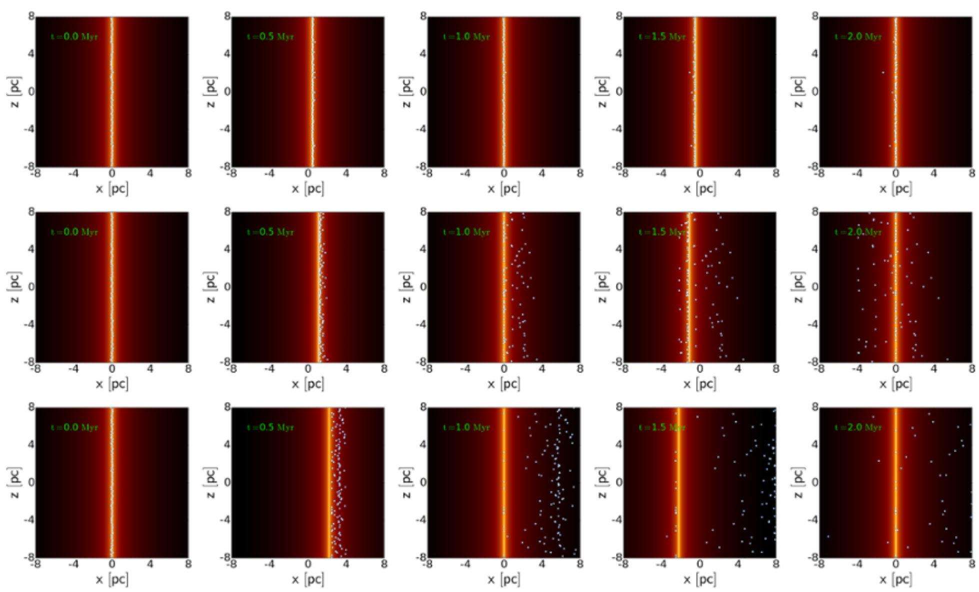

4. Dynamically Shaping the IMF

The ejection of a protostar due to the Slingshot also terminates its growth. Therefore the Slingshot provides a dynamical means of shaping the IMF.

The shape is determined by the oscillation amplitude and period of the gas filament, the accretion rate of the protostars and the coupling strength of the protostars to the gas.

On the right we show an illustrative example.

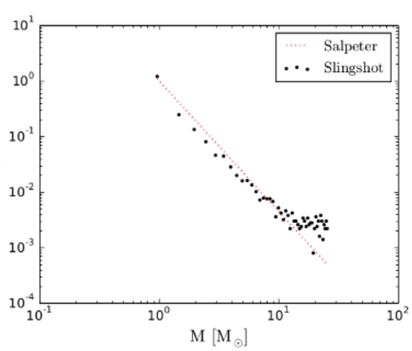

5. Discussion

We have shown that the Slingshot Mechanism can explain
- the spreading out of young stars in gas filaments
- the shape of the IMF

Alternative explanations such as stellar encounters and ejections fail as observations show that the ISF is a gas-dominated system.
The upcoming Gaia data, with accurate positions and proper motions will allow us to further scrutinize the dynamics of stars in gas filaments.

References:
Stutz and Gould 2016, Boekholt et al. 2017, Stutz 2017, Schleicher and Stutz in prep.

Stellar black hole binary mergers in open clusters

Sara Rastello
Università di Roma, La Sapienza

The recent detections of gravitational waves by the LIGO/VIRGO collaboration, produced by the merging of two massive black holes of stellar origin, provides the first evidence that such massive objects exist and may merge within the Hubble time. To investigate on the merger process, we studied the dynamical evolution of a massive black hole binary (BHB) in a star cluster of the size of typical Open Clusters in our galaxy (mass $\approx (0.8-4)\times 10^3 M_\odot$), using the NBODY7 code. Although preliminary, our results indicate that in these young, low density and dynamically active stellar systems, repeated stellar encounters can drive the BHB coalescence on reasonable time scales in a fraction of the investigated cases ($\approx 1\%$), in dependence on the host cluster properties.

Stellar Black Hole Binary Merging in Open Clusters

S. Rastello [1], I. Tosta e Melo [1,2], M. Arca Sedda [3], R. Capuzzo Dolcetta [1], G. Fragione [4]

[1] Sapienza-Università di Roma, P.le A. Moro 5, I-00165 Rome, Italy
[2] CAPES Foundation, Ministry of Education of Brazil, DF 70040-020, Brasilia, Brazil
[3] Astronomisches Rechen Insitute, Zentrum fur Astronomie der Universitat Heidelberg, Monchhofstrasse 12-14, 69120 Heidelberg, Germany
[4] Racah Institute for Physics, The Hebrew University, Jerusalem 91904, Israel

MODEST[17] , Modelling and observing dense stellar systems
Charles University September,
Prague, 18-22 September , 2017

Introduction

The recent detections of gravitational waves by the LIGO/VIRGO collaboration, produced by the merging of two massive stellar black holes, provides the first evidence that such massive objects exist and may merge within the Hubble time. To investigate the merger process, we studied the dynamical evolution of a massive black hole binary (BHB) in a star cluster of the size of typical Open Clusters in our galaxy, $M_{OC}\sim(0.8\text{-}4)10^3\ M_\odot$, using the NBODY7 code. Our results indicate that in these young, low density and dynamically active stellar systems, repeated stellar encounters can drive the BHB coalescence on reasonable timescales.

Method

In order to span a wide range of physical models, we prepared a suit of initial conditions summarized in **Table 1**: the physical parameters selected for the stellar environment are based on observations, while the BHB system is modeled on the basis of the recent LIGO/VIRGO detection (Abbott et al., 2016). We created 4 realizations of an isolated Open cluster (models S0, S1, S2 and S3), varying the total number of cluster stars (512, 1024, 2048 and 4096, respectively). Each cluster is modeled with a Plummer density profile (r_c = 1pc), a Kroupa IMF and $Z_\odot$. The BHB is initially placed in the very center of the cluster. It is formed by two equal-mass BHs (M_{BH} = 30$M_\odot$) placed at an initial distance r^i_{BHB}=0.01 pc each other. Case *a* and *b* denotes a BHB on an initial circular orbit (e_a=0.0) and on an initial eccentric orbit (e_b=0.5). We followed the dynamical evolution of such BHB for a total time of about 3 Gyr running, for each model, 150 simulations with **NBODY7** (Aarseth, 2012).

Cluster Models			BHB Models			Sets		
N_*	M_{cl} ($M_\odot$)	ρ_{cl}	M_{BHB} ($M_\odot$)	r^i_{BHB} (*pc*)	e^i_{BHB}	S_{tot}	S_{eff}	Name
512	$\sim 4\cdot10^2$	Plummer	60	0.01	0.0	150	140	S0a
					0.5	150	146	S0b
1024	$\sim 7\cdot10^2$	Plummer	60	0.01	0.0	150	146	S1a
					0.5	150	149	S1b
2048	$\sim 1\cdot10^3$	Plummer	60	0.01	0.0	150	148	S2a
					0.5	150	143	S2b
4096	$\sim 2\cdot10^3$	Plummer	60	0.01	0.0	150	144	S3a
					0.5	150	140	S3b

Tab.1: Summary of the initial conditions adopted in this work.

Results

We explored the fraction of cases, for each model, in which the BHB is ejected from the cluster as a bound system, BHB^b_{esc}, the BHB is disrupted (unbound) and expelled from the cluster, BHB^u_{esc}, and it merges BHB_{merg} (**Table 2** column 2, 3 and 4). In very low density stellar systems (S0a & S0b) the BHB is never ejected from the cluster while systems with higher density show a progressive percentage increasing of BHBs bound ejected. On the other hand, the disruption of the BHB has more scattered results with a maximum percentage of BHB^u_{esc} in model S3a. This results may indicate that high density stellar systems are more likely to eject heavy objects and binary systems.

Model S1 (*a* & *b*), shows a low percentage of merger (0.7%). As the mass of the cluster increases, the percentage of merger increases with a maximum in model S3a (7%). Both in model S2 and S3 the larger number of merger is found in case *a*. All the mergers detected occur inside the clusters, between 10 and 400 Myr with only two exceptions, at 800 Myr and 1 Gyr.

Model	BHB^b_{esc} %	BHB^u_{esc} %	BHB_{merg} %
S0a	0.0	2.9	0.0
S0b	0.0	0.7	0.0
S1a	0.7	5.5	0.7
S1b	3.4	5.4	0.7
S2a	4.7	8.1	2.1
S2b	7.7	4.9	1.4
S3a	8.3	9.1	7.0
S3b	7.1	5.7	1.5

Tab.2: Percentage fraction of BHBs escaped from the cluster bound (BHB^b_{esc}), unbound (BHB^u_{esc}) and BHBs that merge (BHB_{merg}) inside the cluster for each model.

In order to understand if the ejected (bound) BHB would merge outside the cluster in a Hubble time, we plot the distribution of the semi major axis (a) and the eccentricity (e) for all BHB^b_{esc} in each model (**Fig.2**). The colormap indicates the corresponding time of gravitational wave emission (Peters, 1964). The three red curves indicate the expected values of a and e for three fix T_{gw} (10, 15 & 20 Gyr). We observed that a small fraction of BHBs is likely to merge in a Hubble time (model S3a, S3b), while the majority of the other models will never merge in such time (T_{gw} > 20 Gyr).

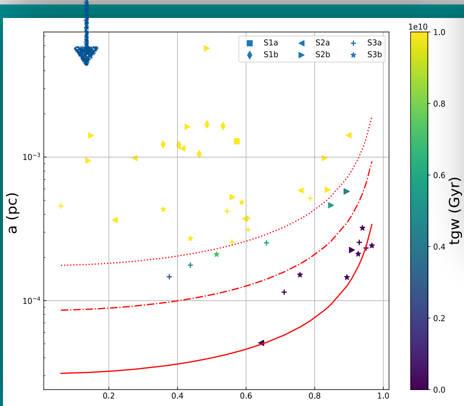

Fig. 2: The red curves indicate the expected a and e for three fix T_{gw}, (10 straight , 15 dashed and 20 Gyr, dotted, line).

To investigate the degree of shrinkage of the BHB as result of dynamical encounters with the cluster stars, we studied the evolution of its pericenter (r_p) for each model. **Fig. 3** shows the histograms of the distribution of r_p for four models (S0b, S1a, S2a, & S3b). In each plot, three histograms are overlapped, referred respectively to the following time range: 0-1 Gyr, 0-2 Gyr and 0-3 Gyr. In each histogram the dashed line indicates r_p at the beginning of the simulation $r^i_{p(a)}$=1.0e-02 pc and $r^i_{p(b)}$=3.3e-03 pc. The results for all the models are summarized in **Table 3**. Globally all these results show that the mean pericenter, $<r_p>$, decreases as time pass. This is also evident in Fig. 3 where the "peak" moves to the left as time increases. This trend gives evidence of a general decreasing of the BHB separation which, in the majority of the models, occurs soon after 1 Gyr. In some cases, there is also a "tail" at very low r_p (Fig. 3 and Table 3, column 5).

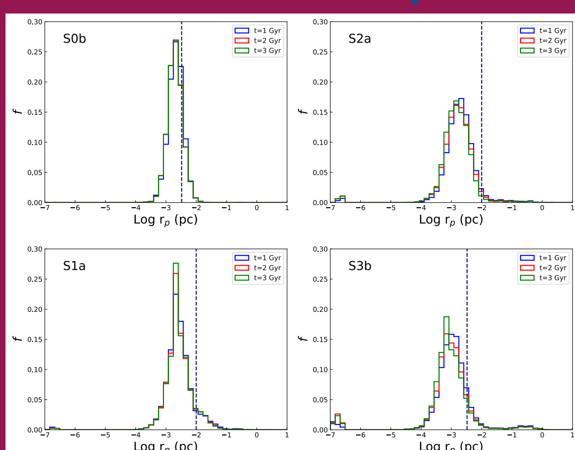

Fig. 3: Distribution of the BHB pericenters for all the simulation of model S0b, S1a, S2a and S3b *(from top left to bottom right)*. The x-axis is the logarithmic of the BHB pericenter in pc (r_p) and the y-axis the frequency (*f*).

Tab.3: Evolution of the mean BHB pericenters for all the models.

Model	r^i_p pc	T Gyr	$<r_p>$ pc	r^{min}_p pc
S0a	1.0e-02	1	2.5e-03	6.5e-05
		2	2.4e-03	3.1e-05
		3	2.4e-03	3.1e-05
S0b	3.3e-03	1	2.2e-03	1.8e-07
		2	2.0e-03	1.3e-07
		3	2.0e-03	1.3e-07
S1a	1.0e-02	1	2.5e-03	1.4e-07
		2	2.4e-03	1.4e-07
		3	2.4e-03	1.4e-07
S1b	3.3e-03	1	2.4e-03	8.7e-08
		2	2.5e-03	8.7e-08
		3	2.6e-03	8.7e-08
S2a	1.0e-02	1	2.5e-03	1.8e-08
		2	2.6e-03	1.8e-08
		3	1.5e-03	1.8e-08
S2b	3.3e-03	1	1.7e-03	9.9e-08
		2	1.6e-03	1.6e-08
		3	1.5e-03	1.6e-08
S3a	1.0e-02	1	1.1e-03	1.6e-08
		2	9.0e-04	1.5e-08
		3	8.0e-04	1.5e-08
S3b	3.3e-03	1	1.1e-03	3.9e-08
		2	9.0e-04	3.9e-08
		3	8.0e-04	3.9e-08

Conclusions

The results of our study indicate that a massive black hole binary which evolves in a low density stellar cluster may merge in a Hubble time within the cluster itself in a percentage that even if low is not negligible. Moreover, a small fraction of BHBs may coalescence outside the stellar system after they have been ejected, on reasonable time scales. In addition, in low density environments, the repeated encounters and dynamical interactions between the stars and a massive black hole binary can thus drive the shrinkage of the BHB semi major axis soon after 1 Gyr (**Rastello** et al., in prep.).

References
Aarseth S. J., 2012, MNRAS, 422, 841 422,(2012)
Abbott B. P., et al., 2016, ApJL, 818, L22
Peters, P. Phys. Rev. 136, B1224 (1964).
***Rastello** S., Arca Sedda M., Tosta e Melo I., Fragione G., Capuzzo Dolcetta R., in prep.*

Email: sara.rastello@uniroma1.it

Noise, discreteness effects and the continuum limit in N-body systems, revisited

Pierfrancesco Di Cintio
CNR-IFAC & INFN Firenze

By means of active and frozen N-Body simulations we revise the role of discreteness effects and external noise in the dynamics of self gravitating systems and non-neutral plasmas. In particular, we show that the use of frozen N-body realization may, in certain cases, lead to misleading conclusions.

Noise, discreteness effects and the continuum limit in N-body systems

Pierfrancesco Di Cintio[1,2]

[1] CNR-IFAC "Nello Carrara" Institute of Applied Physics, via Madonna del Piano 17 50022 Sesto Fiorentino, Italy;
[2] INFN-Sezione di Firenze, via Sansone 1 50022 Sesto Fiorentino, Italy

Introduction

The dynamics of $N-$body gravitational systems, due to the long-range nature of the $1/r^2$ force, is principally dominated by *mean field* effects rather than by inter-particle collisions for large N. Due to the extremely large number of particles it is often natural to adopt a description in the continuum ($N \to \infty$, $m \to 0$) collisionless limit in terms of the Collisionless Boltzmann Equation (CBE, see e.g. [2]) for the phase-space distribution $f(\mathbf{r}, \mathbf{v}, t)$

$$\partial_t f + \mathbf{v} \cdot \nabla_{\mathbf{r}} f + \nabla \Phi \cdot \nabla_{\mathbf{v}} f = 0, \tag{1}$$

coupled to the Poisson equation $\Delta\Phi(\mathbf{r}) = 4\pi G\rho(\mathbf{r})$.

In real systems, such as elliptical galaxies, N is always finite though large ($N \sim 10^{11}$) while the typical relaxation times excede the age of the universe. It is nevertheless interesting to question the validity of the continuum limit.

Several authors (see e.g. [8, 9, 6, 7, 10]) rely to frozen $N-$body models, namely following the dynamics of a tracer particle in the potential built up by N fixed particles for different values of N.

Here we revisit those studies and consider also the dynamics of individual tracer particle in active equilibrium $N-$body models, aiming at understanding whether information extracted from frozen models is relevant in the context of the real $N-$body problem.

Numerical methods

Initial conditions

In both frozen and active models we consider two different spherically symmetric density profiles, the flat cored Plummer profile

$$\rho(r) = \frac{3Mr_c^2}{4\pi\left(r^2 + r_c^2\right)^{5/2}}; \tag{2}$$

and the centrally cusped Hernquist profile

$$\rho(r) = \frac{M}{2\pi r_c^2 r(1 + r/r_c)^3}, \tag{3}$$

Where M is the the total mass and r_c a scale radius. Potentials generated by those distributions are integrable thus admitting only regular orbits. In order to generate the velocities for the active simulations, we use the standard rejection technique to sample the isotropic equilibrium phase-space distribution function f obtained from ρ with the Eddington inversion [4] as

$$f(\mathcal{E}) = \frac{1}{\sqrt{8}\pi^2}\frac{\mathrm{d}}{\mathrm{d}\mathcal{E}}\int_{\mathcal{E}}^{0}\frac{\mathrm{d}\rho}{\mathrm{d}\Phi}\frac{\mathrm{d}\Phi}{\sqrt{\Phi - \mathcal{E}}}. \tag{4}$$

The integrator

We use a family of symplectic integrators with order between 1 and 4. When the Hamiltonian $H(\mathbf{p}, \mathbf{q})$ is separable in kinetic and potential part such that

$$H(\mathbf{p}, \mathbf{q}) = K(\mathbf{p}) + U(\mathbf{q}), \tag{5}$$

symplectic integrators in the operator splitting form are best suited to solve the associated Hamilton equtions $-\partial H/\partial q = \dot{p}$; $\partial H/\partial p = \dot{q}$. In our case where the potential is given by the static density distribution, the Hamiltonian of our problem becomes

$$H = \frac{\mathbf{p}^2}{2m} + U(\mathbf{q}); \quad \mathbf{p} = m\mathbf{v}, \mathbf{q} = \mathbf{r}, \tag{6}$$

where $U = \Phi(\mathbf{q})$.

Let us now for reasons of simplicity consider a one degree of freedom case $H(p, q)$ and substitute the canonical pair of coordinates with $z = (q, p)$. The Hamilton equations become in terms of Poisson brackets $\dot{z} = [z, H(z)] = \mathcal{D}z$, whose solution in terms of matrix exponential is given by

$$z(\tau) = \exp(\tau\mathcal{D})z(0), \tag{7}$$

where τ corresponds to the suitable discretization of time. Expanding the operator $\mathcal{D}$ in terms of Kinetic and potential terms on has

$$\exp(\tau\mathcal{D}) = \prod_{i=1}^{k}\exp(c_i\tau\mathcal{K})\exp(d_i\tau\mathcal{U}) + O(\tau^{k+1}). \tag{8}$$

The sum in k of the real constants c_i and d_i yields 1. Turning back to conjugate coordinates p and q this corresponds to a iterable symplectic combination of mappings of the form

$$q_{n+1/2} = q_n + \tau c_i\frac{\partial K}{\partial p}(p_n), \quad p_{n+1/2} = p_n \tag{9}$$

and

$$q_{n+1} = q_{n+1/2}, \quad p_{n+1} = p_{n+1/2} - \tau d_i\frac{\partial U}{\partial q}(q_{n+1/2}). \tag{10}$$

The order of the algorithm is given by the number k of iterations required during a timestep τ while, in general, the values of the coeffcients c_i and d_i are not obtainable analytically in terms of simple functions but can be obtained recursively according to the Baker-Campbell-Hausdorff formula.

Results I

In order to compare on the same scale different simulations, we use normalized units where positions times and velocities are given in units of r_c, $t_* = \sqrt{r_c^3/GM}$ and $v_* = r_c/t_*$, respectively.

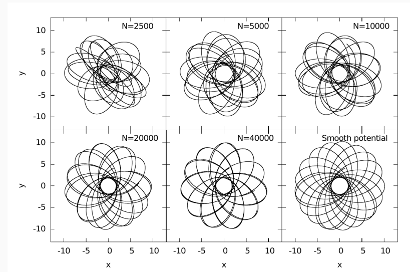

Consistently with previous work [6, 10], the orbits evolved in the frozen $N-$body potential qualitatively resemble orbits integrated in the parent smooth potentials as N increases, see Fig. above for a Plummer model.

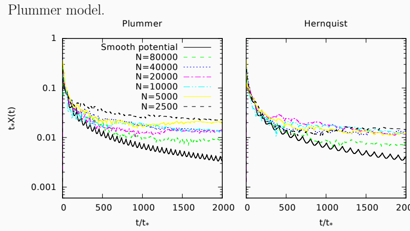

Using the Benettin-Galgani-Strelcyn technique [1] we evaluate the maximum Lyapunov exponent $\Lambda_{\max}$ for all orbits as the limit for large t of

$$\chi(t) = \frac{1}{n\Delta t}\sum_n \ln\left|\frac{\delta Z(n\Delta t)}{d}\right|, \tag{11}$$

where δZ is the distance between the reference orbit and the evolved perturbation implemented as an euclidean norm in 6D, and d is the distance between the initial condition and the perturbation. The perturbation is typically taken of the order of 10^{-9} in double precision while using a third order scheme for the numerical integration with $\Delta t = t_*/200$. From the figure above appears clear that for both models explored the maximum Lyapunov exponent of the orbits evolved in forzen potentials rapidly relaxes to a small finite value while (as expectable), it stedily goes to 0 for the orbits evolved in smooth (integrable) potential. Remarkably, such value seamingly does not depend much on N when $N < 15000$.

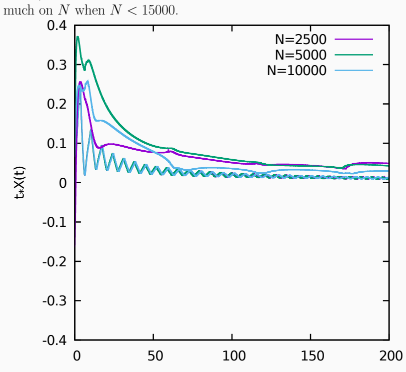

Surprizingly, $\Lambda_{\max}$ shows little dependence on N for active systems and rapidly converges to *lower* values than its counterpart for frozen systems even though individual orbits in configuration space appear to be less regular.

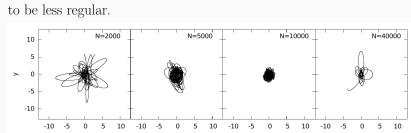

We interpret this fact as a hint that the continuum limit shall be questioned at least concerning the concept of $N-$body chaos [5]. In particular, the diffusion in phase-space (connected to relaxation phenomena such as violent relaxation and phase mixing) should be quite different in the two cases since in a froze model the single particle energy is always conserved independently on N, while in active $N-$body models particles could exchange energy, even in the limit of $N \to \infty$.

Results II

We introduce now the so-called emittance [7], a quantity introduced in the context of charged particles beams associated to the diffusion in phase-space, defined by

$$\epsilon = (\epsilon_x\epsilon_y\epsilon_z)^{1/3}, \quad \epsilon_i = \sqrt{\langle r_i^2\rangle\langle v_i^2\rangle - \langle r_i v_i\rangle^2}, \tag{12}$$

where $\langle ...\rangle$ indicate ensamble averages.

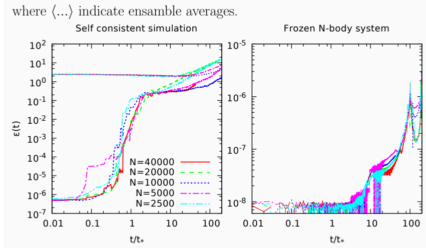

The emittance of a cluster of tracers in an active $N-$body simulation is compared to the same quantity for a subset of active particles and that of a cluster in a frozen $N-$body simulation. For large N ϵ grows in the same fashion for both tracers and active particles in the self-consistent simulation, while it retains lower values for the frozen case. This is apparenlty in contraddiction with what observed for $\Lambda_{\max}$. However, a lower emittance in the frozen cases is simply a consequence of the long lasting correlations among tracer particles given by the fixed distribution of scatterers (i.e. finite N noise) and has nothing to do with the chaoticity of the model.

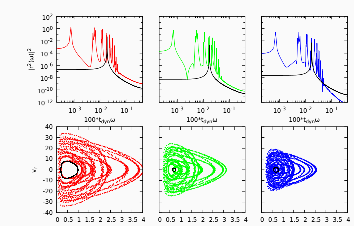

On the other hand, orbits integrated in the self consistent simulation experience stronger diffusion in phase-space associated with a more complex strucure of their frequency spectrum, that does not become continuum (as expected for wildly chaotic orbits) but is still characterized by a finite number of frequencies (peaks).

Conclusions

The main results of this preparatory study can be summarized as follows:

- Orbital structure in frozen models approaches that of continuum potentials, however the dependance on N of this trend is not trivial.
- Orbits in frozen models and active self consistent models have (obviously) different mixing properties and have, in general, different maximal Lyapunov exponents. $\Lambda_{\max}$ depends more on N in frozen systems.
- The concept of regular and chaotic orbits for large N models can not be naively extrapolated from that for lower degrees of freedom systems.
- Given that orbits in potentials of integrable models (in the continuum limit) behave differently in frozen simulations and self consistent simulations, nothing can be deduced from studies with tracer particles in frozen $N-$body models reproducing non-integrable models, such for example triaxial systems [3].

References

[1] Benettin, G.; Galgani, L.; Strelcyn, J.-M. *Phys. Rev. A* **14**, 2338 (1976)
[2] Binney, J.; Tremaine, S. Galactic dynamics 2nd edition, Princeton University Press NJ (2008)
[3] Di Cintio, P.F.; Sala, M., in preparation (2017)
[4] Eddington, A., *MNRAS* **76**, 525 (1916)
[5] Hemsendorf, M.; Merritt, D. *ApJ* **580**, 606 (2002)
[6] Kandrup, H.E.; Sideris, I.V. *ApJ* **585**, 244 (2003)
[7] Kandrup, H.E.; Sideris, I.V.; Bohn, C.L. *Phys. Rev. St Acc. B.* **7**, 14202 (2004)
[8] Kandrup, H.E.; Sideris, I.V. *Phys. Rev. E* **64**, 56209 (2001)
[9] Sideris, I.V.; Kandrup, H.E. *Phys. Rev. E* **65**, 66203 (2002)
[10] Meschiari, S. Bs Thesis, Bologna University (2006)

Supernova Kicks and Dynamics of Compact Remnants in the Galactic Centre

Elisa Bortolas
University of Padova / INAF-OAPd

The Galactic Centre (GC) is a unique place to study the extreme dynamical processes occurring near a massive black hole (MBH). In this work I study the role of supernova (SN) explosions occurring in massive binary stellar systems lying in a discy structure within the innermost pc. In this poster I show the results of a suite of 3-body simulations of binaries orbiting the central MBH, while the primary star undergoes a SN explosion. The associated kicks scatter the lighter stars in the pair on completely new orbits, with higher eccentricity and inclination. In contrast, stellar black holes (BHs) and massive stars retain memory of the orbit of their progenitor star. My results suggest that SN kicks are not sufficient to eject BHs from the GC: all BHs that form in situ in the central parsec of our Galaxy probably remain in the GC, building up a cluster of dark remnants. I also present the implications of this study on the observed dearth of NSs in the GC and I speculate on the possible origin of peculiar GC objects, such as the S-stars, G1 and G2.

Supernova Kicks and Dynamics of Compact Remnants in the Galactic Centre

Elisa Bortolas
Universita` di Padova
INAF - Osservatorio Astronomico di Padova
✉elisa.bortolas@phd.unipd.it

Introduction

The Galactic Centre (GC) is an ideal laboratory to study the extreme dynamical processes occurring in proximity of a super-massive black hole (SMBH).

The GC is a very crowded and puzzling place, and it still poses a plethora of questions:

- What is the origin of the S-cluster of young B stars around the SMBH?
- What is the nature of G1 and G2, two dusty objects recently spotted near the SMBH?
- Why pulsars seem to be missing in the GC?
- Why do we observe a cored distribution of red giants instead of a cuspy one?

We make use of **3-body simulations** to understand **what is the role of Supernova (SN) explosions occurring in binary stellar systems within the GC** ?

SN kicks may:

- reshuffle the orbits of pulsars, other dark remnants and red giants
- push low mass stars into highly eccentric orbits, such as the ones of G1and G2

Methods

- We perform 30k **regularized** 3-body simulations
- *In each run:*
  1. a stellar binary is placed within the clockwise disk and orbits around the SMBH
  2. the more massive (primary) star explodes as a SN
  3. the perturbed stellar system is evolved around the SMBH for 1 Myr

An example in the right Fig.

Orbits of the two stars before and after the SN kick in a selected run

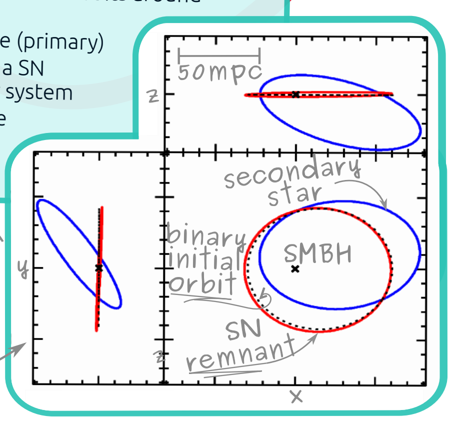

Results

- After the kick, the **lighter stars** (i.e. neutron stars or low mass secondary binary components) are generally scattered on completely **different orbits**, with higher eccentricities and inclinations.

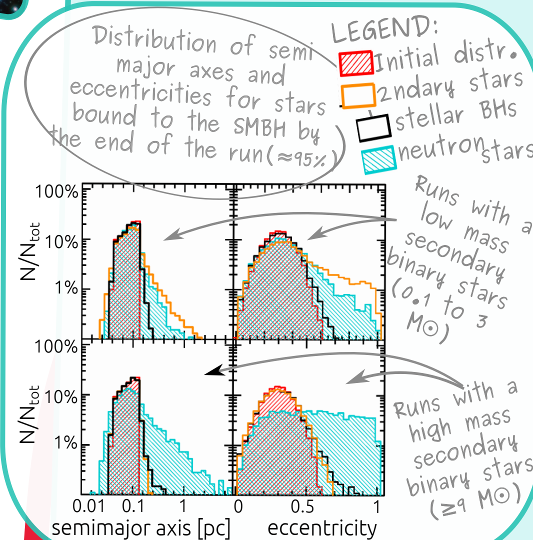

- Stellar mass **black holes** (BHs) and **massive secondary stars retain memory of their initial orbit** instead (Fig. on the left).
- ~40% of remnants stay bound to the companion after the SN kick → up to 70% of them might become **X-ray binaries** through Roche lobe filling.
- ~3% of the low mass secondary star orbits are compatible with those of **G1** and **G2** (right scatter plot).

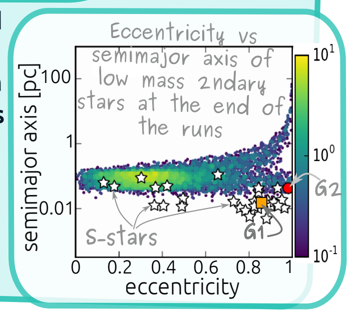

Conclusion

- **BHs** do not change their orbits significantly →a **cusp of BHs** may have formed around the SMBH
- **Neutron stars** are generally scattered away from the SMBH → the missing pulsars problem may be a result of SN natal kicks.
- **G1**and **G2** might have been low-mass stellar companions to massive GC stars.

Bortolas, Mapelli & Spera 2017, MNRAS, 469, 1510

Binary Star Cluster Population in the Milky Way and LMC

Mochamad Ikbal Arifyanto
Dept. of Astronomy, Institut Teknologi Bandung

We present the statistical analysis of binary star cluster population in Milky Way (MW) and Large Magellanic Cloud (LMC). The data is collected from several published catalogues, complemented by original data produced in our study. We determined the empirical distribution of MW and LMC's binary star clusters. From the established distributions, it can be deduced that the binary clusters tend to be young (less than 100 Myr) while their locations coincide with the locations of star forming complexes. There is an indication that the binary fraction increases with the rise of star formation rate in the last millions years. In the LMC, the increasing of binary fraction at $t \approx -100$ Myr can be associated to the last episode of close encounter with the Small Magellanic Cloud at $t \approx -150$ Myr. This observational evidence supports the theory of binary cluster formation through fission of molecular clouds where the encounter between galaxies enhanced the clouds velocity dispersion, which in turn increased the probability of cloud-cloud collisions that produce binary clusters.

Binary Star Cluster Population in the Milky Way and LMC

Rhorom Priyatikanto[1] and Mochamad Ikbal Arifyanto[2]
[1]Space Science Center, National Institute of Aeronautics and Space, Indonesia | rhorom.priyatikanto@lapan.go.id
[2]Department of Astronomy, Institut Teknologi Bandung, Indonesia | ikbal@as.itb.ac.id

Background

- Star clusters were born from giant molecular clouds that contracted gravitationally and fragmented.
- Hierarchical fragmentation during cluster formations may produce cluster families or even binary clusters with typical lifetime $\sim$ 100 Myr.
- Binary clusters can also be formed through sequential formation and tidal capture, but cloud fission induced by oblique collision is believed to contribute more.
- Improved census of clusters in the Milky Way (MW) and neighboring Large Magellanic Cloud (LMC) provide clue about binary star population and their formation history.

Objectives

- To identify binary cluster candidates in the Milky Way and LMC.
- To construct empirical distributions of binary cluster, in particular the age distribution that shed light on the formation history of this population.

Data and Methods

- Cluster catalogue used in this study:
  - **Milky Way Star Clusters** (Kharchenko et al. 2013) – 3006 clusters with position, distance, age, size, and proper motion. The catalog is complete up to 1.8 kpc from the Sun, consist of 1414 clusters.
  - **The LMC Extended Objects** (Bica et al. 2008) – 3086 clusters with position and size. Cluster ages are compiled from Bica et al. (1996), Pietrzynski et al. (2000), Glatt et al. (2010), Popescu et al. (2012), and complemented by original data produced in our study using CMD fitting.
- There are 104 MW clusters identified as the member of pairs/groups with physical separation $s \leq 30$ pc. The average binary fraction is 7%.
- In the LMC, 634 clusters identified in pairs/groups. Based on Monte Carlo simulations, it was found that approximately 310 clusters are possibly chance pairs. Thus, binary fraction for the LMC cluster is $\sim$ 10%.

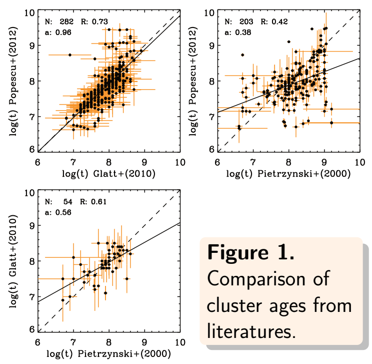

Figure 1. Comparison of cluster ages from literatures.

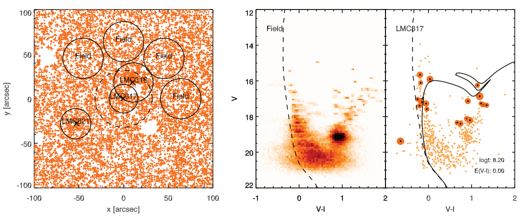

Figure 2. Photometry data from MCPS (Zaritsky et al. 2004) and OGLE (Udalski et al. 1997) were analyzed in order to estimate LMC clusters' ages. For each cluster, the CMD was decontaminated from field stars before isochrone fitting.

Results and Discussion

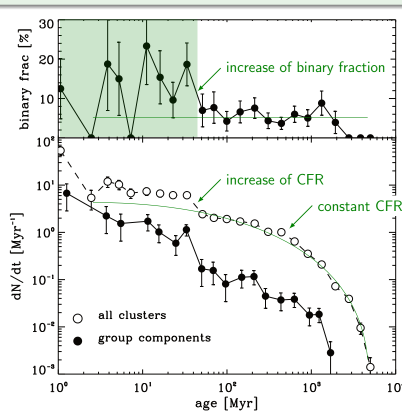

Figure 3. Age distribution of clusters in the Milky Way (open circle) and clusters in pairs/groups (filled circle). Binary fraction is defined as the ratio between the number of clusters in pairs/groups and the overall clusters in every age bin.

At $t = -40$ Myr, binary fraction significantly increased along with the rise of cluster formation rate (CFR). Young clusters tend to be in pairs/groups.

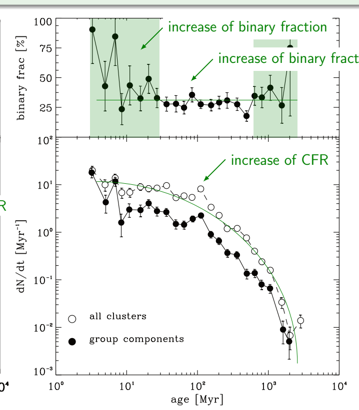

Figure 4. Age distribution and the variation of binary fraction in the LMC. Not all clusters analyzed here have determined age, such that the obtained binary fraction is higher than the actual value.

High binary fraction for young clusters is observed. The increase of both CFR and binary fraction are prominent at $t \approx -150$ Myr $\rightarrow$ related to the latest episode of LMC-SMC encounter (Bekki & Chiba 2005).

Distribution of pair separation (Figure 5) exhibits positive trend with obvious fluctuation, or multimodal distribution. For the case of MW cluster pairs, the first two peaks are located at 7 and 15 pc. Fore the case of LMC, the peaks are at 6 and 12 pc.

Multimodal distribution is likely to be related to the stability of binary clusters from dynamical point of view (e.g. Priyatikanto et al. 2016). A gap at 10 pc may be related to the merger-separation boundary resulted from the dynamical simulation of typical binary clusters with planar prograde orbit.

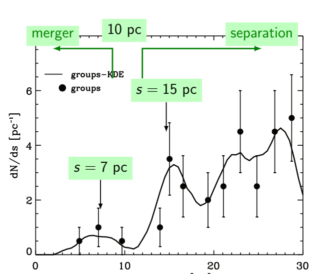

Figure 5. Distribution of pair separation in MW.

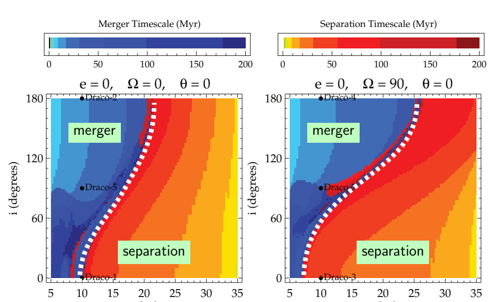

Figure 6. Estimation of binary cluster life time in MW from Priyatikanto et al. (2016).

Conclusions

- Clusters tend to be formed in groups and the rise of cluster formation rate is usually in line with the increase of binary fraction.
- The increase of binary fraction at $t \approx -150$ Myr supports the theory of binary cluster formation through oblique collision of molecular clouds.
- Multimodal distribution of 'physical separation' of cluster pairs in MW is likely to be related to the stability issue.

Acknowledgement

This research is supported by Hibah Riset Desentralisasi Ristekdikti. MIA acknowledge the travel grant from Institut Teknologi Bandung through P3MI.

References

Bekki & Chiba. 2005, MNRAS 356:680
Bica et al. 1996, ApJS 102:57
Bica et al. 2008, MNRAS 389:678
Glatt et al. 2010, A&A 517:A50
Pietrzynski & Udalski. 2000, ActAstr 50:355
Popescu et al. 2012, ApJ 751:122
Priyatikanto et al. 2016, MNRAS 457:1339
Udalski et al. 1997, ActAstr 47:319
Zaritsky et al. 2004, AJ 128:1606

A new spherical basis set for halo expansions

Edward Lilley
Institute of Astronomy, University of Cambridge

Halo expansion (HEX) techniques can provide a compact way of describing numerically constructed cosmological haloes, incorporating non-spherical effects; and they can provide the basis functions for self-consistent field expansion algorithms for evolution of N body systems. We construct a completely new family of biorthogonal basis sets using the Hankel transform of the Laguerre polynomials. The lowest-order density profiles are cusped at small radii as $r^{(-2+1/a)}$, and have asymptotic density fall-off like $r^{(-3-1/(2a))}$. Here, a is a parameter satisfying $a > 1/2$. The family therefore spans the range of inner density cusps found in numerical simulations, but has much shallower and hence more realistic outer slopes than the corresponding members of the family deduced by Zhao (1996) and exemplified by Hernquist & Ostriker (1992). We focus on the $a = 1$ case, whose lowest-order density has a $1/r$ cusp and falls off as $r^{(-3.5)}$, similar to NFW.

A new family of basis sets for halo expansions

Edward Lilley*, Jason Sanders, N. Wyn Evans

Institute of Astronomy, University of Cambridge

*ejl144@cam.ac.uk

Overview of bi-orthogonal basis sets

- Calculating the force on each particle in an N-body simulation is expensive, requiring $O\left(N^2\right)$ steps. Things are considerably simplified if we have a set of potential-density pairs satisfying

$$\int d^3\vec{r}\ \Phi_i\,\rho_j^* \propto \delta_{ij}, \qquad \nabla^2\,\Phi_i = 4\pi G\,\rho_i$$

- We can approximately represent any density ρ and potential Φ using a truncated series of basis functions

$$\Phi\left(\vec{r}\right) = \sum_i C_i\,\Phi_i\left(\vec{r}\right), \qquad \rho\left(\vec{r}\right) = \sum_i C_i\,\rho_i\left(\vec{r}\right)$$

- If the density is formed of a cloud of N point-like particles, finding the coefficients C_i is simply a sum over those N points,

$$\rho(\vec{r}) = \sum_j^N m_j\,\delta\left(\vec{r}-\vec{r}_j\right), \qquad C_i = \int d^3\vec{r}\ \Phi_i\,\rho = \sum_j^N m_j\,\Phi_i(\vec{r}_j)$$

- We call a basis set *spherical* when the angular part of the basis functions is expressed using spherical harmonics. If we fix the maximum radial order to $n_{\max}$ and the maximum angular order to $l_{\max}$, we have $\left(n_{\max}+1\right)\left(l_{\max}+1\right)^2$ terms in total

$$\Phi_{nlm}\left(\vec{r}\right) \equiv \Phi_{nl}(r)\,Y_{lm}(\theta,\phi), \qquad \rho_{nlm}\left(\vec{r}\right) \equiv \rho_{nl}(r)\,Y_{lm}(\theta,\phi),$$

$$\Phi\left(\vec{r}\right) = \sum_{n=0}^{n=n_{\max}}\sum_{l=0}^{l=l_{\max}}\sum_{m=-l}^{m=l}\Phi_{nlm}\left(\vec{r}\right).$$

- The complication comes when trying to find a simple form for the radial basis functions $\Phi_{nl}(r)$ and $\rho_{nl}(r)$; these must obey

$$\int r^2\,dr\,\Phi_{nl}\,\rho_{n'l} \propto \delta_{nn'}, \qquad \left(\nabla^2 - \frac{l(l+1)}{r^2}\right)\Phi_{nl} = 4\pi G\,\rho_{nl}, \qquad \forall\, l\in\mathbb{Z}^+$$

- We have developed a general method of calculating basis functions that obey this condition, by Hankel-transforming sets of functions that are orthogonal on $(0,\infty)$.

Our family of basis sets

- While basis sets for cylindrical systems are abundant in the literature, spherical basis sets are somewhat rarer, and all those currently in use are in fact special cases of that of Zhao (1996), who generalised both the original basis set of Clutton-Brock (1973) and the subsequent one of Hernquist & Ostriker (1992).
- It is desirable that the lowest-order term in the expansion capture the overall form of the system as well as possible. Zhao's basis set illustrates this well, as the form of the lowest-order density function is (in units where the scale length equals unity)

$$\rho_{000}^{\text{Zhao}} \propto \frac{1}{r^{2-1/\alpha}\left(1+r^{1/\alpha}\right)^{\alpha+2}},$$

which reproduces the well-known models of Plummer and Hernquist when $\alpha = 1/2$ and $\alpha = 1$ respectively.

- We introduce a new basis set whose lowest-order in density is

$$\rho_{000}^{\text{LSE}} \propto \frac{1}{r^{2-1/\alpha}\left(1+r^{1/\alpha}\right)^{\alpha+3/2}}.$$

Here the $\alpha = 1/2$ basis set gives de Zeeuw's perfect sphere at lowest order, and was discovered (in a slightly different form) by Rahmati & Jalali (2009). Basis sets with $\alpha > 1/2$ are completely new, and we note particularly the $\alpha = 1$ case,

$$\rho_{000}^{\text{SH}} \propto \frac{1}{r\,(1+r)^{5/2}},$$

which we dub the *super-Hernquist* (SH) model. It has properties intermediate between those of the NFW and Hernquist models, and has an analytical distribution function in the spherically-symmetric case.

- Our basis functions are all expressed in terms of well-known analytical functions. For example, the SH radial density basis functions are written using the Gegenbauer polynomials,

$$\rho_{nl}\left(\vec{r}\right) \propto \frac{r^{l-1}}{(1+r)^{5/2+2l}}\left[(3/2+n+2l)\,C_n^{(3/2+2l)}\left(\frac{r-1}{r+1}\right) - (1/2+n+2l)\,C_{n-1}^{(3/2+2l)}\left(\frac{r-1}{r+1}\right)\right].$$

Expanding flattened NFW halos

We take the $\alpha = 1$ *super-Hernquist* (SH) member of our family of basis sets and use it to represent flattened NFW models; we compare this with the Hernquist & Ostriker (1992) (HO) basis set (the $\alpha = 1$ member of Zhao's family), which is the basis set most commonly used in the literature to expand halos, for example to study stellar streams – see e.g. Lowing et al. (2011); Ngan et al. (2015).

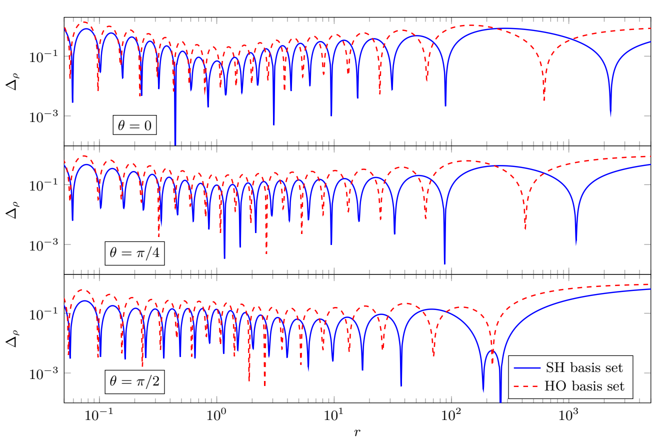

Fig. 1: Expansion of a flattened ($q = 0.8$) NFW density. Viewing angle θ is shown on each plot. Both expansions use radial terms up to $n = 20$ and angular terms up to $l = 12$. The error measure is $\Delta_\rho \equiv log\left|1-\rho_{\text{approx}}/\rho_{\text{exact}}\right|$ (lower is better; the dips are due to the oscillations around the true value).

Expanding numerical halos

We analysed a suite of numerical dark matter halos, each consisting of around 10 million particles. We fit the zeroth-order basis functions to the halo to find the scale-length and the parameter α (typically $1 < \alpha < 1.5$) and then represent the halo using a truncated series of basis functions.

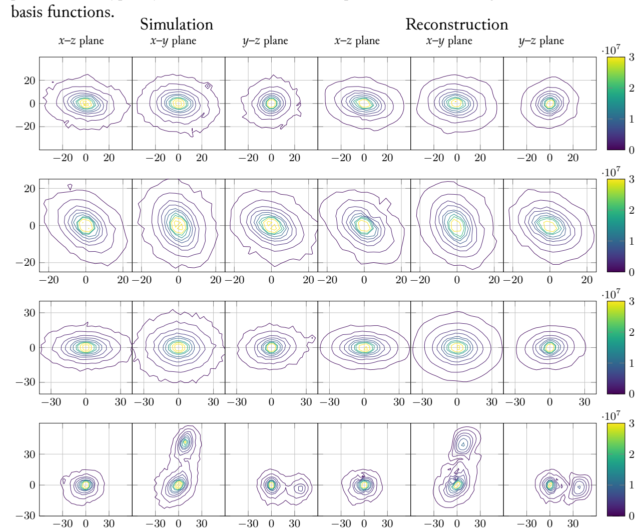

Fig. 2: From left to right: the three principal planes of the original numerical halo, then the same three principal planes of the halo as reconstructed with basis functions up to $n = 20$ and $l = 12$. Distances are in kpc, and the densities are in $M_\odot\,\text{kpc}^{-3}$.

Bibliography

References

Clutton-Brock M., 1973, Ap&SS, 23, 55

Hernquist L., Ostriker J. P., 1992, ApJ, 386, 375

Lowing B., Jenkins A., Eke V., Frenk C., 2011, MNRAS, 416, 2697

Ngan W., Bozek B., Carlberg R. G., Wyse R. F. G., Szalay A. S., Madau P., 2015, ApJ, 803, 75

Rahmati A., Jalali M. A., 2009, MNRAS, 393, 1459

Zhao H., 1996, MNRAS, 278, 488

Acknowledgements

Edward Lilley and Jason Sanders acknowledge financial support from the UK Science and Technology Facilities Council. We thank Denis Erkal for providing us with the suite of numerically constructed cosmological halos.

Initial Dynamical Evolution of Star Clusters near the Galactic Centre

So-Myoung Park
Kyung Hee University

Recent observations have shown that star-forming regions are clumpy, substructured, and filamentary, but star clusters are bound, gas-free, and spherical. In this study, we investigate how initial fractal star clusters evolve near the galactic centre with N-body simulations. We find that clusters have to initially be contained within their (nominal) tidal radii to survive. Because our fractal star clusters have high initial densities, they very rapidly evolve into dense and spherical star clusters, therefore they are almost indistinguishable from initially spherical clusters. The density at which Galactic Centre clusters like the Arches must have formed is therefore set by their formation distance from the GC, and if the Arches formed at 100pc from the GC its initial density could have been several times lower than its current value.

Initial Dynamical Evolution of Star Clusters Near the Galactic Centre

So-Myoung Park[1], Simon P. Goodwin[2], & Sungsoo S. Kim[1,3]

smpark12@khu.ac.kr

[1]School of Space Research, Kyung Hee University
[2]Department of Physics & Astronomy, University of Sheffield
[3]Department of Astronomy & Space Science, Kyung Hee University

ABSTRACT

We investigate how initial Plummer and fractal star clusters evolve near the Galactic centre (GC) with N-body simulations to examine which initial conditions can give us the Arches-like young massive star cluster. We find that clusters have to initially be contained within their (nominal) tidal radii to survive. Because our star clusters have high initial densities, they very rapidly evolve into dense and spherical star clusters, therefore they all look extremely similar after 2 Myr, no matter how they start. The density at which Galactic Centre clusters like the Arches must have formed is therefore set by their formation distance from the GC. That is, a lower limit of the initial density of the Arches cluster is ~ 600 $M_\odot$ pc^{-3} at ~30 pc from the GC and ~ 200 $M_\odot$ pc^{-3} at ~100 pc from the GC.

INTRODUCTION

One of the important routes to understanding star formation are star clusters. Many young stars are observed in dense, spherical clusters (Lada & Lada 2003) even in regions where the tidal field is strong, e.g. the Arches and Quintuplet clusters whose *projected* distance is ~30 pc from the GC. Star forming regions, however, are often found to be substructured (Arzoumanian et al. 2011). Numerical simulations have shown that dense, spherical star clusters can form from initially fractal distributions without a tidal field (Allison et al. 2009). But do Arches-like star clusters have to form as we now see them, or can they collapse from larger, substructured distributions? In this poster, we present the results of simulations of star cluster evolving in a (very) strong tidal field.

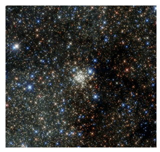

Arches Cluster
(Credit: NASA/ESA)

METHOD & INITIAL CONDITIONS

Method

- We use NBODY6 code modified by Kim et al. (2000).
- The strong tidal fields are applied: 30 pc & 100 pc from the GC.
  → Enclosed mass: 5.5×10^7 $M_\odot$ & 6.4×10^8 $M_\odot$, respectively. (Launhardt et al. 2002)
- We make three star clusters: low, intermediate, and high densities.

Initial conditions

* M: The mass of cluster * R_t: Tidal radius * R_{gc}: Galactocentric radius * IMF: Initial Mass Function

Initial distributions	M	R_t		IMF
Fractal (Goodwin & Whitworth 2004)	~ 2 × 10^4 $M_\odot$ (Kim et al. 2000)	~ 2 pc (R_{gc} ~ 30 pc)	~ 3 pc (R_{gc} ~ 100 pc)	Maschberger 2013
Plummer (Aarseth, Henon & Wielen 1974)				

RESULTS

* ▲ : The 10 most massive stars * R_c: The total (outer) cluster radius * Q: Virial ratio

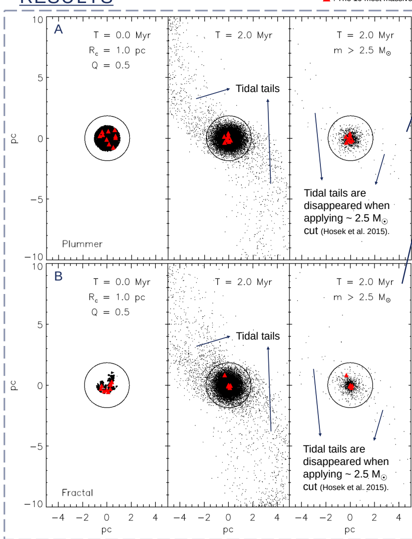

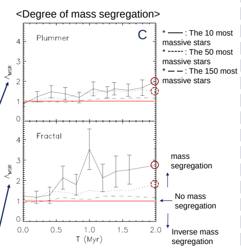

I. Well-contained clusters (R_{gc} = 30 pc)

1. Plummer (A): In 2 Myr, it has not evolved significantly.

2. Fractal (B): In 2 Myr, it rapidly evolves like a Plummer sphere, erasing initial substructures, because of a *violent relaxation* (Allison et al. 2009).

→ In Fig. C , the fractal is slightly more mass segregated then the Plummer sphere.

∴ *Fractals are more dynamically evolved than the Plummer spheres because of a rapid violent relaxation.*

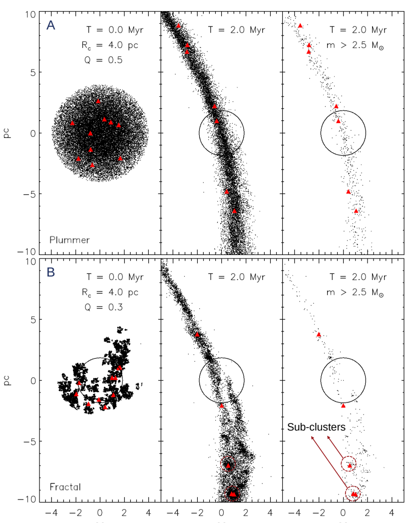

III. Overflowing clusters (R_{gc} = 30 pc)

1. Plummer (A): It shredded apart in 2 Myr.

2. Fractal (B): It also shredded in 2 Myr, but some sub-clusters can survive.

∴ *The Plummer spheres and fractals cannot survive as a single cluster, however, there are some surviving sub-clusters in the fractal case.*

IV. R_{gc} = 100 pc:

Usually the results are simply scaled-up versions of those at 30 with some subtle differences.

1. Well-contained clusters: As in the 30 pc case, both Plummer and fractal initial conditions evolve very similar to each other by 2 Myr. However, *if R_c = 2 pc, their dynamical evolution is slightly slower so they mass segregate to a slightly lesser degree than for well-contained clusters at 30 pc*.

2. Just-contained clusters: Both Plummer and fractal initial conditions evolve very similarly to the 30 pc case. However, *the Plummer sphere is destroyed on a longer time scale because of the weaker tidal field and a longer dynamical timescales.*

3. Overflowing clusters: As at 30 pc case, the Plummer spheres are completely destroyed. However, *in the fractal case, there are considerable surviving overdensities, often in a long 'filament', because of the weaker tidal field.*

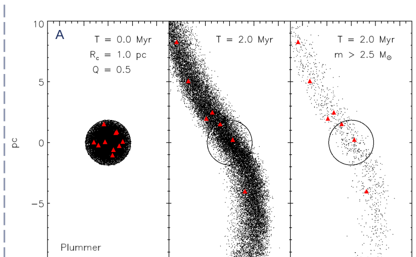

II. Just-contained clusters (R_{gc} = 30 pc)

1. Plummer (A): In 2 Myr, it has not survived as a cluster.

2. Fractals:
 a. Tepid (Q = 0.5) fractal (B): In 2 Myr, it has survived as a star cluster *within the tidal radius*.
 b. Cool (Q = 0.3) fractal (C): In 2 Myr, we can see a surviving substructures *on the tidal arms*.

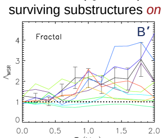

→ In Fig. B′, we run 10 ensembles of Fig. B by only changing the random number seed. *Around half of them shows significant mass segregation.*

∴ *The Plummer spheres cannot survive as a cluster while fractals can.*

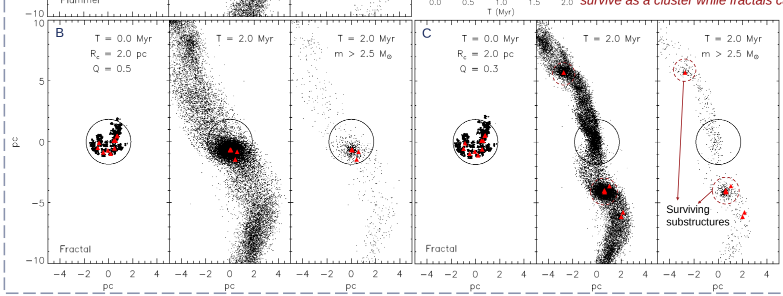

CONCLUSION

We investigate the early evolution of ~ 2 × 10^4 $M_\odot$ Plummer and fractal initial conditions in a strong tidal fields at ~ 30 and ~ 100 pc from the GC where the nominal tidal radii are ~ 2 and ~3 pc respectively.

We perform *N*-body simulations using NBODY6 code with full tidal fields (Kim et al. 2000).

1. Both Plummer sphere and fractal initial conditions that are well-contained within the nominal tidal radii survive for 2 Myr as distinct bound clusters.
 - Fractals evolve dynamically faster than Plummer spheres, erasing initial substructures due to a rapid violent relaxation. Hence all surviving clusters look very similar at 2 Myr.
 - They give rise to tidal tails of low-mass stars that would be difficult to observe at the GC.

2. If the initial conditions completely fill the tidal radius then if a single significant cluster survive depends somewhat on the initial conditions.
 - Plummer spheres are destroyed.
 - Tepid (virial ratio 0.5) fractals survive, but cool (virial ratio 0.3) fractals destroyed (but substructure often survives).

3. Any initial conditions that overflow the nominal tidal radius are destroyed.
 - But if the initial conditions are fractal then significant 'subclusters' can survive.

∴ *If a single significant cluster like the Arches cluster survives then after 2 Myr it appears as a mass segregated Plummer-like object irrespective of the initial conditions.*
→ *If the Arches-like cluster formed at 30 or 100 pc from the GC, this sets a lower limit on the formation density > 600 $M_\odot$ pc^{-3} and at 30 pc, or > 200 $M_\odot$ pc^{-3} at 100 pc.*

REFERENCES

Aarseth S. J., Hênon M., Wielen R., 1974, A&A, 37, 183
Allison R. J., Goodwin S. P., Parker R. J., de Grijs R., Portegies Zwart S. F., Kouwenhoven M. B. N., 2009, 700, L99
Arzoumanian D. et al., 2011, A&A, 529, L6
Goodwin S. P., Whitworth A. P., 2004, A&A, 413, 929
Hosek M. W., Lu J. R., Anderseon J., Ghez A. M., Morris M. R., Clarkson W. I., 2015, ApJ, 813, 23
Kim S. S., Figer D. F., Lee H. M., Morris M., 2000, ApJ, 545, 301
Lada C. J., Lada E. A., 2003, ARA&A, 41, 57
Launhardt R., Zylka R., Mezger P. G., 2002, A&A, 384, 112
Maschberger T., 2013, MNRAS, 429, 1725

Hypervelocity runaways from the Large Magellanic Cloud

Douglas Boubert
University of Cambridge

We explore the possibility that the observed population of Galactic hypervelocity stars (HVSs) originate as runaway stars from the Large Magellanic Cloud (LMC). Pairing a binary evolution code with an N-body simulation of the interaction of the LMC with the Milky Way, we predict the spatial distribution and kinematics of an LMC runaway population. We find that runaway stars from the LMC can contribute Galactic HVSs at a rate of three every million years. This is composed of stars at different points of stellar evolution, ranging from the main-sequence to those at the tip of the asymptotic giant branch. We find that the known B-type HVSs have kinematics which are consistent with an LMC origin. Massive runaways will themselves go supernova, producing a remnant whose velocity will be modulated by a supernova kick. This latter scenario has some exotic consequences, such as pulsars and supernovae far from star-forming regions.

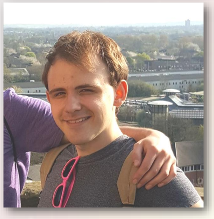

Hypervelocity Runaways from the Large Magellanic Cloud

D. Boubert, D. Erkal, N. W. Evans & R. G. Izzard 2017, MNRAS, 469, 2151
Institute of Astronomy, University of Cambridge
Get in touch at d.boubert@ast.cam.ac.uk!

1. Context: We do not know the origins of the hypervelocity stars.

Hypervelocity stars are defined to have velocities greater than the escape speed of the Milky Way. We know of twenty two B type hypervelocity stars between 50 and 120 kpc from the Earth. The other peculiar characteristic of these stars is that they are not distributed evenly across the sky. In this figure we show the footprint of SDSS DR9 in grey, corresponding to the region that was searched by Brown et al. (2006, 2007, 2014), and the hypervelocity stars that were found in red.

If the hypervelocity stars are born in the Milky Way then they must be produced through the Hills mechanism (Brown, 2015). In the Hills mechanism binary stars are tidally disrupted during a close encounter with the massive black hole at the centre of the Galaxy. This cannot explain why the hypervelocity stars are preferentially found in one part of the sky.

However, the location and past orbit of the LMC (shown in purple in the figure below) are intriguingly aligned with where we see the hypervelocity stars. The LMC is travelling at 378 km/s past the Milky Way and thus a star ejected at 200 km/s in the direction of travel of the LMC would escape the LMC and become a hypervelocity star.

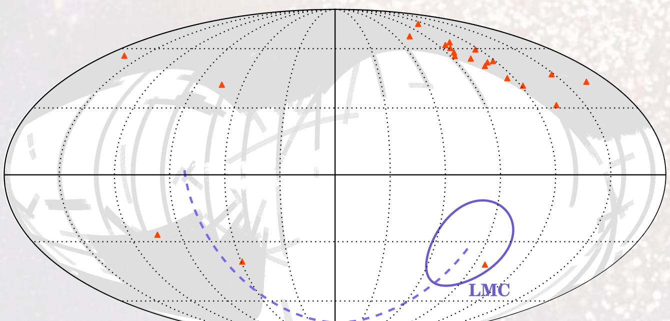

2. Are they hypervelocity runaway stars?

If a star only has to be ejected faster than 200 km/s we can consider a less extreme mechanism. The binary supernova scenario first described by Blaauw (1961), where a star is ejected by the core-collapse supernova of its companion, is observed to produce runaway stars with velocities in excess of 200 km/s.

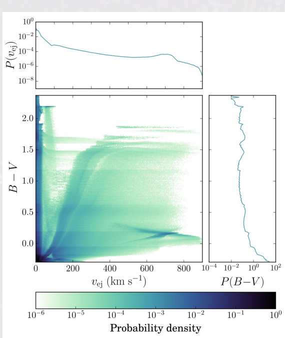

We simulate a sample of runaway stars formed over the past 2 Gyr in the LMC by assuming a SFR of $0.2\ M_\odot\ yr^{-1}$ and sampling binary stars from analytic distributions for their initial properties. We evolve these binaries to identify the runaway stars that are formed using binary_c (Izzard et al., 2004, 2006, 2009). In this figure we show the PDF for the ejection velocity and colour of the runaway stars that are formed. Interestingly, all the stars that have velocities in excess of 200 km/s have interacted with their binary companion prior to the supernova.

A key technical advance of this work is that we follow the single star evolution of the runaways after they are ejected. This allows us to predict stellar properties at present day.

3. Eject the runaways in a model of the LMC-MW and find out where they go.

Once we have the time and supernova velocity kick for the runaway stars formed in the LMC over the past 2 Gyr, we pick a random starting location in the LMC disc and a random orientation for the supernova kick. We also randomly sample velocity dispersions from the LMC disc and add on the rotation velocity of the disc.

We integrate the orbits of the runaway stars until present day in a live N-body model of the LMC flying past the Milky Way, taken from Mackey et al. (2016). In this figure we show the particles which represent the LMC potential at the final timestep. The features top and bottom are due to the tidal disruption of the LMC by the Milky Way.

4. The runaway stars can perfectly reproduce the hypervelocity stars.

We predict that there are 10,000 main sequence runaway stars that have escaped the LMC and are now hypervelocity stars of the Milky Way.

In the figures on the right we show density contours for the simulated runaway stars where the red triangles are the known hypervelocity stars. The first plot on the right is in Galactic coordinates and demonstrates that the clump of hypervelocity stars is naturally explained as the tip of a leading arm of hypervelocity stars. The second plot shows that our model can replicate the radial velocities of the hypervelocity stars. Our model can also match their proper motions and distances.

The major caveat of this model is that the high ejection velocities require binaries to experience common envelope evolution, a process that is not entirely understood.

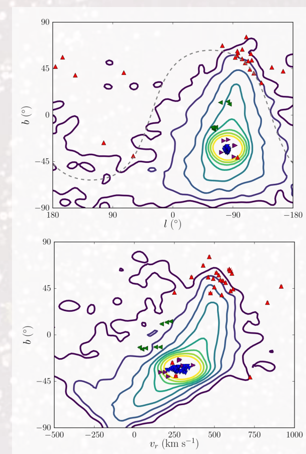

5. Gaia DR2 will provide a definitive test.

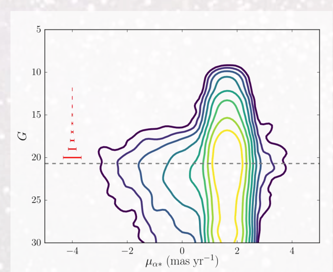

Searches for hypervelocity stars in the past have been limited to parts of the sky which are covered by deep surveys. With Gaia the entire sky will be mapped down to G = 20.7 and, as shown in the figure on the left, this is sufficiently deep to discover the leading arm of hypervelocity stars from the LMC. The proper-motion errors of Gaia are magnitude-dependent and estimates of these are also shown. Not only will Gaia detect these stars, it will measure their proper motions.

6. Conclusions

- We can explain the hypervelocity stars as runaway stars that have escaped the Large Magellanic Cloud.
- The known hypervelocity stars are the tip of a leading arm of 10,000 hypervelocity stars stretching $100°$ on the sky from the Large Magellanic Cloud to the constellation of Leo.
- We predict that Gaia will have discovered stars in this leading arm and measured their proper motions by the end of the five year mission.

Featured in:

Scan the QR code to get to the ADS entry!

Bibliography:

• Blaauw 1961, BAIN, 15, 265 • Boubert et al. 2017, MNRAS, 469, 2151 • Brown et al. 2006, ApJ, 640, L35 • Brown et al. 2007, ApJ, 671, 1708 • Brown et al. 2014, ApJ, 787, 89 • Izzard et al. 2004, MNRAS, 350, 407 • Izzard et al. 2006, A&A, 460, 565 • Izzard et al. 2009, A&A, 508, 1359 • Mackey et al. 2016, MNRAS, 459, 239

Boxy Orbital Structures in Rotating Bar Models

Luis Leonardo Chaves Velasquez
INAOE, México

We investigate regular and chaotic orbits of stars in models of a galactic potential consisting in a disk, a halo, and a bar, in order to find the origin of 3D boxy components, which are part of the bar. Our models originate in snapshots of an N-body simulation presented by Machado & Athanassoula (2010), which develops a conspicuous bar component at times $t = 4.2$ Gyr, $t = 7.0$ Gyr, and $t = 11.2$ Gyr. For the orbital study we treat each snapshot independently, as an autonomous Hamiltonian system. The calculated corotation-to-bar-length ratios indicate that in all three cases the bar rotates slowly. We calculated the characteristic curves of the three models and we found that in all cases, the ellipticity and the orientation of the main family of periodic orbits vary along these curves. The shape of the characteristic of the main family also evolves from model to model. In all three cases we present in this paper it has a complicated shape and changes directions at several energies between the center of the system and corotation. In order to study the regular, chaotic, or sticky character of the orbits and their contribution to the appearance of specific morphological features, we have used the GALI2 index. We characterize the orbits as regular, sticky, or chaotic after integrating them for 10 Gyr period. We study the non-periodic orbits in the outer parts of stability islands, or with sticky orbits around them. By perturbing such orbits in the vertical direction we find a class of non-periodic orbits that are characterized by boxy projections both in their face-on and side-on views, since they are 3D boxy structures.

Boxy orbital structures in rotating bar models

L. Chaves-Velasquez[1], P.A Patsis[2], I. Puerari[1], Ch. Skokos[3], and T. Manos[4]

[1]Instituto Nacional de Astrofísica, Óptica y Electrónica, Puebla, Mexico
[2]Research Center for Astronomy, Academy of Athens, Athens, Greece
[3]Department of Mathematics and Applied Mathematics, University of Cape Town, Cape Town, South Africa
[4]Institute of Neuroscience and Medicine, Brain and Behaviour (INM-7), Research Centre Jülich, Jülich, Germany

Abstract

We investigate regular and chaotic two-dimensional (2D) and three-dimensional (3D) orbits of stars in models of a galactic potential consisting in a disk, a halo and a bar, to find the origin of boxy components, which are part of the bar or (almost) the bar itself. Our models originate in snapshots of a cosmological N -body simulation, which develops a strong bar. We consider three snapshots of the simulation and for the orbital study we treat each snapshot independently, as an autonomous Hamiltonian system. The calculated corotation-to-bar-length ratios indicate that in all three cases the bar rotates slowly, while the orientation of the orbits of the main family of periodic orbits changes along its characteristic. We characterize the orbits as regular, sticky, or chaotic after integrating them for a 10 Gyr period by using the GALI$_2$ index. Boxiness in the equatorial plane is associated either with quasi-periodic orbits in the outer parts of stability islands, or with sticky orbits around them, which can be found in a large range of energies. We indicate the location of such orbits in diagrams, which include the characteristic of the main family. They are always found about the transition region from order to chaos. By perturbing such orbits in the vertical direction we find a class of 3D non-periodic orbits, which have boxy projections both in their face-on and side-on views.

Introduction

In the present study we want to investigate what kind of orbits support 2D and 3D boxy morphologies in the successive snapshots, and how they evolve in time, i.e. from the model of the earlier snapshot to the model for the final one. We want to examine whether this dynamical mechanism is associated with orbits just beyond the vertical 2:1 resonance region, or if it can be applied in a large energy range in which we can find bar-supporting orbits. For this purpose we do not investigate in detail the structure of phase space in a large number of energies, for this purpose we investigate the system's global dynamics.

Modelling the N-body Snapshots

The N-body simulation is described in Manos & Machado (2014) [3]. We approximate the morphology of the snapshots by using the following components.

- The bar (Ferrers 1877) [2]:

$$\Phi_B = -\pi G abc \frac{\rho_c}{3}\int_\lambda^\infty \frac{du}{\Delta(u)}(1-\mu^2(u))^3, \qquad (1)$$

- The disk (Miyamoto and Nagai 1975) [4]:

$$\Phi_D = -\frac{GM_D}{\sqrt{x^2+y^2+(A+\sqrt{z^2+B^2})^2}}, \qquad (2)$$

- The spherical dark mater halo (Dehnen 1993) [1]:

$$\Phi_H = -\frac{GM_H}{a_H(2-\gamma)}\left[1-\left(\frac{r}{r+a_H}\right)^{2-\gamma}\right], \qquad (3)$$

Autonomous Hamiltonian system and the GALI$_2$ index

The Hamiltonian of the system is given by

$$H = \frac{1}{2}(p_x^2+p_y^2+p_z^2)+\Phi(x,y,z)-\Omega_b(xp_y-yp_x) = E_J \qquad (4)$$

The equations of motion are:

$$\dot{x} = p_x+\Omega_b y, \quad \dot{y} = p_y-\Omega_b x, \quad \dot{z} = p_z,$$
$$\dot{p}_x = -\frac{\partial\Phi}{\partial x}+\Omega_b p_y, \quad \dot{p}_y = -\frac{\partial\Phi}{\partial y}-\Omega_b p_x, \quad \dot{p}_z = -\frac{\partial\Phi}{\partial z} \qquad (5)$$

The variational equations are given by:

$$\dot{\delta x} = \delta p_x+\Omega_b\delta y, \quad \dot{\delta y} = \delta p_y-\Omega_b\delta x, \quad \dot{\delta z} = \delta p_z,$$
$$\dot{\delta p_x} = -\frac{\partial^2\Phi}{\partial x^2}\delta x-\frac{\partial^2\Phi}{\partial x\partial y}\delta y-\frac{\partial^2\Phi}{\partial x\partial z}\delta z+\Omega_b\delta p_y,$$
$$\dot{\delta p_y} = -\frac{\partial^2\Phi}{\partial x\partial y}\delta x-\frac{\partial^2\Phi}{\partial y^2}\delta y-\frac{\partial^2\Phi}{\partial y\partial z}\delta z-\Omega_b\delta p_x, \qquad (6)$$
$$\dot{\delta p_z} = -\frac{\partial^2\Phi}{\partial x\partial z}\delta x-\frac{\partial^2\Phi}{\partial z\partial y}\delta y-\frac{\partial^2\Phi}{\partial z^2}\delta z.$$

The GALI$_2$ index is given by (Skokos et al. 2007) [5]:

$$\mathrm{GALI}_2(t) = |\hat{\mathbf{w}}_1(t)\wedge\hat{\mathbf{w}}_2(t)|. \qquad (7)$$

- For chaotic orbits:

$$\mathrm{GALI}_2(t) \propto \exp\left(-(\lambda_1-\lambda_2)t\right) \qquad (8)$$

- For regular orbits:

$$\mathrm{GALI}_2(t) \propto constant. \qquad (9)$$

The degree of chaoticity of the orbits

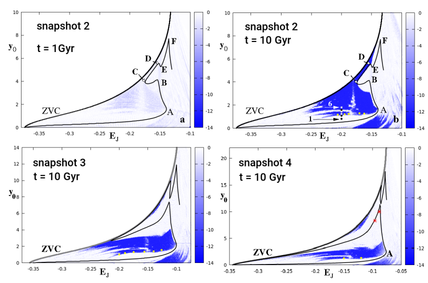

Figure 1: The chaoticity of the planar orbits on the equatorial plane of models 2,3,4. Dark areas correspond to chaotic initial conditions according to their GALI$_2$ value (see colour bars to the right of the panels)

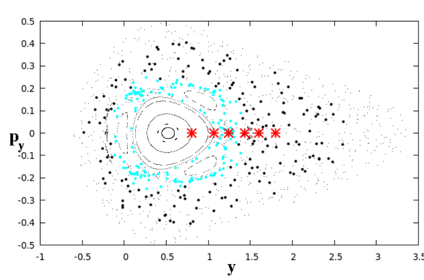

Figure 2: The Poincaré surface of section of model 2 for $E_J = -0.2$.

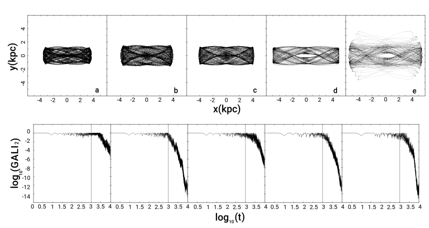

Figure 3: Five orbits with boxy character on the equatorial plane of the model of snapshot 2.

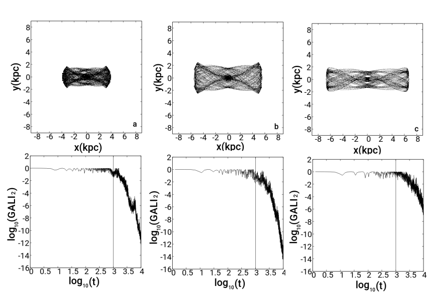

Figure 4: Three orbits with boxy character on the equatorial plane of the model of snapshot 3.

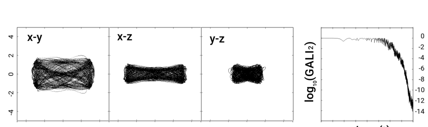

Figure 5: 3D orbit associated with 3D boxy structures in the model of snapshot 2.

Conclusions

1. In models where the family of x1 ellipses exists we can find a class of sticky chaotic orbits with a 2D and/or 3D boxy structure. The shape of these orbits, after integrating them for 10 Gyr and the evolution of their GALI$_2$ index show that they can be used as building blocks for structures that last for several Gyr. They exist in a large range of E_J's.
2. 2D non-periodic boxy orbits can be found on the outermost invariant curves around x1 on a surface of section, or in regions in the immediate neighbourhood of the stability islands. We find them in all E_J's we encounter x1 periodic orbits that match the size of the N-body bar.
3. For finding 3D orbits with boxy morphology in both face-on and edge-on views, one has to perturb in the vertical direction the boxy planar orbits. There is always a Δp_z interval in the initial conditions of the perturbed, initially planar, orbits in which the 3D orbits will have a boxy structure. These are 3D sticky chaotic orbits. Their face-on projections are different from those of the quasi-periodic orbits close to x1 and its 3D bifurcations, at all E_J's we find them.
4. In the face-on projections of these sticky boxy orbits we find the formation of an X embedded in the boxy structure.
5. Such orbits can be used to construct models with boxy isophotes inside the face-on views of the bars. The areas of the boxy isophotes in these cases correspond to the extent of the edge-on boxy bulges, in agreement with the result of
6. The degree of boxiness of a bar, or of a part of it, indicates which orbits are populated. If quasi-periodic orbits in the immediate neighbourhood of the periodic orbits of the central family prevail, the face-on projections will be elliptical. On the other hand if the majority of the non-periodic orbits building the bar, or its part, are at the edges of the stability islands and/or sticky chaotic orbits next to them, then the supported shape in the face-on views will be boxy. In both cases we can have boxy edge-on profiles.

References

[1] W. Dehnen.
MNRAS, 265:250, November 1993.

[2] N. M. Ferrers.
Quart.J.Pur.Appl.Math., 14:1, 1877.

[3] T. Manos and R. E. G. Machado.
MNRAS, 438:2201–2217, March 2014.

[4] M. Miyamoto and R. Nagai.
PASJ, 27:533–543, 1975.

[5] C. Skokos, T. C. Bountis, and C. Antonopoulos.
Physica D Nonlinear Phenomena, 231:30–54, July 2007.

For more information see Chaves-Velasquez et al. 2017 (submitted)

Contact Information

- Email: leonardochaves83@gmail.com
- Phone: +52 (222) 739-29-20

Global Stabilities in Isolated and Perturbed Barred Models

Diego Valencia-Enríquez
INAOE

It has been known that the origin of stellar bars in isolated disc galaxies depends on the angular momentum exchange and on the properties of the model -the ratio between disc mass and halo mass, halo concentration, velocity dispersion, etc.- which they can be characterized by the Global Stabilities. However, it remains unclear what is the lower limit on these Global Stabilities to get a model stable or unstable to bar formation, and how they behave during the evolution of a disc. In this work, we explore Global Stabilities from numerical models where we only change the spin parameter to get two classical models -disc dominate and halo dominate models- and follow them through the time. As we expect, disc dominate models develop a bar while halo dominate ones do not. However, we find while the Global Stabilities are closer from its stabilities limit, the bar formation is more delayed, the spiral structures are stronger, the pattern speed of the bar is slower, and the bar catches surprisingly more particles at the buckles phase. Besides, we perturb these models by a flyby elliptical galaxy to analyse the evolution of the Global Stability Limits of the galaxy and the bar growth under perturbation.

Global Stabilities in Isolated and Perturbed Barred Galaxy Models

Diego Valencia-Enríquez[1], Ivânio Puerari[1], and Irapuan Rodrigues[2]

valencia@inaoep.mx, diegovalencia5@gmail.com

[1]Astrophysics Dpt. at Instituto Nacional de Astrofísica, Óptica y Electrónica, Puebla, Mexico.

[2]Universidade do Vale do Paraíba, Brasil.

Abstract

It remains unclear what are the lower limits of the Global Stabilities parameters to get a model stable or unstable to bar formation, and how they behave during the evolution of a disc. In this work, we explore the Global Stabilities parameters from N-body simulations in which we only change the spin parameter to get two classical models -disc dominate and halo dominate models- and follow them through the time. As we expect, disc dominate models develop a bar while halo dominate ones do not. We find that while the Global Stabilities parameters are closer to their stabilities limit, the bar formation is delayed, the spiral structures are stronger, the pattern speed of the bar is slower, and the bar catches surprisingly more particles at the buckles phase. Besides, we perturb these models by a flyby elliptical galaxy to analyse the evolution of the Global Stability Limits of the galaxy model and the bar growth under perturbation.

Global disc instabilities

We focus on the behavior of global instabilities that can trigger a bar in isolated and perturbed models. [1] suggested a criterion for bar instability characterized by the parameter

$$\epsilon_m = \frac{V_{max}}{\sqrt{GM_d/r_d}}, \quad (1)$$

where V_{max} is the maximum circular velocity, M_d and r_d are the disc mass and disc radial scale length, respectively. The parameter ϵ_m has the advantage of being expressible in terms of quantities that are easy to obtain observationally.

In addition, [2] show that disc stability is characterized by a lower limit of the spin parameter λ_d. They showed that a disc can be unstable to bar formation if

$$0.7 \leq \epsilon_m \leq 1.2 \qquad \text{and} \qquad \lambda_d < \lambda_{crit}. \quad (2)$$

where,

$$\lambda_{crit} = \left(\frac{\epsilon_{m,crit}}{V_{max}}\right)^2 GM_d \frac{\sqrt{2f_c}}{r_{200} f_r}, \quad (3)$$

with $\epsilon_{m,crit} \approx 1$ being the critical value of ϵ_m for disc stability, f_c is a function which depends of the halo concentration c, f_r is a function which depends of the scale radius of the disc r_d, and r_{200} is the radius where the mean enclosed dark matter density is 200 times the critical density.

Simulations

Isolated models:

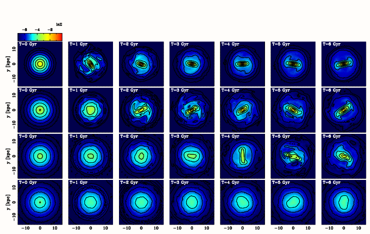

Figure 1 : Description in the text.

Figure 1 shows the face-on surface density maps -in a log scale- for our models and at times of 0, 1, 2, 3, 4, 5, 6 Gyr. From top to bottom, we present the evolution of models $A\lambda03$, $A\lambda04$, $A\lambda05$, and $A\lambda06$, respectively.

Perturbed models:

In Figure 2 the angular velocity of the companion at the perigalacticon in all encounters is around of $40 \mathrm{km/s/kpc}$; we can observe that those interactions produce well defined strong spiral arms and extended tidal features, such as bridges and tails, that are all transient, but distinct in nature.

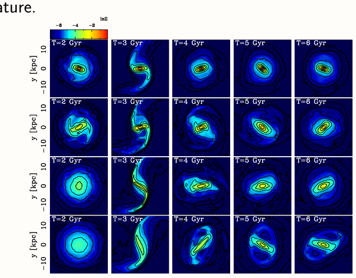

Figure 2 : As in figure 1, interactions of our Pm set. From top to bottom, we present the evolution of models $PmA\lambda03$, $PmA\lambda04$, $PmA\lambda05$, and $PmA\lambda06$, respectively.

Measurement of Global Stabilities

Isolated models:

We observe in Fig. 3 how the bar models begin in the range $0.7 < \epsilon < 1$ and evolve asymptotically toward the unity, while the stable model keeps ϵ_m beyond the unity.

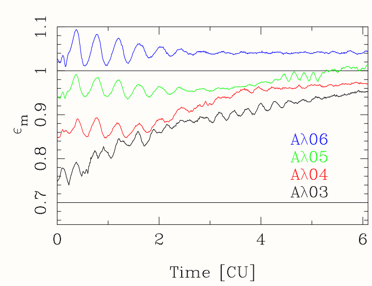

Figure 3 : Evolution of the stability experimental parameter ϵ_m for the isolated models.

Perturbed models:

We observe in Fig. 4 how the parameter ϵ_m falls into the range $0.7 < \epsilon < 1$ due to the passing of the perturbation for all models.

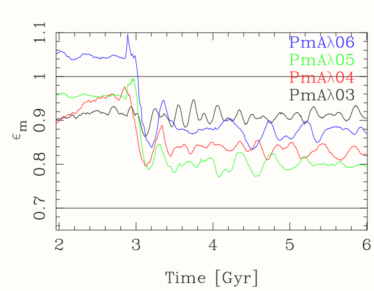

Figure 4 : Evolution of the stability experimental parameter ϵ_m for the perturbed models.

Isolate models:

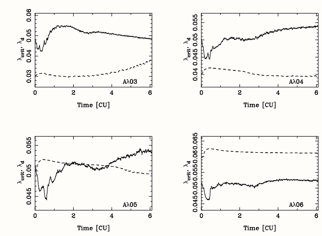

Figure 5 : The spin parameter of the disc λ_d (dashed line) and the critical spin parameter λ_{crit} (continuous line) as a function of time for the isolated models.

We can observe that models forming a bar have $\lambda_d < \lambda_{crit}$, and the stable model against the bar formation has $\lambda_d > \lambda_{crit}$.

Perturbed models:

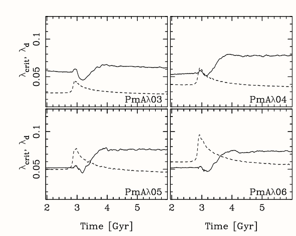

Figure 6 : As in Figure 5, but for perturbed models.

In general, once the perturbation passes and it is far from the studied galaxy, the λ_d parameter tends to return to the equilibrium values that it had before the flyby. Furthermore, the λ_{crit} parameter tends to rise to higher values causing the disc to become more unstable, and the ϵ_m parameter is almost constant through the rest of the simulation with a lower value compared to the initial one.

Table 1 : Evolution of stability parameters.

Model	λ_i	Initial	Final	Final Status
$A\lambda03$	0.03	$\lambda_d < \lambda_{crit}$	$\lambda_d < \lambda_{crit}$	Strong Bar
$A\lambda04$	0.04	$\lambda_d < \lambda_{crit}$	$\lambda_d < \lambda_{crit}$	Bar
$A\lambda05$	0.05	$\lambda_d \approx \lambda_{crit}$	$\lambda_d \leq \lambda_{crit}$	Weak Bar
$A\lambda06$	0.06	$\lambda_d > \lambda_{crit}$	$\lambda_d > \lambda_{crit}$	Stable
$PmA\lambda03$		$\lambda_d < \lambda_{crit}$	$\lambda_d < \lambda_{crit}$	Strong Bar
$PmA\lambda04$		$\lambda_d < \lambda_{crit}$	$\lambda_d < \lambda_{crit}$	Strong Bar
$PmA\lambda05$		$\lambda_d \approx \lambda_{crit}$	$\lambda_d < \lambda_{crit}$	Bar
$PmA\lambda06$		$\lambda_d > \lambda_{crit}$	$\lambda_d < \lambda_{crit}$	Bar

Conclusion

We get a stable disc against bar formation when the model begins with the spin parameter greater than its critical spin parameter, and the experimental parameter ϵ_m is larger than the unity. On the other hand, we get an unstable disc to bar formation when its spin parameter is less than its critical spin parameter and the parameter ϵ_m is in the range from 0.7 to 1. The perturbed models also show that behavior.

References

[1] Efstathiou, G., Lake, G., & Negroponte, J. 1982, MNRAS, 199, 1069

[2] Mo, H. J., Mao, S., & White, S. D. M. 1998, MNRAS, 295, 319

INDICATE: an INdex to Define Inherent Clustering And TEndencies

Anne Buckner
University of Leeds

StarFormMapper (SFM) is an EU H2020 funded international collaborative project whose aim is to constrain the mechanisms that underlie massive star and cluster formation. We present our new novel automated statistical clustering tool INDICATE (Buckner et al., submit.). Traditional clustering algorithms find clusters centroids and members in datasets - but this is insufficient for studies of e.g. mass segregation and substructure in young star clusters/forming regions. INDICATE enables the user to quantitatively trace how "clustered" individual objects are in distribution and how this changes as the system evolves. We will show that for both observed & simulated data INDICATE is robust against noise and can be applied in any specified parameter space without preference for the data sets size, shape or number of dimensions (2D, 3D, 6D).

INDICATE

INdex to Define Inherent Clustering And TEndencies

A. Buckner[1] and the StarFormMapper Collaboration

1 School of Physics and Astronomy, University of Leeds, Leeds LS2 9JT , United Kingdom

What is it?

A new novel automated statistical clustering tool (Buckner et al., in prep.).

Traditional clustering algorithms find cluster centroids and members in datasets- but this is insufficient for studies of e.g. mass segregation and substructure in young star clusters/forming regions. INDICATE enables the user to quantitatively trace how “clustered” individual objects are in distribution and how this changes as the system evolves.

Why do YOU want to use it?

INDICATE has been developed as a tool for the community to quantitatively trace:

- **Mass Segregation**
- **Stellar Substructure**
- **Dynamical Evolution of a Cluster System**
- **Spatial Evolution of Individual Stars in Cluster Mergers**

As stars indexes are derived through direct comparisons to generated uniform distributions, direct comparisons of the Index values derived for individual stars in the cluster system, as well as between multiple cluster systems, is possible.

Thus INDICATE grants the ability to trace how the degree of clustering varies for individual stars, whole cluster systems, and globally, with e.g. stellar/cluster mass, age, position etc.

How does it work?

Calculates a 'clustering' index for every vector in a discrete distribution.

The Index:

- quantitatively describes the degree (or lack of) of spatial clustering in the local neighbourhood of the vector
- derived by comparing the number density of the vector's local neighbourhood with a generated evenly spaced uniform distribution (i.e. definitively non-clustered) with the same overall number density of the distribution
- as such, is independent of shape (circular, filamentary etc.), size and spatial compactness of distributions sub/structure
- can be derived for 2D, 3D and/or 6D discrete distributions
- is calibrated against random distributions

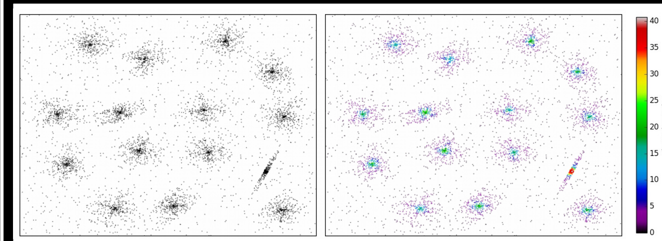

Figure 1. Demonstration of applying INDICATE to a discrete 2D dataset. ***(Left:)*** Synthetic 2D dataset of 6000 vectors and 15 Gaussian clusters with different degree of cluster overlapping (augmented from original form by Fränti & Virmajoki, 2006) ***(Right:)*** after applying INDICATE. The higher the clustering index, the more (absolutely) spatially clustered the vector is.

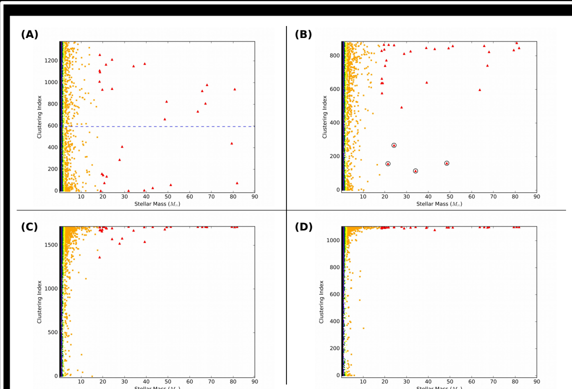

Figure 2: Plots Stellar Mass vs Clustering Index for massive clusters (~10^4 M_{sun}) generated using McLuster (Kuepper et al., 2011) with a ZAMS stellar population of 20,000 members between 0.08-100 M_{sun}; no binaries; half-mass radius of 1pc; and ***(A)*** S=0.0 ***(B)*** S=0.25 ***(C)*** S=0.50 and ***(D)*** S=0.99 degree of mass segregation respectively. As a visual aid stars are tentatively colour coded by spectral type based on mass ranges given for MS stars by Pecaut & Mamajek (2013) [O-red, B-orange, A-yellow, F-green, G-blue, K-purple, M-black] and the blue dashed line on (A) marks the median Clustering Index of the cluster.

Example: Mass Segregation

Mass segregation can be defined as a difference in distribution of stars as a function of stellar mass, such that the more massive stars are more spatially concentrated than their lower mass counter parts.

Thus INDICATE (which quantifies the spatial concentration of objects) allows the variation in the spatial distribution of stars as a function of mass to be easily seen. Advantageously, it is independent (and does not require prior knowledge) of cluster centres, radii or density profiles. An example is shown in **Figure 2**: cluster ***(A)*** has no mass segregation so the Indexes of the most massive stars are randomly distributed about the median value of the cluster. Comparatively, clusters ***(B) (C)*** & ***(D)*** show a trend of increasing higher clustering indexes for the individual massive stars with greater degrees of mass segregation.

However, the true power of INDICATE for mass segregation applications is the ability to quantitatively describe and compare the spatial clustering of individual stars of similar masses. For example in ***(B)*** there are 4 O-type stars [circled] which have a Index value that is statistically significantly lower than the other stars in the cluster with similar masses. Therefore INDICATE has identified/quantified which massive stars are not spatially clustered (respectively) – information which can then be used as a focal point for further studies into e.g. the effects of local environment formation conditions on the dynamical history's of cluster members and cluster spatial structure.

The StarFormMapper Project

INDICATE was developed for, and this research was conducted on behalf of, the StarFormMapper (SFM) project. The key aim of the project is to combine data from two of ESA’s major space missions, Gaia and Herschel, together with ground based facilities and simulations to constrain the mechanisms that underlie massive star and star cluster formation.

SFM has received funding from the European Union’s Horizon 2020 research and innovation programme under grant agreement No 687528. It is a joint collaboration between the University of Leeds, University of Cardiff, Université Grenoble Alps and Quasar Science Resources, S.L.

Scan me to discover the SFM Website!

References

A.Buckner et al., *“The Spatial Evolution of Young Massive Clusters I. – A New Tool to Quantify Substructure & Mass Segregation”*, A&A, in prep.

Fränti & Virmajoki, (2006), Pattern Recognition, 39 (5), 761-765.

Kuepper et al., (2011), MNRAS, 417, 2300.

Pecaut & Mamajek (2013) , ApJS, 208, 9.

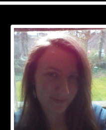

Poster by A. Buckner, Postdoc @ Uni. of Leeds

Star Clusters in outskirts of the Magellanic Clouds and the Bridge

Monika Sitek
Astronomical Observatory of Warsaw University

The Magellanic System (MS), consisting of the Large Magellanic Cloud (LMC), the Small Magellanic Cloud (SMC) and the Magellanic Bridge (MBR), contains diverse sample of star clusters. Their spatial distribution, ages and chemical abundances may provide important information about the history of formation of the whole System. We use deep photometric maps derived from the images collected during the fourth phase of The Optical Gravitational Lensing Experiment (OGLE-IV) to construct the most complete catalog of star clusters in the Magellanic System using the homogeneous photometric data. We present the collection of star clusters (877) found in the area of about 600 square degrees in the outer regions of the Magellanic Clouds and the Bridge. Our sample contains 303 visually identified new star cluster candidates, 77 of which were not published yet, and 226 were already published by us in M. Sitek et. al. 2016. The new clusters are mainly young small open clusters or clusters similar to associations. The main goal of this research project is to prepare the most recent, full census of star clusters in the Magellanic System, based on rich photometric data of the OGLE project. Considering that the OGLE project covers whole Magellanic System on unprecedented scale, it is anticipated that we will be able to determine very accurate parameters of all known clusters, with possible new findings in that area.

Star Clusters in outskirts of the Magellanic Clouds and the Bridge

Monika Sitek and The OGLE Team

Astronomical Observatory, University of Warsaw

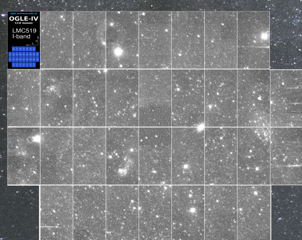

An example field of OGLE-IV observations from central part of Large Magellanic Cloud

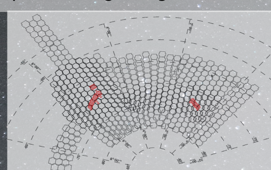

Comparison of OGLE-IV (black poligons) and OGLE-II (red rectangles) Magellanic System sky coverage.

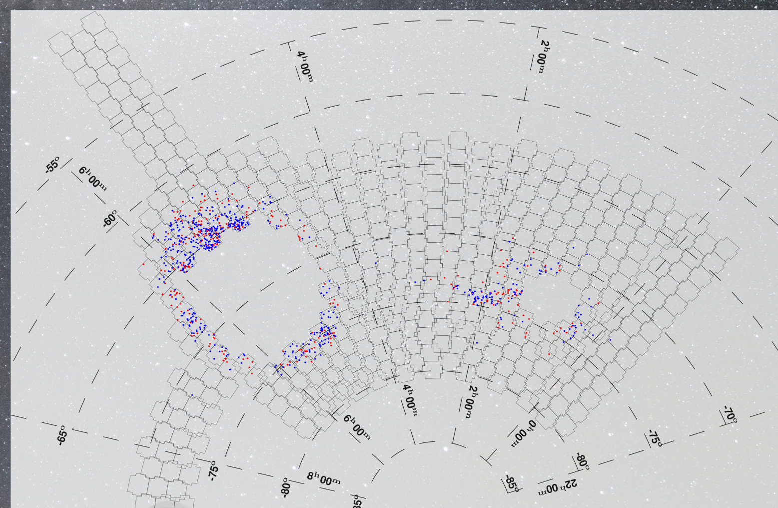

OGLE FACTS

~ in operation since 1992
~ since 2010 as OGLE-IV
~ 1.3m telescope with 32-chip mosaic CCD
~ 1.3 billion stars monitored every night
~ 665 deg^2 Magellanic System coverage
~ 3500 deg^2 whole sky coverage
~ over 17 000 microlensing detections
~ more than 50 exoplanets discovered
~ 1 000 000 new variable stars

our star clusters

known 574 (blue dots)

new 303 (red dots)

The Magellanic System (MS), consisting of the Large Magellanic Cloud (LMC), the Small Magellanic Cloud (SMC) and the Magellanic Bridge (MBR), contains diverse sample of star clusters. Their spatial distribution, ages and chemical abundances may provide important information about the history of formation of the whole System. We use deep photometric maps derived from the images collected during the fourth phase of The Optical Gravitational Lensing Experiment (OGLE-IV) to construct the most complete catalog of star clusters in the Magellanic System using the homogeneous photometric data. We present the collection of star clusters (877) found in the area of about 600 square degrees in the outer regions of the Magellanic Clouds and the Bridge. Our sample contains 303 visually identified new star cluster candidates, 77 of which were not published yet, and 226 were already published by us in M. Sitek et. al. 2016. The new clusters are mainly young small open clusters or clusters similar to associations.

The main goal of this research project is to prepare the most recent, full census of star clusters in the Magellanic System, based on rich photometric data of the OGLE project. Considering that the OGLE project covers whole Magellanic System on unprecedented scale, it is anticipated that we will be able to determine very accurate parameters of all known clusters, with possible new findings in that area. The catalog will contain the basic parameters of detected clusters: size, number of objects and variable stars in each cluster, reddening, estimated age, etc. Those parameters will be derived in the most accurate way possible, using different methods and multiple tests in order to obtain good statistics.

Pietrzyński et al. (1998, 1999) published a catalog of 615 (including 126 new findings) star clusters in the SMC and LMC, based on observations of the OGLE-II project. This was by far the largest collection of clusters in LMC and SMC based on the data of single observation project, but only in central parts of Magellanic Clouds. Now we have found 877 star clusters only in the outskirts of the Magellanic Clouds and in the Bridge. Our sample contains almost all star clusters from the biggest catalog of extended objects (Bica et. al. 2008) in this area and 303 new objects.

Methods of searching and analyzing star clusters are not new idea in astronomy but still challenging. Construction, testing and application of algorithms which will work effectively in highly distinct environments such as LMC and SMC centers and vast, mostly empty regions of the Bridge have been never done before in such scale of a single, homogeneous set of data.

Together with other OGLE projects regarding the Magellanic System which are currently underway this project should yield and up-to-date view of the structure and content of one of the most important stellar systems in astronomy.

This work was supported from the National Science Center, grant agreement no. 2013/11/D/ST9/03445 and from the European Research Council under the European Community's Seventh Framework Programme(FP7/2007-2013) / ERC grant agreement no. 246678.

Bibliography:

1. "OGLE collection of star clusters. New objects in the outskirts of tle Large Magellanic Cloud", M. Sitek et. al. Acta Astron. 2016, 66,255
2. "OGLE-IV: Fourth Phase of the Optical Gravitational Lensing Experiment", A. Udalski et al. Acta Astron.,2015,65,1
3. "A general catalogue of extended objects in the Magellanic System", E.Bica et al. MNRAS,389,p.678
4. "The Optical Gravitational Lensing Experiment. The catalogue of star clusters from the LMC", G. Pietrzyński et al., Acta Astron.,1999,49,521
5. "The Optical Gravitational Lensing Experiment. The catalogue of star clusters fro the SMC", G.Pietrzyński et al., Acta Astron.,1998,48,175

The secular evolution of the Nuclear Star Cluster of the Milky Way

Sara Rastello
Università di Roma, La Sapienza

Nuclear Stellar Clusters are stellar systems (up to 10^7 stars in few parsec radius) so dense that their dynamics cannot be followed with the high precision, direct summation available N-body codes over a long integration time. This poster introduces the main idea of our project, that is of studying the dynamics of the MW NSC by means of a new approach to work in a direct summation code. The focus is on setting an inner region of the MW NSC containing a "treatable" number of stars (10^5 to 10^6 stars) where we run the direct N-body simulation with the advanced code NBODY6++GPU while modeling the region surrounding the subset sphere "boundary" by a suitable method preserving precision and speed. This strategy will allow us to study the evolution of the NSC over its 2-body relaxation time with an acceptable numerical effort by mean of a massive computational platform.

Features of globular clusters dynamics with intermediate mass black holes

Marina Ryabova
Southern Federal University, Russia

Recent photometric and spectroscopic analysis of several Galactic globular clusters (e.g., 47 Tuc, Omega Cen, NGC 5286, NGC 6266, NGC 6388, NGC 6624) is evidence that the clusters probably contain black holes of intermediate mass (around 1% of the cluster mass). Using N-body simulations, we follow the dynamical evolution of globular cluster in the presence of an intermediate-mass black hole. Black hole forms a hard binary system that affects kinematics of central region of the cluster, and black holes with masses exceeding 1.5% of the total cluster mass are able to prevent core collapse.

A chemical study of blue straggler stars in the open cluster M67

Clio Bertelli Motta
ARI - ZAH - University of Heidelberg

Blue straggler stars (BSS) are among the most puzzling objects found in stellar clusters. Since their discovery in globular clusters, they have been shown to exist also in old open clusters of the Milky Way. Their formation is currently explained by two main theoretical scenarios (collision and mass transfer), but the observational evidence in support of the one or the other is still incomplete, especially with respect to the chemical composition of these stars. Using APOGEE observations of the old open cluster M67, we performed a membership analysis based on kinematic criteria (radial velocity and proper motions from the PPMXL catalogue). Among the selected stars, we found 10 whose position on the colour-magnitude diagram suggests a blue straggler nature. Since no abundances were available for these objects from the APOGEE pipeline ASPCAP, we conducted an independent chemical analysis of the sample. We found that the BSS candidates share the same surface chemical composition as the stars situated at the turn-off of M67. In particular, their carbon abundances do not show any anomaly, and thus seems to support a collisional formation scenario for these stars. Furthermore, we note that the abundances of the yellow straggler 2MASS J08515020 + 1146069 are consistent with the abundances of the red clump stars in M67, confirming the evolved nature of this object.

The viscous evolution of circumstellar discs in young star clusters

Francisca Concha-Ramírez
Leiden Observatory

Stars with circumstellar disks form in environments with high stellar and gas densities which affects disks through processes such as truncation from dynamical interactions, ram pressure stripping, and external photoevaporation. Circumstellar disks also undergo internal viscous evolution, leading to disk expansion and mass accretion onto the central star. Previous work indicates that dynamical truncation and viscous evolution play a major role in determining circumstellar disk size and mass distributions. However, it remains unclear under what circumstances which of these two processes dominates. Here we present results of simulations of young clusters taking into account dynamical interaction between stars and the viscous evolution of disks. Coupling viscous disk evolution with direct N-body code is done using the AMUSE framework. Cluster gas is modelled as a time variable background potential. We compare these results with actual observations of size, mass, and accretion rates of circumstellar disks inside star clusters. We argue that the relative importance of dynamical truncation and the viscous evolution of disks changes with time and cluster density. Viscous evolution causes the importance of dynamical encounters increase with time. The presence of gas results in more dynamical encounters, compared to simulations without gas. Gas expulsion causes the cluster to expand, making the moment of gas expulsion a critical variable in the importance of dynamical truncation. Simulation results for disk masses and accretion rates are in agreement with observations of the Trapezium cluster. Disk sizes are overestimated by our model, suggesting the need to include other physical processes that might be triggering disk truncation.

Hydrodynamic simulations of the central molecular zone with realistic Galactic potential

Jihye Shin
Korea Institute for Advanced Study

We present hydrodynamic simulations of gas clouds inflowing from the disk to a few hundred parsec region of the Milky Way. A gravitational potential is generated to include realistic Galactic structures by using thousands of multipole expansions that describe 6.4 million stellar particles of a self-consistent Galaxy simulation. We find that a hybrid multipole expansion model, with two different basis sets and a thick disk correction, accurately reproduces the overall structures of the Milky Way. Through non-axisymmetric Galactic structures of an elongated bar and spiral arms, gas clouds in the disk inflow to the nuclear region and form a central molecular zone (CMZ)-like nuclear ring. We find that the size of the nuclear ring evolves into ≈ 240 pc at $T \approx 1500$ Myr, regardless of the initial size. For most simulation runs, the rate of gas inflow to the nuclear region is equilibrated to ≈ 0.02 $M_{\odot}/yr$. The nuclear ring is off-centered, relative to the Galactic center, by the lopsided central.

Globular Clusters within Dark Matter Halos - 47 Tuc, NGC 1851 and M 15

Joowon Lee
Kyung Hee University

From the observation and numerical studies, Globular clusters (GCs) are known to have a very small amount of or no dark matter (DM). GCs must have lost the majority of the DM through dynamical processes such as mass segregation or tidal stripping even if GCs formed within individual DM halos. Nevertheless, further studies are necessary to see if there is any GC that has been formed with a significant amount of DM. For our study, we select three Galactic GCs, 47 Tuc, NGC 1851, and M 15, which have different origins and properties since the clusters' origins can affect the initial amount of DM. Using the Fokker-Planck (FP) calculations, we investigate the dynamical evolution of the three GCs with an assumption that they were formed in mini DM halos. We compare the FP results to the present-day observational data to trace the amount of initial DM of the three clusters. We find that these three GCs must have initially had insignificant amounts of DM, less than 10% of the initial stellar mass less than 10% of the initial stellar mass of each cluster.

nProFit: a toolkit for the analysis of intensity profiles of n objects in an image

Bolivia Teresa Cuevas Otahola
INAOE

We present here nProFiT, a profile fitting tool designed specifically to compute and analyze intensity profiles of extra-galactic star clusters and compact galaxies. The tool, developed in PyRAF, starts by obtaining intensity profiles in elliptical rings around user-given coordinates using the IRAF/STSDAS task ellipse. Subsequently, the tool allows the user to fit the observed profiles with a number of commonly used theoretical/empirical profiles (King, Moffat-EFF, Sersic, Nuker, etc.) to derive the structural parameters associated to the fitted objects. Critical image-related parameters such as background level, the rms, the ellipticity, position angle of the object and the fitting radius, are automatically determined by the tool. Unlike other publicly available toolkits like GALFIT and iSHAPE, nProFit allows complete characterization of structural parameters for each object in a list automatically. We also present the structural parameters distributions of Super Stelar Clusters in the M82 disk, contained in the Maya et al. (2008) catalogue, computed using nProFit, for 146 objects in the HST passbands F435W(B), F555W(V) y F814W(I). The best fits where obtained using Moffat-EFF profile.